Development of Intelligent Exoskeleton Grasping Through Sensor Fusion and Slip Detection

by Brielle JB. Lee

Thesis submitted to the faculty of the Virginia Polytechnic Institute and State University in partial fulfillment of the requirements for the degree of

Master of Science
In
Mechanical Engineering

Pinhas Ben-Tzvi, Chair
Alfred L. Wicks
Alan Asbeck

May 9, 2018
Blacksburg, Virginia

Keywords: Exoskeleton, Mechatronics, Robotic Systems, Slip Detection, Assistive Glove, Rehabilitation

Development of Intelligent Exoskeleton Grasping Through Sensor Fusion and Slip Detection

by Brielle JB. Lee

ABSTRACT

This thesis explores the field of hand exoskeleton robotic systems with slip detection and its applications. It presents the design and control of the intelligent sensing and force-feedback exoskeleton robotic (iSAFER) glove to create a system capable of intelligent object grasping initiated by detection of the user's intentions through motion amplification. Using a combination of sensory feedback streams from the glove, the system has the ability to identify and prevent object slippage, as well as adapting grip geometry to the object properties. The slip detection algorithm provides updated inputs to the force controller to prevent an object from being dropped, while only requiring minimal input from a user who may have varying degrees of functionality in their injured hand. This thesis proposes the use of a high dynamic range, low cost conductive elastomer sensor coupled with a negative force derivative trigger that can be leveraged in order to create a controller that can intelligently respond to slip conditions through state machine architecture, and improve the grasping robustness of the exoskeleton. The mechanical and electrical improvements to the previous design, the sensing and force-feedback exoskeleton robotic (SAFER) glove, are described while details of the controller design and the proposed assistive and rehabilitative applications are explained. Experimental results confirming the validity of the proposed system are also presented. In closing, this thesis concludes with topics for future exploration.

Development of Intelligent Exoskeleton Grasping Through Sensor Fusion and Slip Detection

by Brielle JB. Lee

GENERAL AUDIENCE ABSTRACT

Exoskeletons are robotic systems that have rigid external covering, such as links, joints, and/or soft artificial tendons or muscles, for the desired body part to provide support and/or protection. These are typically used to enhance power and strength, provide rehabilitation and assistance, and teleoperate other robots from a distance. While the US Army developed exoskeletons for strengthening purposes, another potential purpose of exoskeletons, which is serving medical needs, such as rehabilitation, attracted a lot of attention.

Among numerous illnesses and injuries that may lead to impaired hand functionality, the U.S. Department of Health and Human Services estimated that approximately 470,000 people survive strokes every year in the United States and require continuous rehabilitation to recover their motor functions. Though medical professionals believe that the intensity and duration of rehabilitation is the key for maximizing the rate of recovery, it is often limited due to many reasons, such as cost or difficulty in attending rehabilitation sessions. To augment the availability and quality of rehabilitation, the study of exoskeletons has earned popularity. Beyond the capability of providing simple movements, such as passive rehabilitation, many scientists researched to provide active rehabilitation, which involves active participation from the patients. Furthermore, detecting the patient's intention to activate the rehabilitation glove became a topic of interest, and many types of sensors were utilized in research.

This thesis explores the design and control of the intelligent sensing and force-feedback exoskeleton robotic (iSAFER) glove, which detects the user's intentions to activate the system through motion amplification. The iSAFER glove performs soft initial grasp until the fingers touch an object. After the object is gently grabbed and lifted, the grasp is autonomously adjusted through slip detection until there is no more slip. To facilitate this idea, a low cost force sensor was created and leveraged to improve the grasping control of the exoskeleton. The mechanical and electrical improvements to the previous design, the sensing and force-feedback exoskeleton robotic (SAFER) glove, are described while details of the controller design and the proposed assistive and rehabilitative applications are explained. Experimental results confirming the validity of the proposed system are also presented. In closing, this thesis concludes with topics for future exploration.

ACKNOWLEDGMENTS

Firstly, I would like to thank my family and friends, especially my mother Young Ok Lee, father Sang Sub Lee, grandfather Min Don Lee, uncle Kyo Young Lee, and friend Terry Filarecki, for all their love, unfailing support, and continuous encouragement throughout my years of study and the process of researching. I would also like to offer special thanks to my old friend, KJ Shin, who shared dreams of engineering with me. Though our promise is not possible to be kept anymore, smiles and memories of him inspired me to stay positive, and it will always be.

My thesis would not have been successful without the help of many people. I would like to thank my advisor, Dr. Pinhas Ben-Tzvi for his guidance and supports. He was always available to help and cared about his students. I deeply appreciate the opportunities he has provided me at the Robotics and Mechatronics Lab at Virginia Tech. I also would like to acknowledge, Adam Williams, Hailin Ren, Anil Kumar, and Bijo Sebastian for their encouraging words and ceaseless support. Not only did they help with my research, they also helped me remain strong-minded and regain my confidence.

Finally, I would also like to thank my committee members, Dr. Alfred L. Wicks and Dr. Alan Asbeck, for their guidance. I am grateful for their concerns and recommendation that helped to improve my research and thesis.

TABLE OF CONTENTS

LIST OF FIGURES

LIST OF TABLES

CHAPTER 1

INTRODUCTION

1.1 Background

Numerous illnesses and injuries may lead to impaired hand functionality, from stroke to cerebral palsy to impact injuries that result in fractures and nerve damage. Loss of hand dexterity and strength often causes a drastic decrease in the patient's quality of life and makes it difficult to perform activities of daily living (ADL). Illnesses and injuries in combination with an aging population will drive future increases in the rate of patients who need rehabilitation and assistance, resulting in greater demand for healthcare services and a rise in related costs [1]–[6].

Common treatment aimed at returning hand functionality following such an illness or injury often includes some form of rehabilitation treatment. This involves performing strength training exercises and dexterity building activities, usually overseen by a licensed occupational therapist [7]. While the frequency and intensity of active rehabilitation increase the rate of recovery, involvement in this level of rehabilitation can often be limited due to the cost or difficulty in attending such sessions for injured or elderly patients [1], [7], [8]. Similarly, passive rehabilitation, through guided motions, can alleviate joint pain while helping the patients to combat muscle and bone atrophy prior to beginning active rehabilitation, or maintain progress once active rehab has begun [8]. However, as passive rehabilitation requires another person or device to perform the exercises on the patients, the access is again limited. This challenge has led to the

expansion of research into using assistive robotic technology to improve the accessibility of rehabilitative services for hard to reach demographics [9]–[12].

In addition to the exploration of rehabilitative devices, a complementary active research topic is the investigation of utilizing assistive wearable gloves and orthoses that serve to augment and amplify the abilities of the wearer. Whether improving grip strength and reducing fatigue like the NASA/GM RoboGlove [13] or aiding persons with impaired hand mobility to grasp everyday objects with soft robotic gloves, these systems are intended to be worn by the targeted user to improve their manual capabilities [14]. While the earliest robotic exoskeleton gloves had large footprints and were heavy to use, the focus has been in the reduction in weight, size, and actuation requirements in order to increase the adoption of the use of robotic assistive devices. However, there are tradeoffs made in the design of such systems. For instance, while soft systems are often lightweight, they also incorporate the use of fluidic actuation systems that require the inclusion of a pump or compressor. Hard frame exoskeletons, on the other hand, struggle to maintain a feasible weight and face actuation hurdles as well with large battery packs/actuation units.

Key to the design of these platforms is the intended motions and interactions of the user. These then inform not only the physical design process but the design of the control and operation of the system as well. In many cases, a force control paradigm is used, whether implemented via PID, impedance control, sliding mode control, or some other paradigm [15]–[17]. However, this method depends on the prior calibration or calculation of what the required force input must be for successful motion, grasping, interaction, or other desired action. In addition, the wearer must have the sensory and control capability

to adjust the force input if the action is unsuccessful. Even when possible, this may prove difficult at times for wearers with broader impairment. For these reasons, robotic exoskeletons would greatly benefit from further exploration of intelligent grasping paradigms.

Outside of the realm of robotic exoskeletons, there has been far more extensive research into intelligent grasping as applied to robotic manipulators and prosthetics. One of the key elements of intelligent grasping is the detection of slip conditions, as this signals a failure in the grasp that is then utilized to trigger an error correction behavior [18]–[22]. The extant work in robotic hand provides a basis for the application of a slip-aware intelligent grasping paradigm to a robotic exoskeleton for the first time.

1.2 Motivation

When it comes to strokes, the U.S. Department of Health and Human Services estimates that approximately 470,000 people survive strokes every year in the United States and require continuous rehabilitation to recover their motor functions [7]. Many stroke survivors who lose their motor functions also suffer emotional distress because of losing their independence. Relearning basic skills, such as eating, bathing, toileting, and dressing, can be very stressful to some patients, and failing to perform these skills without the help of others may lead to loss of confidence and negative expectation regarding the recovery, thereby aggravating the condition [23]. As a result, the use of rehabilitation devices such as exoskeletons has emerged in popularity within recent decades.

Before the rehabilitation exoskeletons earned their popularity, many exoskeletons

with different purposes were developed since the 20th century. Beginning with the Hardiman developed by General Electric in the United States around 1966, there was a rich evolution in the history of the exoskeleton robot system [24]. Originally starting from power augmentation systems, mostly aimed for the military usage, the exoskeletons that assist rehabilitation eventually emerged. Due to the technical limitations and lack of knowledge at that time, the rehabilitation exoskeletons were presented to the market recently, but their great potentials for multiple applications were broadly recognized since the 1960s.

To maximize the rate of recovery, medical professionals often emphasize that the rehabilitation should begin as soon as a stroke patient is stable [7] as only 25 percent of patients recover physical functioning which matches the physical functioning of persons who have not had a stroke [2]. Starting from an acute hospitalization for acute stroke patients to inpatient and outpatient rehabilitation for subacute stroke patients to individual goal setting for chronic stroke patients [2], [25], each stroke patient at a different stage of stroke needs appropriate rehabilitation concepts. Among different types of the recommended rehabilitation approaches, a number of approaches such as muscle strengthening exercises and mirror therapy [25], as well as the passive movement, stood out because these were recommended for all the stages of stroke. Many medical papers described that the patients also suffer spasticity-related pain, also known as a “frozen” joint, in addition to the discomfort of having difficulty to perform ADL [2], [7], [25]. Due to lack of movement in a joint after the illnesses and injuries, the tendons and ligaments around the joint can thicken, causing the pain and decreased the range of motion (ROM). Therefore, this passive movement, also known as passive stretching,

involving a gentle move, flex, or stretch of the impaired limb and joints by a therapist or caregiver, is essential to prevent or thaw the frozen joint. This will not only alleviate the pain [7], [12], [26] but also help patients to maintain the condition of their recovered joints [8]. As mentioned earlier in subsection 1.1, using assistive robotic technology to improve the accessibility of rehabilitative services has attracted the attention of many researchers. As a result, numerous robotic technologies were developed and validated for medical purposes. While many researchers and medical professionals still question whether assistive robotic technology is as efficient as or better than the traditional rehabilitation methodology, some of them confirmed the effectiveness of the robot-aided rehabilitation and assistance [12], [26]–[30], and many others concluded their research with positive expectations for the future [6], [31], [32].

Furthermore, to provide an exoskeleton that can help patients to perform cognitive processes, which represent the processes of inference, planning, and actions of human acquiring various senses such as visual, tactile, and auditory senses, some of the recent studies focused on human intent measurement. In a traditional way, a pre-programmed rehabilitation system is played to control the exoskeleton for the rehabilitation, and an input signal is triggered by pressing a button or switch to activate a grasp [33]–[37]. Though this traditional way is still practiced, to amplify the effect of recovery by providing active rehabilitation, many studies used sensors such as Electromyography (EMG), muscle stiffness sensor, Electroencephalogram (EEG), and temperature sensor [24], [28], [38]–[40] to understand human intent. However, these sensors also had drawbacks such as the placement of the sensors; a sensor such as the EMG must be directly attached to the skin. The EMG also has a problem quantifying the signals due to

the possibility of interference from the electrical supply and the activity of other muscles [24], [41]. To overcome these disadvantages, researchers developed and utilized various types of sensors that used the measurements such as force, acceleration, and pressure. These new types of sensors proved more reliable than the sensors such as EMG, and they were not required to be attached to the human body. As it could be attached to the exoskeleton itself, this benefit also made the process of wearing the exoskeleton shorter by removing a step of sensor placement and removal for each time.

In summary, the background and history presented above show the importance of providing both passive and active rehabilitation to the patients while expressing the need of exoskeletons that can be used for both rehabilitation and assistance. In addition, to maximize the utilization of the exoskeleton, developing a hybrid exoskeleton with multiple purposes that could be used throughout the stages of rehabilitation while adapting to user's intention is desired. To further facilitate results of active rehabilitation, exploring the intelligent grasping paradigm, which utilizes the twitch as an input signal and slip detection for grip force adjustment, are sought. Following the rehabilitation steps that proved to be effective [26], this thesis aimed to create a control system that has multiple states to provide different rehabilitations such as passive rehabilitation through warm-up movements, which is also comparable to an active mirror therapy since the affected hand is actively moved conveying visual stimuli to the brain, and self-activating active rehabilitation.

1.3 Thesis Structure

The rest of this thesis is organized as follows:

Chapter 1: Presents the brief background of exoskeleton glove as well as the motivation of this thesis

Chapter 2: Provides a comprehensive literature review and detailed analysis on the human hand anatomy and its functionalities as well as current state of the art systems on exoskeleton gloves and robotic manipulators mainly focusing on the slip detection

Chapter 3: Presents the design and thorough review of the prototype which was used and modified for this thesis, and then identifies several factors that can be modified to increase the stability, strength, sensing capabilities, and human-robot interface of the system while improving a system to perform an intelligent object grasping function

Chapter 4: Presents the details of improvements made on the prototype and the modified prototype design

Chapter 5: Provides an overview of the intelligent object grasping system for rehabilitation and assistive purposes

Chapter 6: Presents the sensory data analysis including motion amplification and slip detection

Chapter 7: Describes the experiment setup and discusses the result of experiments

Chapter 8: Concludes the thesis by providing a summary of the work and explores and discusses about several potential future works including the utilization of a forearm exoskeleton called FE.RAP

1.4 Selected Publications

Disclosure: Contents from these publications were used in this thesis.

Conference Paper

1. **J. Lee** and P. Ben-Tzvi, "Design of a Wearable 3-DOF Forearm Exoskeleton for Rehabilitation and Assistive Purposes," in *Proceedings of the 2017 ASME International Mechanical Engineering Congress and Exposition (IMECE 2017) Volume 3: Biomedical and Biotechnology Engineering*, 2017, pp. 1–10.

Journal Paper

1. **B. Lee**, A. Williams, and P. Ben-Tzvi, "Intelligent Object Grasping with Sensor Fusion for Rehabilitation and Assistive Applications," *IEEE Trans. Neural Syst. Rehabil. Eng.*, 2018, *Accepted*

CHAPTER 2

LITERATURE REVIEW

As exoskeletons are worn directly on the human body, they have to be made to fit well with the human body structure. Before an exoskeleton is designed, a basic understanding of the human anatomy is required. Among all human body parts, the hand is known to be complex, performing sophisticated movements, which is also known as an extension of intellect [42]. As the human hand is a prehensile, five-fingered appendage, understanding taxonomy of human grasp types is also important in the development of an exoskeleton for hands. The following subsections will present reviews of hand anatomy and function, taxonomy of human grasp types, and pressure distribution map of the hand. After providing a basic understanding of the human hand anatomy, different types of actuation that were used on the exoskeletons and several state-of-the-art manipulators and prosthetics, which used slip detection to control the grasp, are presented.

2.1 Hand Anatomy and Function

In most cases, the human hand has five fingers, palm, and wrist. Five fingers, which are also known as five digits, are consisted of four fingers (index, middle, ring, and pinky) and one thumb. As shown in Figure 2.1, each finger has three phalanx bones: distal phalanges, middle phalanges, and proximal phalanges, and a thumb only consists of a distal phalanx and proximal phalanx. Including these phalanx bones along with eight short carpal bones of the wrist and metacarpals in the palm area, there are about 27 bones

in the human hand. A number of numerous sesamoid bones in the hand can increase the total number of bones varying with each individual. Similarly, each finger has three joints: Distal Interphalangeal (DIP), Proximal Interphalangeal (PIP), and Metacarpophalangeal (MCP) while a thumb only has two joints: Interphalangeal (IP) and Metacarpophalangeal (MCP). DIP and PIP joints connect distal and middle phalanges together while IP joint connects distal and proximal phalanges, and MCP joints connect proximal phalanges to metacarpals.

As the bones of the fingers and the bones of the thumb have structural similarities, the joints of the fingers and the joints of the thumb also have structural similarities. However,

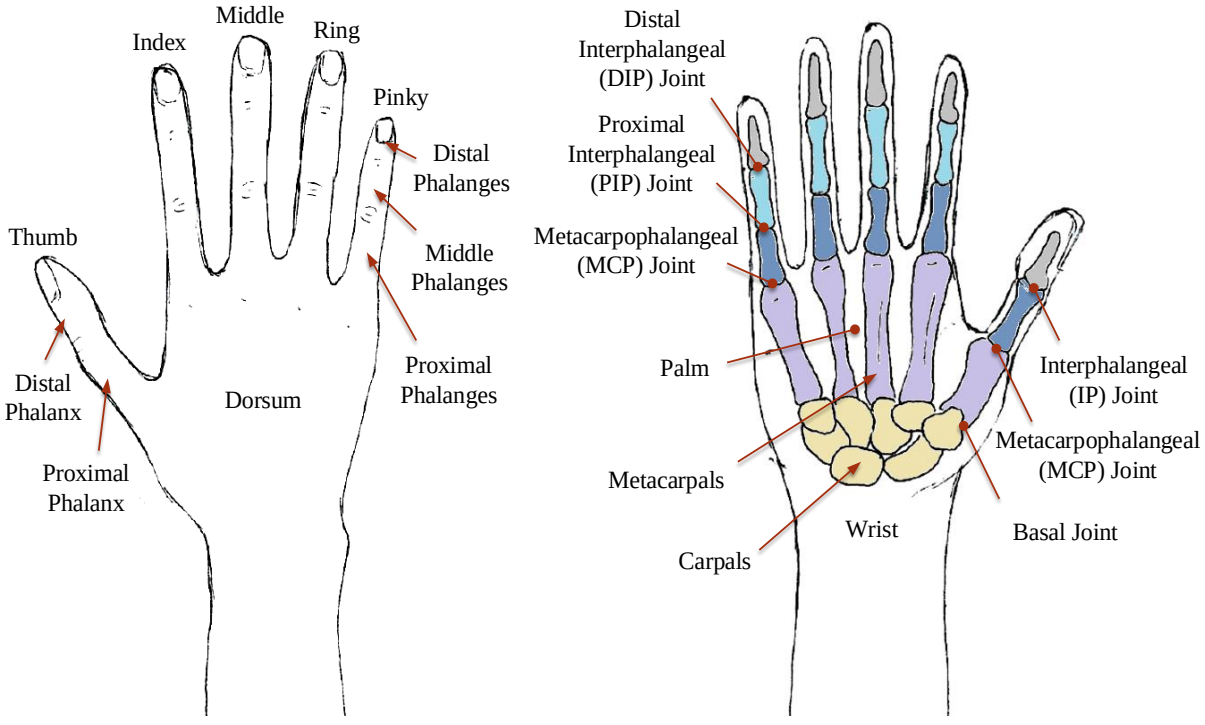

Figure 2.1: Anatomy of the human hand

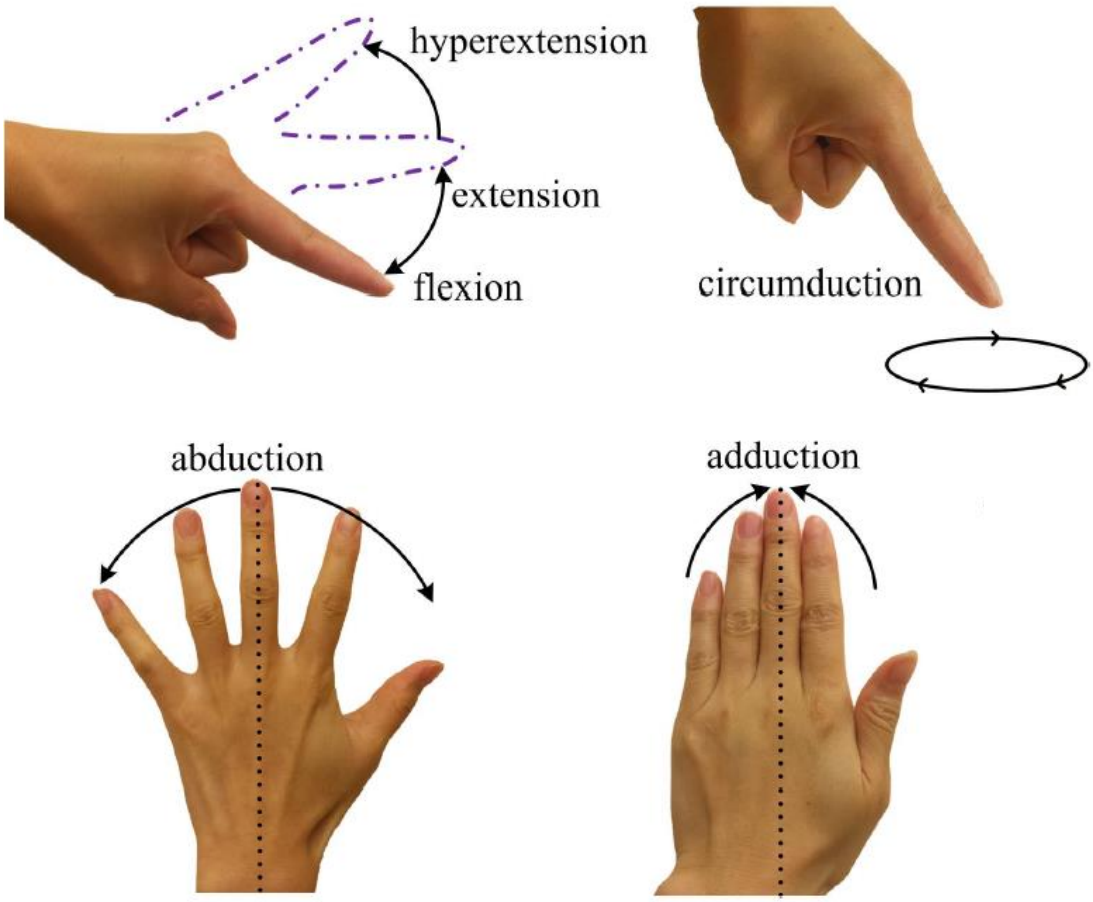

Figure 2.2: Movement of the fingers [43]

the function of the thumb is significantly different from the function of the fingers. According to American Society for Surgery of the Hand organization (ASSH), DIP and PIP joints of the fingers can perform extension and flexion while IP joint of the thumb can perform hyperextension and flexion. MCP joints of both fingers and thumb can perform hyperextension and flexion. Though ASSH did not include circumduction as a movement of fingers or thumb, authors often introduced a term, circumduction, as a movement of joints when a combination of multiple movements, such as flexion, extension, abduction, and adduction, at a joint can create a circular motion [32], [43]–[46] as

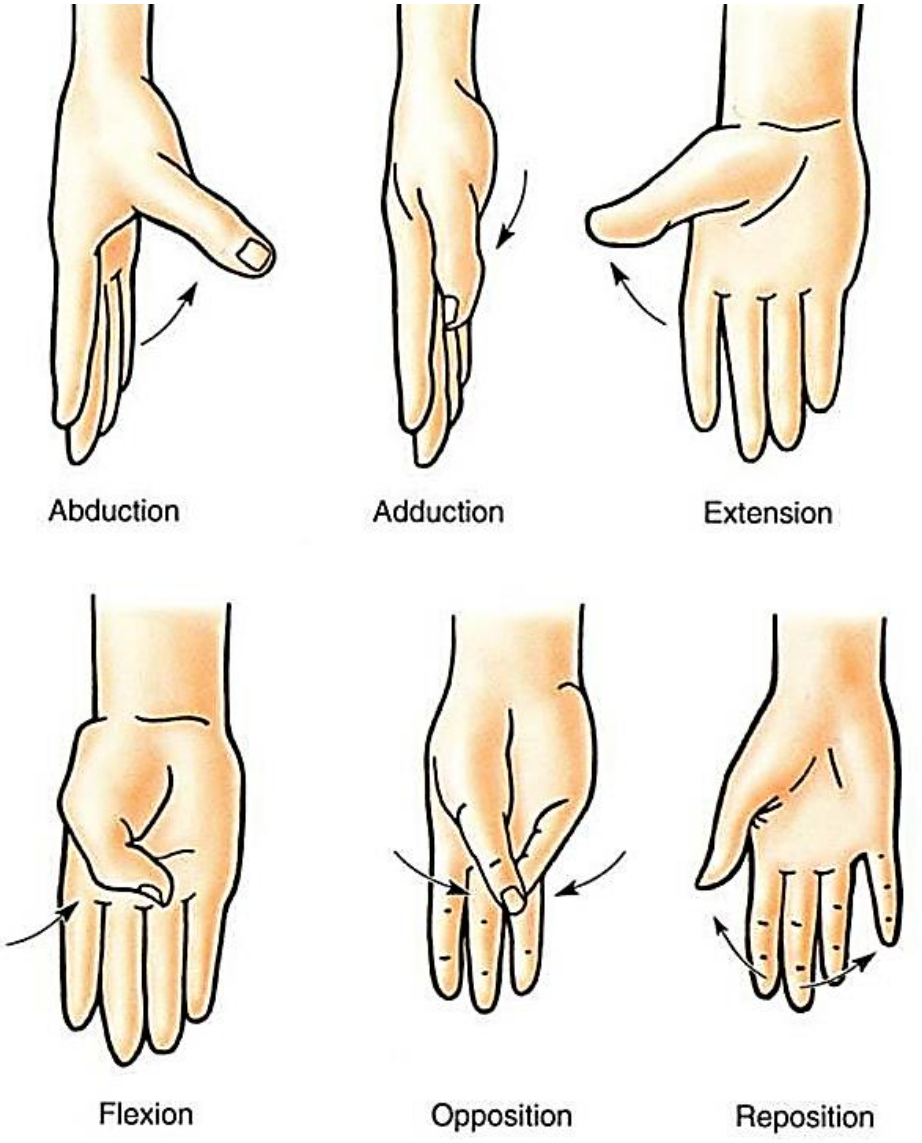

Figure 2.3: Movement of the thumb [47]

illustrated in Figure 2.2. In addition, a basal joint of the thumb, which connects the metacarpal of the thumb and trapezium of carpals, creates the following movements: the palmar abduction and adduction, radial abduction and adduction, opposition, and reposition. Radial abduction and adduction are also known as extension and flexion as depicted in Figure 2.3 [47].

2.2 Taxonomy of Human Grasp Types

As an end part of an arm, a hand is an essential part of the upper limb to perform ADL. There are different activities and components of the ADL with hands where grasping is the essential basic motion that is frequently performed for ADL throughout a day. Ranging from medicine and rehabilitation to robotics and manipulators, understanding a taxonomy of grasps to find common patterns was recognized as an important study to be practiced. Therefore, grasping became one of the numerous human studies to focus, and a number of researchers have studied to organize a taxonomy of human grasp types [48]–[52].

Depending on the authors, each paper claimed different number of grasps that he or she captured and was able to categorize. In 1980, Kamakura defined 14 patterns of object grasping [52]. While studying grasping patterns with 98 objects, seven subjects participated in the study. Besides the quantity of the patterns, the author found another interesting result. Though same objects were used, the subjects sometimes grasped objects using different patterns. Therefore, some of the patterns could not be justified for all population. In recent study, Feix compared 14 publications and found 147 grasp examples. Out of those examples, 45 different grasp types were detected, but then it was further classified into 33 valid grasp types. Considering similar properties of the grasps, Feix also expressed the possibility of merging grasps to reduce it down to 17 grasps [50]. More recently, Feix compared 22 publications and found 211 relevant grasp examples. After the review, Feix was able to categorize them into 47 different grasp types [48]. However, he was again able to reduce them into 17 grasps by merging the similar grasps

as one type. Figure 2.4 depicts those 17 grasp types, and each cell represent each grasp type.

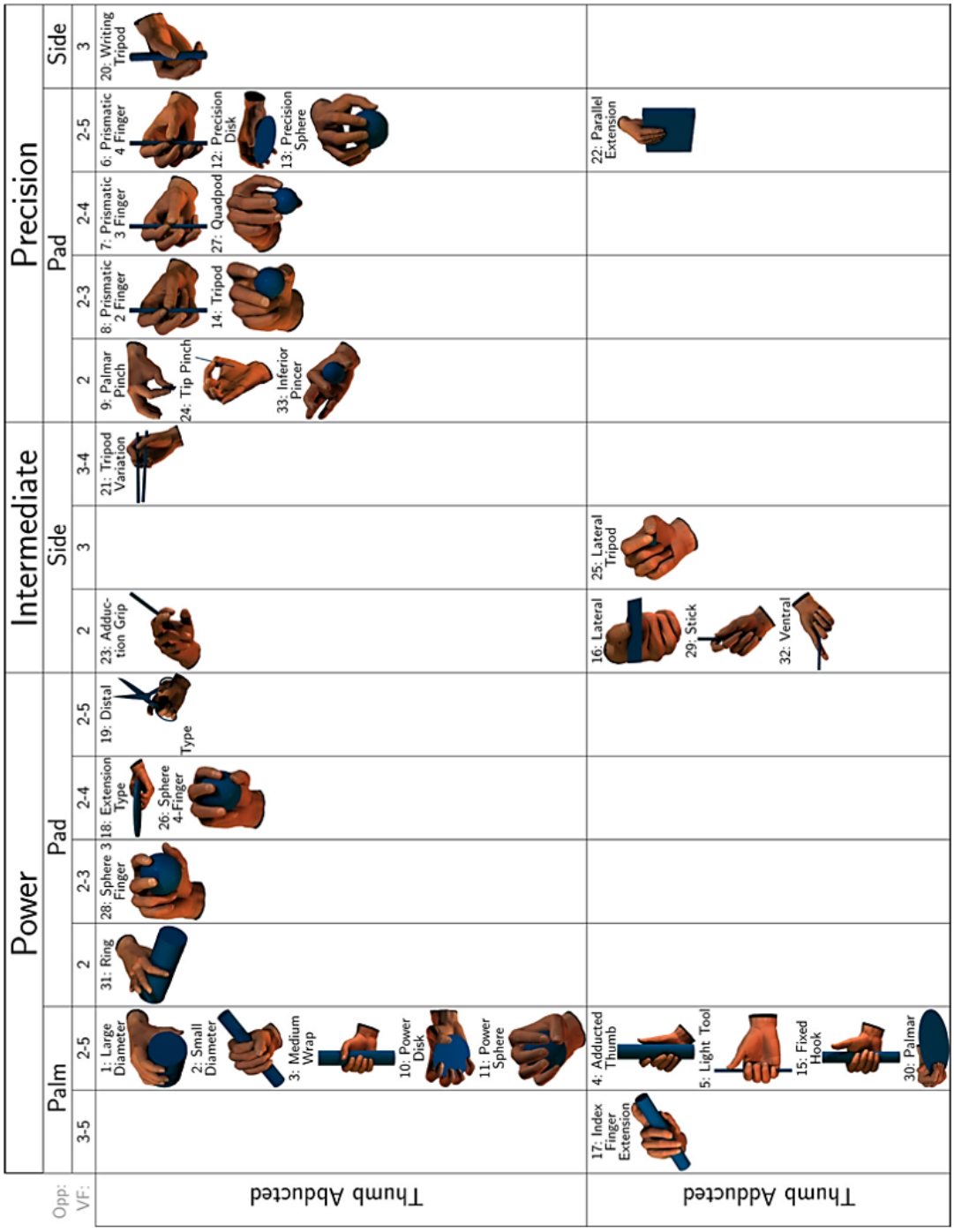

Figure 2.4: Grasp taxonomy showing 17 different grasp types [48]

Despite all the differences between the publications, the authors agreed to use three common categories: power, intermediate, and precision grasps [48]–[52]. Review of different grasp types showed that power and precision grasps were more common than intermediate grasps. When fingers wrapped around the objects, and the thumb is placed against it to support, then this grasp is considered to be the power grasp. In an agreement, wrapping a cylindrical or sphere objects with fingers are categorized in the power grasp in Figure 2.4. Often, the palm is also in contact with objects during the power grasps. Among those power grasps, when the thumb is adducted and does not necessarily assist grasp, but the object is secured by the palm instead, this grasp is called the palmar grasp. When the palm is not involved, an entire pad of finger was often involved in the power grasp. For ring grasp, pads of two fingers, as well as the webbing of the hand, were in contact with the object.

Similarly, a pinch grasp also involves two fingers, but a noticeable difference between the pinch grasp and ring grasp is the contact surfaces. While entire pads of two fingers and the webbing of the hand were in contact with the object for the ring grasp, pinch grasp only used pads of fingertips. Equivalently, the grasps that involved the fingertip contact surfaces were categorized as precision grasp. Theses precision grasps were generally used to hold smaller objects compared to the power grasps.

Following the majority of literature, some grasps were classified as precision grasp when multiple works of literature classified that grasp either as precision or intermediate grasp. However, when such a grasp was classified either as power, precision or intermediate grasp, and if the majority of literature agreed it is in between, that grasp was considered intermediate grasp. The lateral grasp was classified differently in multiple

pieces of literature, but it was classified either as power, precision or intermediate grasp meaning that it takes an intermediate stage between power and precision [48]. Therefore, it was classified as intermediate grasp in Figure 2.4.

Due to the size, the grasps illustrated in Figure 2.4 was reduced in size. To provide a higher quality figure with details, an enlarged figure is included in Appendix A.

2.3 Motor Function Impairment

A loss of hand and arm motor functions is often caused by physical injury or illness in individuals of any age. Illnesses that limit ADL of patients include metabolic bone diseases, strokes, cerebral palsy, neuromuscular disorders, brain injury, spinal cord injury, neuropathy, and arthritis. When the patients survive the illnesses and injuries, multiple tests are regularly performed on the patients to exam the condition of the aftereffects. One of the physical exams that is employed on the patients is called the Modified Ashworth Scale (MAS). It is a clinical scale system rated on a 0-5 scale to

Table 1: MAS for Grading Spasticity [26]

Grade	Description
0	No increase in muscle tone
1	Slight increase in muscle tone, manifested by a catch and release, or by minimal resistance at the end of the ROM when the affected part(s) is moved in flexion or extension
2	Slight increase in muscle tone, manifested by a catch, followed by minimal resistance throughout the remainder (less than half) of the ROM
3	More marked increase in muscle tone through most of ROM, but affected part(s) easily moved
4	Considerable increase in muscle tone, passive movement difficult
5	Affected part(s) rigid in flexion or extension

measure muscle spasticity [12], [26], [53]. It may be referred to as muscle strength testing, motor testing, muscle strength grading, or similar synonyms [54]. While Grade 0 represents complete loss of motor function, slight muscle activation, such as a twitch, is considered as Grade 1. Through the rehabilitation, when the patients recover more ROM, their grades will increase accordingly. Ultimately, the patients aim to reach Grade 5 by achieving full ROM. More details are presented in Table 1.

2.4 Input Control Method

Different exoskeleton systems have covered many of the possible choices of the input control method, such as buttons and switches [35]–[37], EMG and EEG [39], [40], [55]–[58], joint angles [59], or more [6]. It is difficult to say which method is better than the other is as each input control method has its advantages and drawbacks.

For a variety of reasons, buttons and switches are widely used. As a traditional input control method, many studies used buttons and switches for its simplicity. To receive the input in a sophisticated way, EMG and EEG sensors were implemented as one of the input control methods. The use of EMG sensor has increased the potential of powered prostheses, and the use of EEG sensor has broadened the range of users as it monitored electrical activity of the brain. However, even after EMG and EEG sensors earned its popularity, some scientists stayed with buttons and switches due to the drawbacks of EMG and EEG sensors. Most known drawbacks of the EMG and EEG sensors are crosstalk between signals of neighboring muscles, the process of applying the sensors on the skin, muscle activation levels, and interference from the electrical supply [35], [41].

Measuring joint angles of a wrist to activate Exo-Glove [59] was a quite unique method. As detecting a wrist motion was easy and intuitive, detecting intentions of the user would have a high rate of success. However, though it seemed like an ensuring way to control the exoskeleton, the users would have to keep their wrist flexed during lifting or relocating the object. Therefore, a practicability of using this system for ADL was questionable. Moreover, the users who have no motor function on the wrist would not be able to use it.

Deviating from these traditional input control methods, a new method of detecting the user's intention is desired in this thesis.

2.5 Slip Detection Method

During object manipulation activities, such as grasping, the tactile afferents sense the interaction between the hand and objects and convey signals to the brain. The signals can be the physical properties of the object and the transformation of soft tissues of the hand. With this information, the brain implements action-phase controllers, which predicts the activities and tailor next move by generating motor commands to attain goals of activities [60]. In a daily life, when the tactile afferents sense the slippage after the grasp, the brain will predict a drop and tailor firmer grasp instantly to prevent it.

In a similar way, the robot can detect slip and signal the actuation module to react to the condition during the object manipulation, as shown in Figure 2.5. Outside of the realm of robotic exoskeletons, there has been far more extensive research into intelligent grasping as applied to robotic manipulators and prosthetics. Through the research, the detection of slippage was found to be one of the key elements of intelligent grasping, and

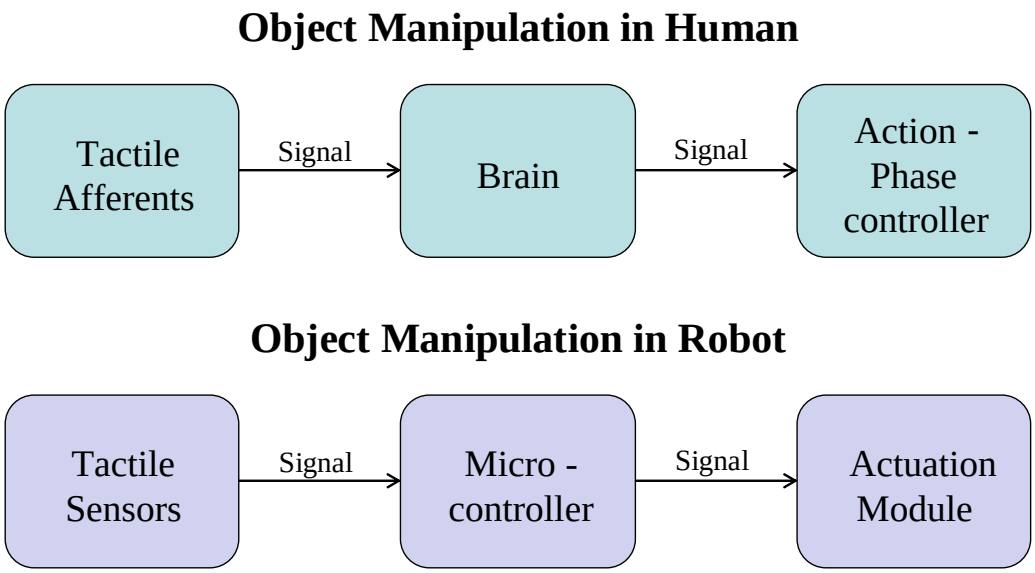

Figure 2.5: Comparison between the object manipulation process in human and robot

by utilizing this grasping process of human, many studies applied slip detection technique to their systems. An approach to detecting the slippage often utilized the tactile sensor [18]–[20], [61]–[67], which used vibration or force, but another method such as an optical tracking was also used in the past [21].

2.5.1 Slip Detection Sensors

Multi-Fingered End Effector with the Photoelastic Slip and Force Sensor [19]

When a robotic end effector is operated to handle the object, it is important to monitor the gripping force to prevent excessive gripping force to the object. The authors proposed the use of tactile sensor to detect the contact parameters at the finger-object interface. To detect applied force as well as object slippage, the photoelastic material was utilized, and

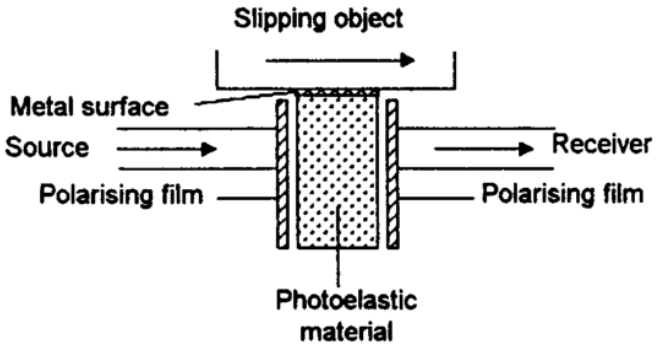

Figure 2.6: Design outline of the photoelastic slip and force sensor [19]

a sensor called ‘photoelastic slip and force sensor’ was designed and proposed in the paper. The proposed design of the photoelastic slip and force sensor is illustrated in Figure 2.6.

As a sensor was developed based on photoelasticity, the sensor’s operation was based on the principle of a photoelastic material. When stress is applied on the photoelastic material, the angle of polarization changes accordingly, and a change in light intensity can also be noticed when polarized light passes through the photoelastic material.

During the experiment, the metal strip between the object and the sensor created the vibration when the object slipped, and this vibration indicated the magnitude of the slip. As the object was slipping while it was pushed against the sensor, the sensor was able to read both the applied force and the cyclic slip signal, as shown in figure 2.7.

Though only touch and a minimum applied force could have been measured for this paper, the signal illustrated in Figure 2.7 clearly showed a drop in the magnitude when the object slipped.

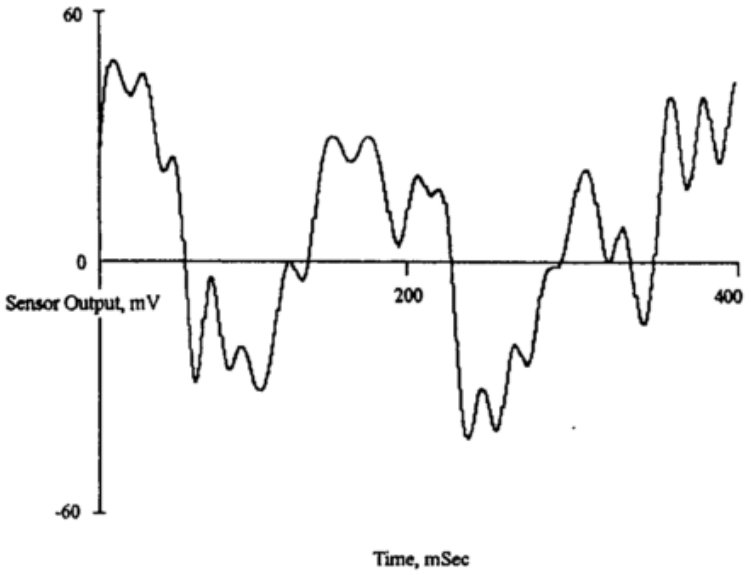

Figure 2.7: Slip signal from the sensor [19]

Integrated Piezoelectric Vibration Tactile Sensors [64]

The authors of this research emphasized important points to consider in development process of tactile sensors: "(1) The tactile sensor needs a high sensitivity to perform with dexterity like human, (2) The tactile sensor needs a wide measurement range to bring a great deal of power and a decay resistance to withstand it, (3) The tactile sensor needs a deformable feature to become flexible like human skin and curved surface shapes of objects, and (4) The tactile sensor needs small sizes and low costs to use various situations widely and easily." In addition, the authors also focused on the difference of forces under the static and dynamic friction. As described in Figure 2.8, a static friction force is greater than a dynamic friction force. Therefore, this change in the force will affect the resultant force and cause the periodic contact loss.

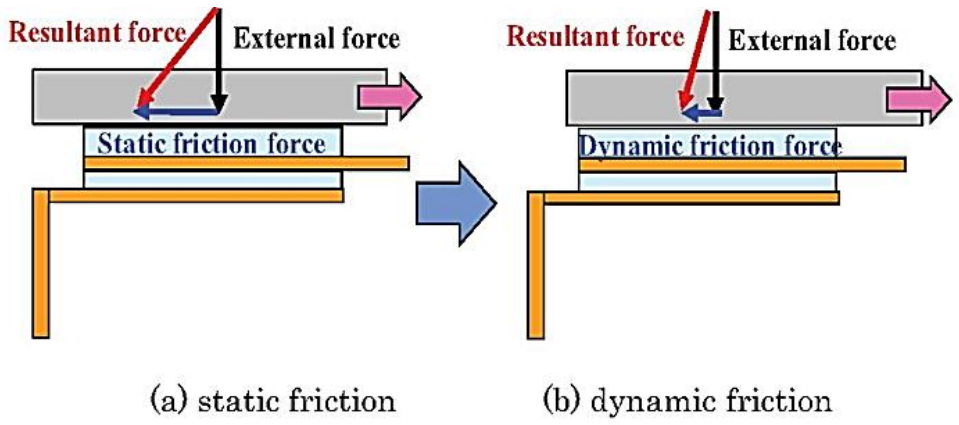

Figure 2.8: Forces relationship during slipping on a sensor element [64]

Implementing this concept, the authors aimed to detect the change of stress as an output and proposed the design of piezoelectric vibration tactile sensor. As a result, the authors validated the possibility of detecting a state of impaction and slipping via the piezoelectric vibration tactile sensor through the experiment. When the force applied to a sensor caused slip representing the transition from static friction force to dynamic friction force, the output voltage suddenly dropped, as shown in Figure 2.9.

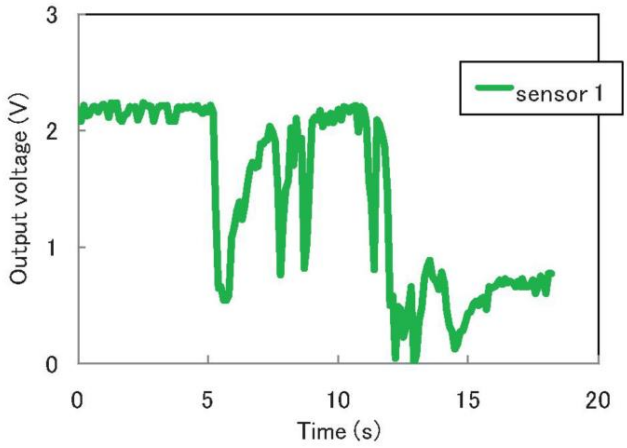

Figure 2.9: Relationship between sensor output and time [64]

The authors concluded the paper stating that the tactile sensor can be mounted on a robot gripper to control the frictional forces effectively.

2.5.2 Manipulators with Slip Detection

Robotic Hand Model with Slip Detection [20]

To further extend the study of slip detection, sensors were applied on the

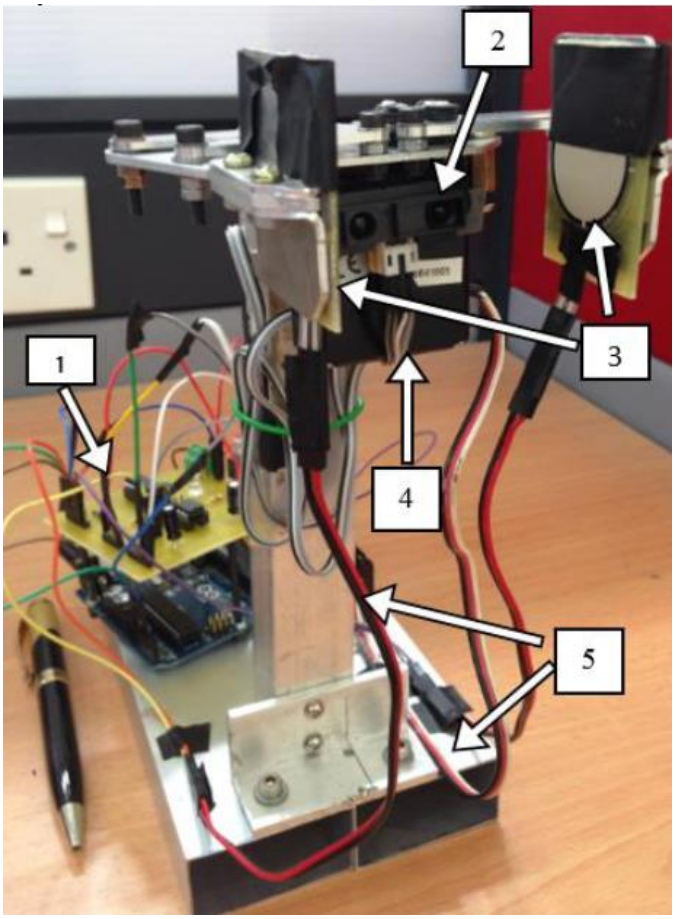

Figure 2.10: Robotic hand model with 1) printed circuit board, microcontroller, and power supply, 2) infrared sensor, 3) pressure sensors, 4) DC servomotor, and 5) robotic hand structure [20]

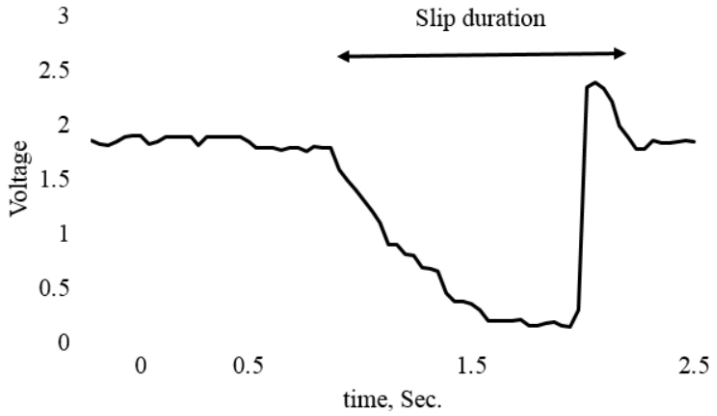

Figure 2.11: Signal response from pressure sensor during an object slipping [20]

manipulators and the data collected via the sensors were analyzed. The prototype shown in the Figure 2.10 is the proposed robotic hand model, which has pressure sensors and DC servomotor. Similar to the results described previously, a signal data collected from a robotic hand model with slip detection illustrated the comparable result. In addition, the authors programmed the microcontroller to control the consequences of the slipping situation.

In the experiment, pressure sensor, also known as a force-sensitive resistor (FSR), has been used to measure the force. As the object started to slip, the magnitude of the voltage decreased, and this pattern was in agreement with the result of both photoelectric slip and force sensor and integrated piezoelectric vibration tactile sensors. The result of the experiment is illustrated in Figure 2.11.

Flexible Fingers Gripper [22]

The authors of this paper realized the importance of tactile sensing due to its improved interaction capabilities such as grasping and manipulation of object related to

touching, detecting surfaces, and collisions. To demonstrate the advantage of flexible fingers gripper in slip detection, the authors proposed a simple and low-cost sensor, which is based on flexible beam deformation. This flexible fingers gripper consists of two symmetric flexible beams as fingers and a DC motor with worm gear for actuation, which creates an underactuated system. Design of the flexible fingers gripper is shown in Figure 2.12, and the Figure 2.13 illustrates how the flexible beams operate to hold an object. In the experiment, a flat surfaced steel plate was used as an object, and this object was initially grabbed before slipping test was conducted. The strain gauges were applied on

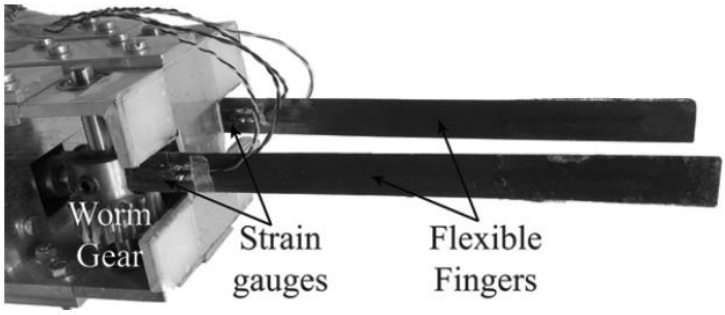

Figure 2.12: Gripper Parts [22]

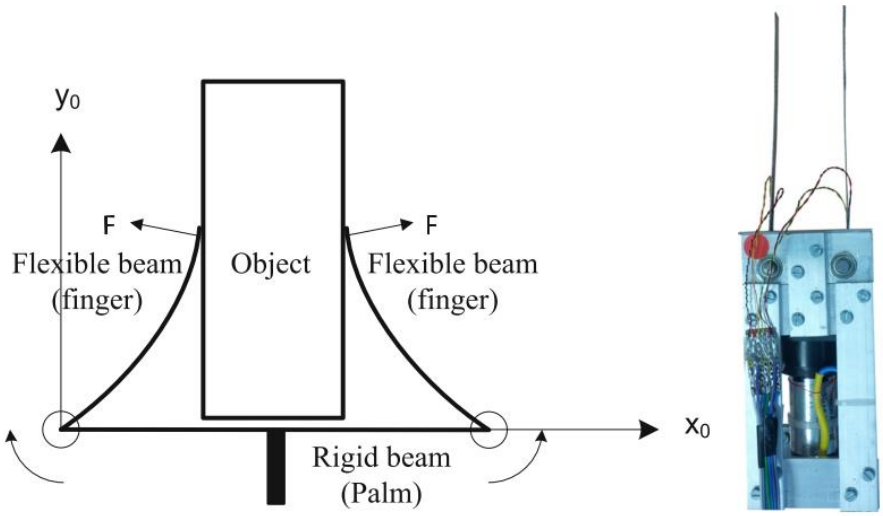

Figure 2.13: Gripper scheme and flexible gripper prototype [22]

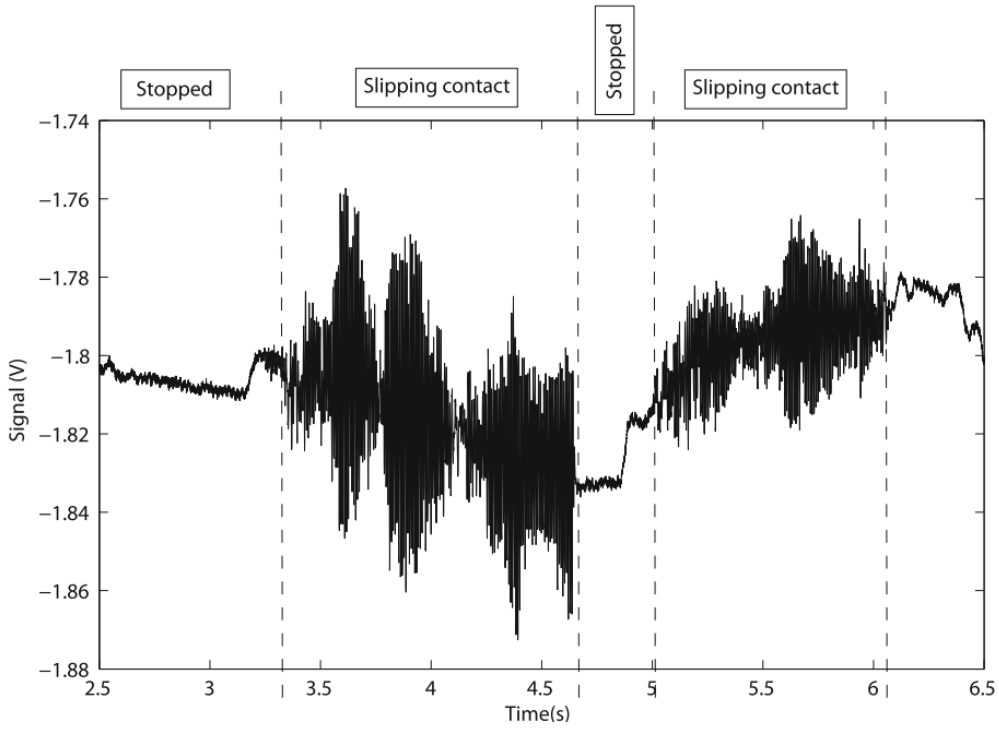

Figure 2.14: Gauge signal of single finger as a function of time [22]

the beams to measure the gauge signal. When the object remained static after the initial grasp, the signal was smooth and almost constant as shown in Figure 2.14. As soon as the object started to slip, a disturbance in signal was recorded. This disturbance represents the vibration caused by the slip, and this information supports a better understanding of the occurrence during grasps, potentially improving manipulation.

2.5.3 Prosthetic Hand with Slip Detection

Adaptive Sliding Mode Control for Prosthetic Hands [16]

As a problem statement, the authors pointed out the drawbacks of using EMG signals. As the EMG signal is fairly noisy, filters with a very slow time constant was used, but

this caused delay in time. Due to the delay, the amputee's intention was not delivered in time correctly, and the object was dropped futilely. To detect and prevent slip, two robust adaptive sliding mode controllers were designed and proposed in the paper, and three slip prevention controllers were evaluated as follows: a sliding mode slip prevention (SMSP) controller, integral sliding mode slip prevention (ISMSP) controller, and proportional derivative (PD) shear force feedback slip prevention controller.

Considering variety of the objects that human grasp every day, it is difficult to determine the coefficient of friction before slip occurs. The first two controllers, SMSP and ISMSP, do not require any knowledge of the coefficient of friction, and the slip will be detected purely by processing the shear force derivative. Unlike the previous study, which utilized low-pass filter, the authors proposed to use band-pass filter on the shear force derivative to amplify vibrations. The difference between two controllers was in the control of the grip force increments. While the grip force was smoothly increased for the ISMSP, discrete predetermined grip forces were applied to SMSP. DP in this research

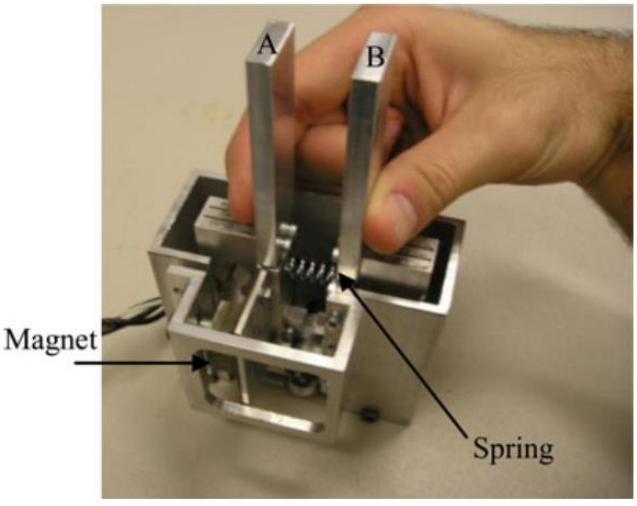

Figure 2.15: Design and components of the manipulandum [16]

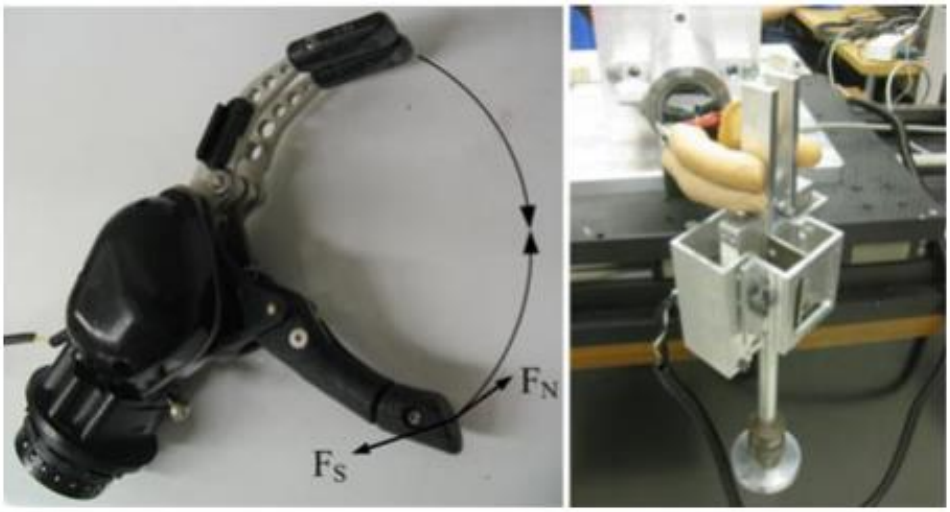

(a) (b)

Figure 2.16: (a) Motion Control Hand: The normal force direction denoted by FN, and the shear direction denoted by FS (b) Motion Control Hand with finger cover grabbing the manipulandum [16]

represented commercially available scheme that has no slip detection and rather increase the grip force proportionally to the measured shear forces.

For the experiment, a manipulandum was designed and built to contain the springs, magnets, and an A1321 Hall effect sensor as shown in Figure 2.15. The Hall effect sensor is applied on the bottom of the manipulandum. It is calibrated to indicate the initial distance between two bars, A and B. Along with load cells, this manipulandum was used to measure the deformation and force. The motion control hand used in the experiment and the experiment set up is depicted in Figure 2.16.

As a result, the ISMSP controller was found to be the best among three controllers due to its advantageous control in smooth increase of the grip force. This controller also resulted the smallest amount of deformation.

Robotic arm with BioTac sensors [18]

Relying on tactile feedback including contact force estimation, human can detect slip when it occurs during the object gripping and lifting events. Using biomimetic sensors, the authors proposed contact-based techniques to evaluate tactile properties, which can be used to detect manipulation events, such as slip. The Barrett arm/hand system equipped with biomimetic tactile sensors, BioTacs, was utilized in this research. Furthermore, machine learning, such as Artificial Neural Networks and Gaussian Mixture Models, are employed to learn the force map.

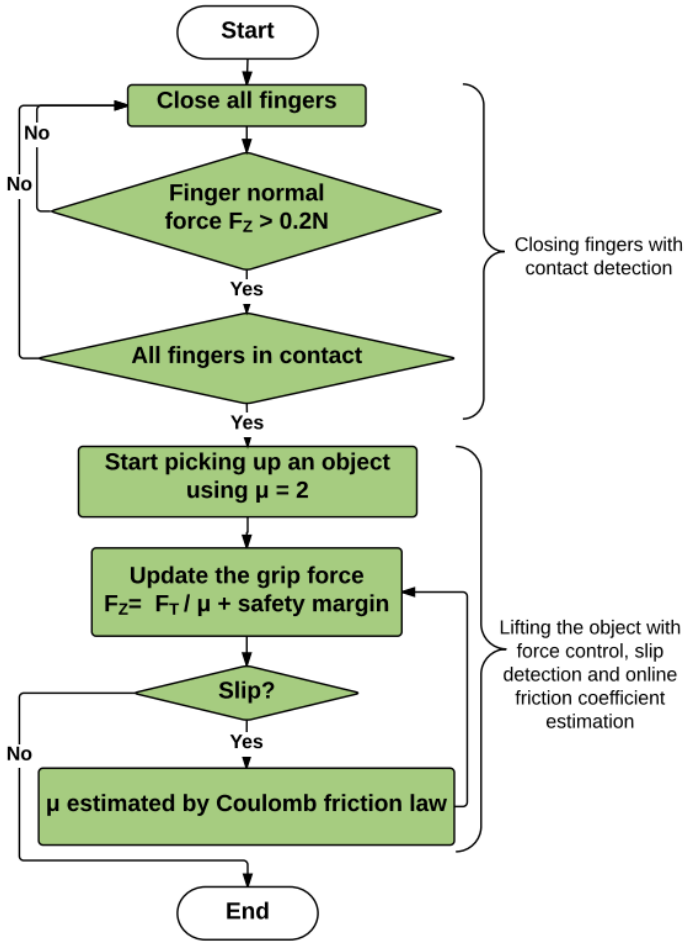

Figure 2.17: Control diagram of the grip controller [18]

The main goal of this research was to develop a grip controller that could control the grip force appropriately without damaging or dropping the fragile objects. The grip controller was designed based on two main stages of grip initiation and object lifting as shown in Figure 2.17. Reviewing the result of an example run of the grip controller

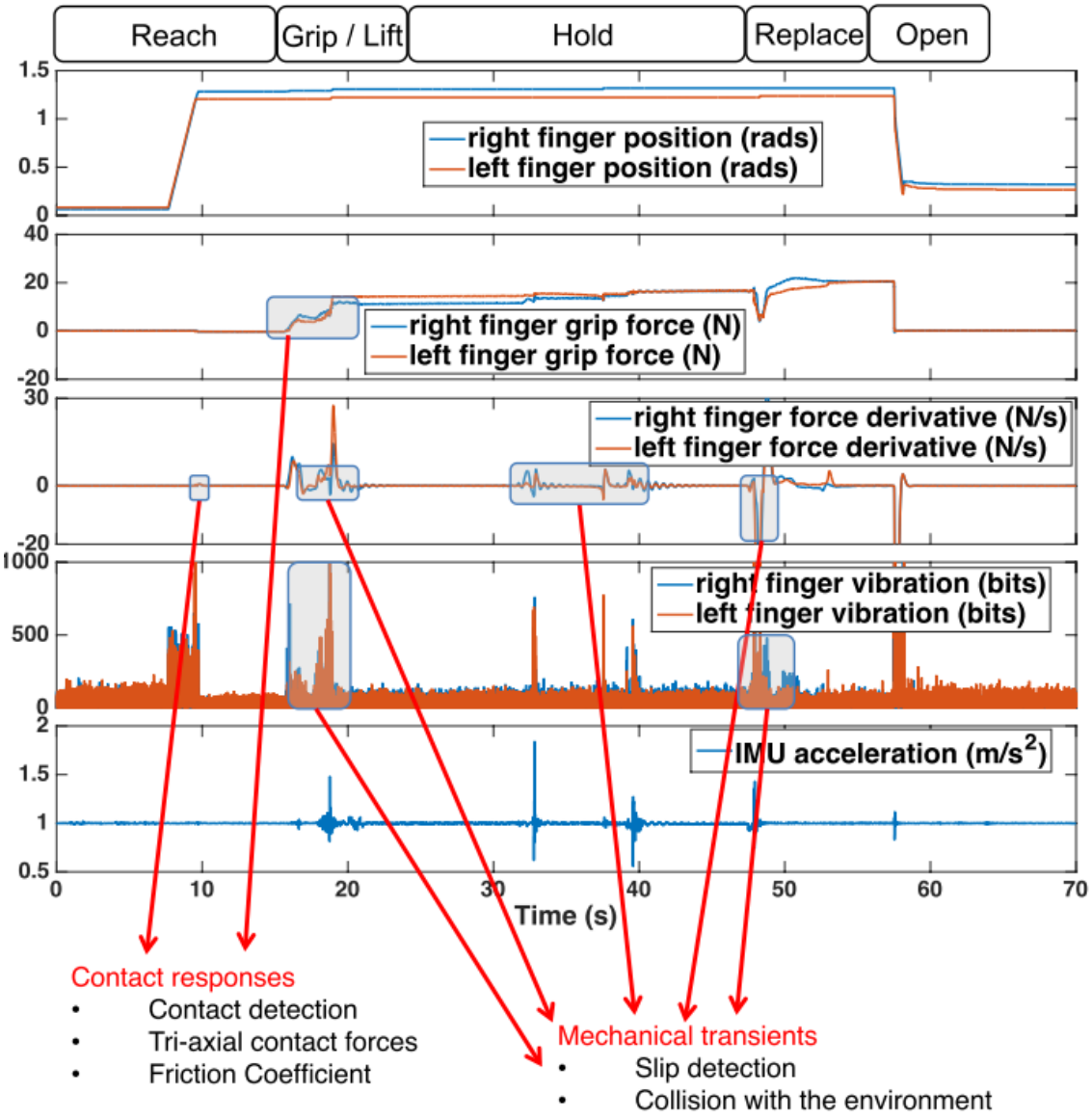

Figure 2.18: An example run of the grip controller that includes all of the grasping phases [18]

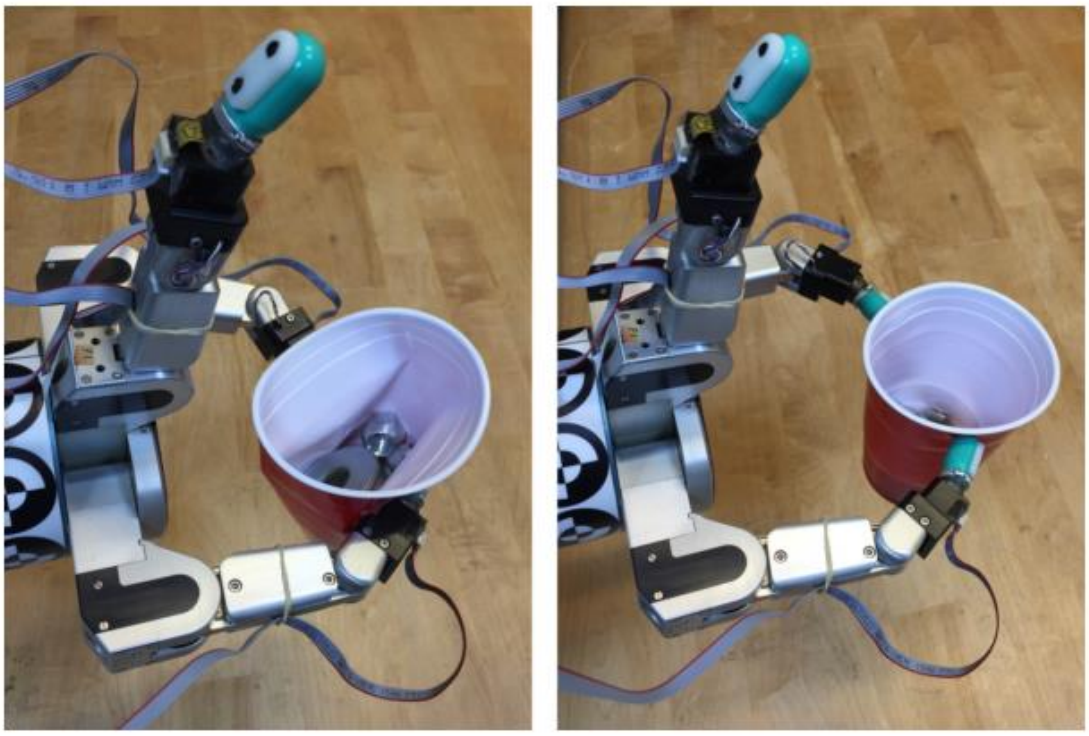

(a) (b)

Figure 2.19: Robotic arm grasping a fragile object (a) using a standard position controller, and (b) using the proposed force grip controller [18]

below in Figure 2.18, familiar patterns were noticed. The highlighted mechanical transients of slip detection had a similar pattern as the slip patterns illustrated in the previous subsections, and they agreed. After slip detection was successfully verified, the grip controller was able to apply appropriate force to a fragile object as shown in Figure 2.19 (b) while the standard position controller, Figure 2.19 (a) failed to protect the fragile object.

Embedded Optical Sensor in Prosthetic Hands [21]

Unlike others, this research implemented an optical sensor to monitor slip. The optical sensor that was used in this study was extracted from a Logitech SBF-96 Optical

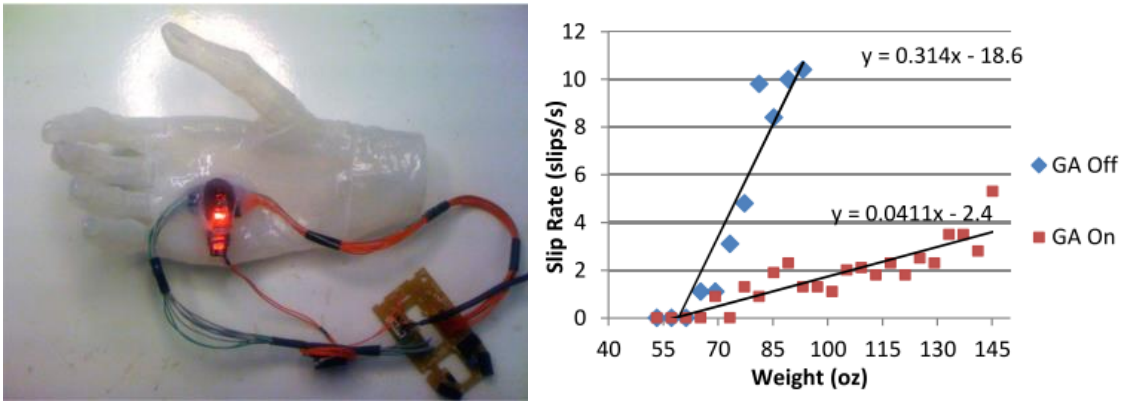

(a) (b)

Figure 2.20: (a) Embedded optical sensor in silicone glove (b) Slip rate comparison for two conditions: grip adjustment (GA) on vs off [21]

Wheel Mouse, and a silicon glove was fabricated to fit over the i-LIMB prosthetic hand. Once the silicon glove was ready, the optical sensor was embedded on the palm side of the glove. Using a closed-loop algorithm, the sensor read the changes in x and y coordinates, detecting the slip. Following the slip detection, a grip adjustment algorithm was also applied. Through the experiment, the authors found that using slip detection and grip adjustment systems decreased the slip rate. Therefore, this result validated their prosthetic hand with optical sensor and control system with slip detection. Figure 2.20 (a) shows the embedded optical sensor in silicone glove while Figure 2.20 (b) presents the different slip rate between two conditions: grip adjustment on and grip adjustment off.

2.5.4 Other Studies Based on the Grip Forces

Tangential Torque Effects on the Control of Grip Forces [68]

Unlike other papers, the authors of this paper studied variety of forces related to the slip. One of the aims was to examine how subjects adapt their normal force to the slip

force during grasp stability experiment. The authors described slip force as normal force at the point of incipient frictional slip. After the relationship between the slip force and the tangential force was studied, the relationship between slip and normal forces was found to be nearly linear as a result. Under zero tangential force condition, the sensor experienced a series of rotate-and-hold trials. Though the normal force was fairly constant during the grab and hold position, the normal force showed sharp, brief pulses as the normal force decreased enough to cause the rotation. While the normal force was acting like a braking force, this pulse pattern shown in the Figure 2.21 below represents the slip occurrence. This phenomenon was also possible because there was small contact.

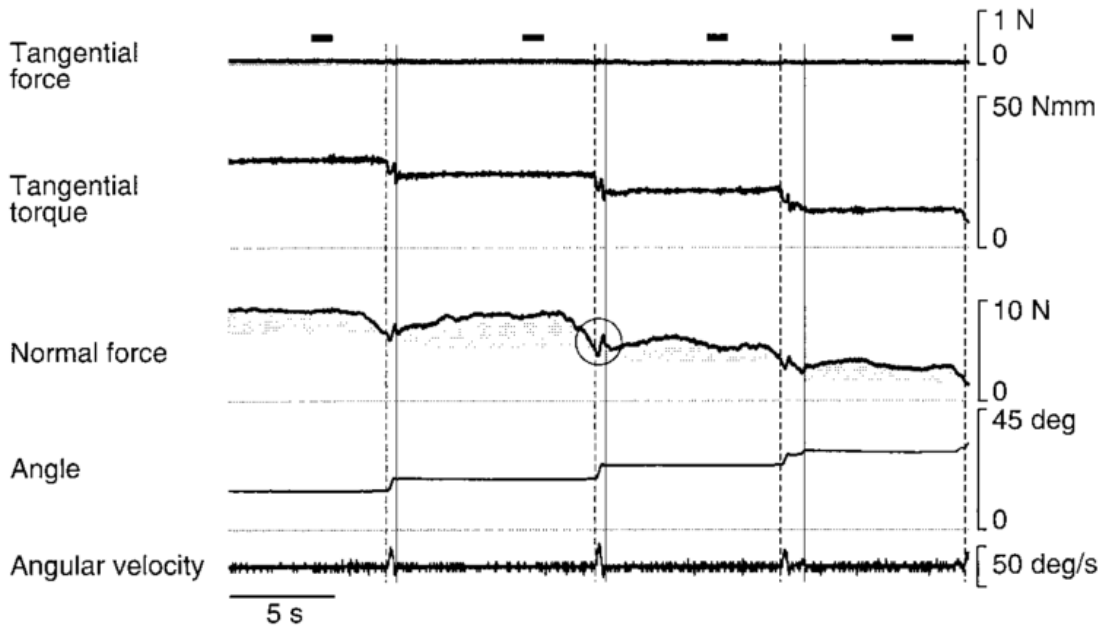

Figure 2.21: Series of rotate-and-hold trials from a single subject under the 0 tangential force condition

2.6 Conclusion

The fundamental knowledge of the human hand including the anatomy, functions, and taxonomy of human grasp types was discussed in this chapter followed by the input control method and slip detection method used on various robotic hand manipulators and prosthetics. Necessity of implementing various grasps within the mechanical limits of the intelligent sensing and force-feedback exoskeleton robotic (iSAFER) glove and feasibility of the tactile sensors as a slip detector was inferred from the information reviewed in this chapter. In addition, as some publications claimed different force directions to detect the slip, verifying the multi-directional responses of a new sensor, which will be proposed in chapter 5, is required.

CHAPTER 3

PROTOTYPE REVIEW & PROBLEM STATEMENT

The Sensing and Force-feedback Robotic (SAFER) glove was designed and experimentally validated in previous work as an assistive and rehabilitative aid [15], [34], [69]–[76]. The SAFER glove, shown in Figure 3.1, consists of articulated linkages that each drive a finger through a cable routing system that ultimately are actuated by miniature DC motors. Antagonistic routing provides full controllability of the system. Following sections will further describe the mechanical design and system of the SAFER glove and the motivation and design evolution of the original system.

After a review of the prototype, describing the design and function of both mechanical and electrical systems of the SAFER glove, the design problems that need to be addressed are further discussed in the later sections of this chapter.

3.1 Mechanical Design and System of SAFER Glove

Starting from a two-finger glove [77], a five-fingered haptic glove was developed as a follow-up prototype. The glove prototype was designed to fit on a bare hand, and the thimbles at the end of the linkages were used to connect each finger. It was also designed to meet its goals such as being a lightweight and portable glove as well as a sensing and actuating system. The mechanical design of each finger of the SAFER glove consists of three main parts: three-link exoskeleton, an actuator unit, and two actuation cables as shown in Figure 3.2. Coupling the Distal Interphalangeal (DIP), Metacarpophalangeal

(MCP), and Proximal Interphalangeal (PIP) joints of each finger with one actuator module resulted in an under actuated system while lightening and simplifying the whole glove. The main reason for choosing cable transmission was due to its compactness, lightweight, cost effectiveness, and unrestrictive nature of the actuator location. The cables were attached to the motor spool and routed around the pulleys representing each joint. A two-cable pull-pull transmission is used, and it was actuated by a DC motor,

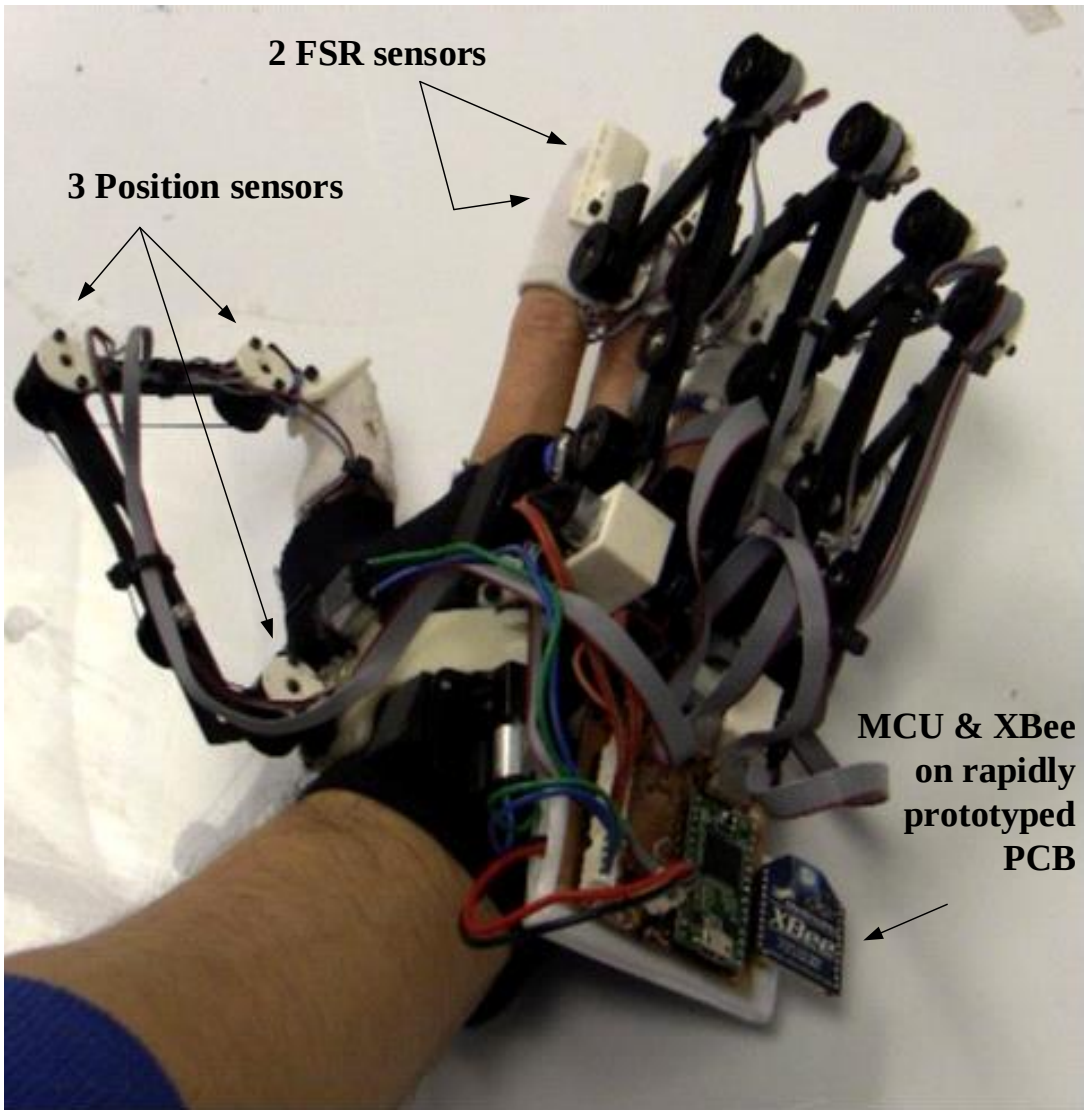

Figure 3.1: Original components of the SAFER glove [23]

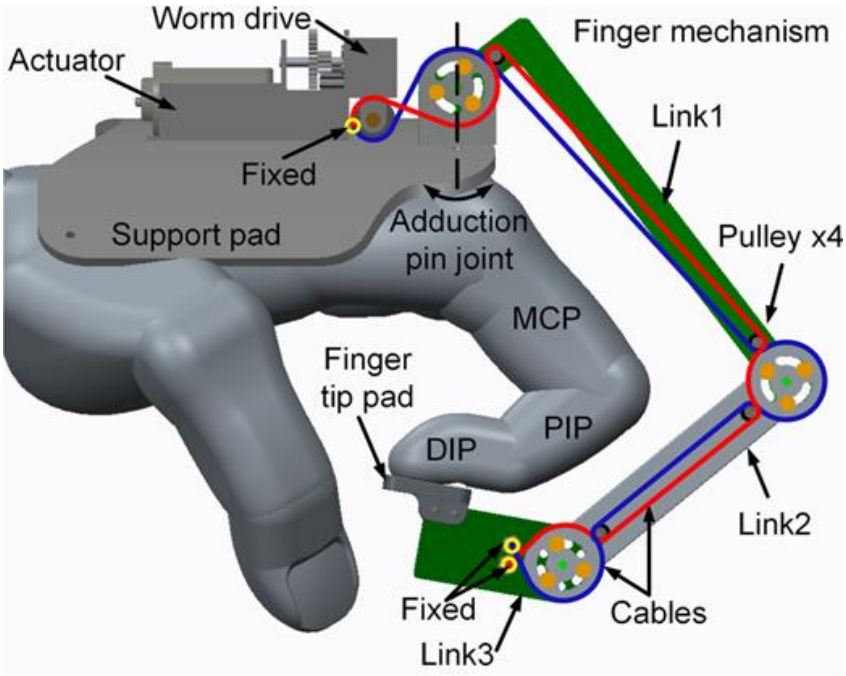

Figure 3.2: CAD model of the index finger mechanism of the glove showing the cable transmission model [19]

which was placed on the dorsum of the hand.

The under actuated multi-link finger mechanism produces flexion and extension at the proximal joints, and the glove mechanism configuration can be adjusted in order to accommodate different finger lengths. Through optimization, the optimal link length for a multi-link finger mechanism with bidirectional tendon actuation was modeled considering workspace size, force transmission ratio, and mechanical design parameters [71].

3.2 Electrical Design and System of SAFER Glove

Each finger has two FSRs on both the pad and the fingernail of the fingertip thimble of SAFER to measure force applied to fingers and three potentiometers on each joint to

calculate the fingertip position [34]. The actuators, controller, and power supply are mounted upon a lightweight platform that is worn on the dorsum of the hand. The self-contained nature of the system lends a high degree of portability to the system.

Microcontroller unit (MCU) of Teensy 3.0 was used on SAFER glove and XBee for the wireless communication. This wireless communication capability with a PC has increased portability. Figure 3.1 shows the SAFER glove with the original components.

3.3 Proposed Rehabilitation Learning System

Along with the proposed mechanical and electrical design of the SAFER glove, a preliminary grasping learning and rehabilitation system was proposed [73], [75]. Before

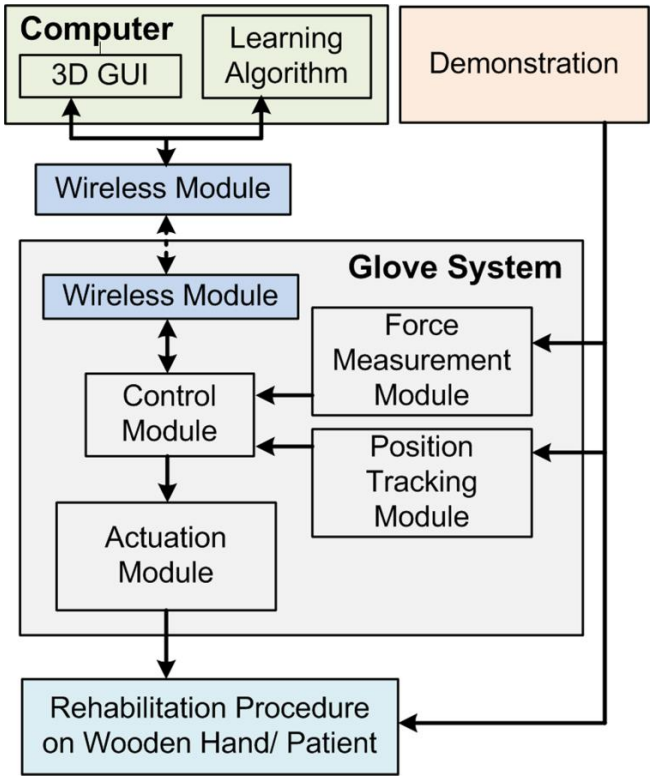

Figure 3.3: Rehabilitation learning system overview [73]

the rehabilitation, this system measured and learned the patterns of grasping motion from the grasping demonstration of healthy human subjects. With measured force and position data, the system was also capable of following the pattern of grasping to provide rehabilitation service to the user. The system overview, shown in Figure 3.3, includes four components: the demonstration procedure of healthy subjects, the SAFER glove system, the learning algorithm with a 3D GUI program, and the rehabilitation and assistive rehabilitation procedure.

3.4 Problems and Possible Improvements

Along with the literature review on several state-of-the-art examples and the slip detection in Chapter 2, the analysis of the prototype highlighted the areas that needed to be improved. Following sections further discusses the design problems that can be improved while presenting the goals of the newer version of the SAFER glove called an intelligent SAFER (iSAFER) glove.

Though the SAFER glove was compact, lightweight, and portable, a couple of problems existed to preserve its condition. The following subsections will present the details of each design issue of the SAFER glove and possible improvements.

3.4.1 Weak Joints

To achieve the lightest weight possible, most of the exoskeleton components are manufactured from 6061 aluminum. However, due to the aluminum's softness and the small profile of the linkages, the retaining ring grooves quickly wore out at the major joints. It was doubtful that replacing the joints with newly manufactured parts would

solve the root cause if the design stayed the same. A modified design of the joints was sought in order to make a more robust joint.

3.4.2 Fragile Force-Sensitive Resistive Sensor

The off-the-shelf product, FSR sensor, was used on SAFER glove. This FSR sensor had a 4 mm diameter active sensing area utilized to detect the force created between the finger and an object. Depending on the point where the force was applied on the finger, the FSR sensor would at times fail to detect the force if the application of force did not align properly with the sensor position.

At first, replacing the FSR sensor with a larger size of the same model was considered. However, the stiff plastic cover on the sensor limited the applicability to a fingertip. Even with the original, smaller sensor, a repetitive bending motion of the finger caused a tear in the sensor, requiring repetitive replacement. As the sensor gets bigger, the risk of damage increases. Therefore, higher risk and stiffness of the sensor on the fingertip rendered this option impractical.

As a result, a custom-made sensor that could accommodate the shape and size of a fingertip and was durable across multiple bending motions was required.

3.4.3 Glove and User Interface

Though the glove was equipped with a wireless communication system and was portable, it was still controlled by the computer input. Considering the feasibility of the glove and the case where a user may not have an access to a computer, a necessity of a better interface between the user and the glove seemed to exist.

By adding an infotainment service to the iSAFER system, the user could have an improved communication and understanding of the rehabilitation and assistance processes. Additionally, informing the users via a media such as screen could guide users through the steps of the rehabilitation without help of a caregiver or technician. In hopes of raising user's confidence, this infotainment service could further increase the independency.

3.4.4 Intelligent Object Grasping and Learning System

The previous SAFER glove system proposed a rehabilitation learning system. It measured and learned the patterns of grasping motion from the grasping demonstration of healthy human subjects. With measured force and position data, the system was also capable of following the pattern of grasping to provide rehabilitation service to the user.

To give various rehabilitation service with different types of grasps involving multiple objects with different shapes and sizes, the system would need to measure and record separate sets of demonstrations for each object. In addition, the force and position measurement of an object used in rehabilitation may not always work to grab and lift the object if the mass of the object changes as the static grip force increases due to the increase in mass [78]. For instance, one rigid plastic water bottle can be used as an example throughout the rehabilitation. However, if the amount of water in the bottle changes, increasing the weight of the bottle, the force data that was used previously to grab the water bottle may not be sufficient to support the weight of the bottle anymore. Therefore, instead of pre-measuring and pre-recording the demonstration data, an algorithm that will continuously measure the force-feedback data in real time to learn and

decide the next action to adapt new mass was desired. Furthermore, creating a system capable of intelligent object grasping initiated by detection of the user's intentions through motion amplification was also sought.

CHAPTER 4

PROTOTYPE IMPROVEMENT

In order to improve the stability, strength, sensing capabilities, and human-robot interface of the system, improvements and modifications were made to the previously described SAFER design, resulting in the iSAFER glove. Figure 4.1 below presents the

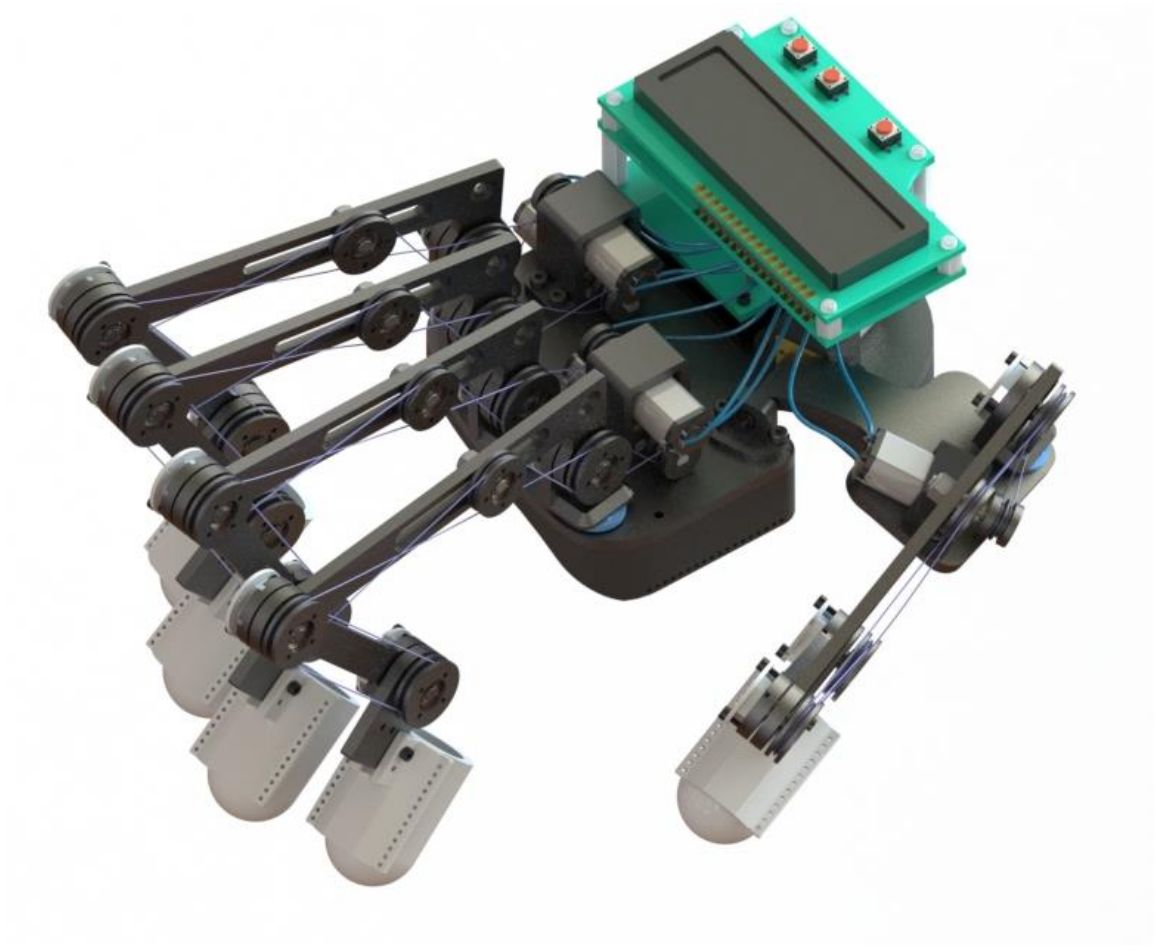

Figure 4.1: New 3D CAD model with updated components representing iSAFER glove

proposed design of the full hand exoskeleton. The following subsections will present the improvements and modifications made to SAFER with more details as some of the improvements and modifications are not visible in Figure 4.1.

4.1 Design of Stable and Robust Joints

To fix the weak spots of SAFER glove, a new joint was designed that would maintain the original functionality. Many options and designs were sought, but at the end, a robustness over a compact design was chosen to keep the joints stable. As a result, instead of the retaining ring with the groove on the outside of the shaft, a hole was drilled in the shaft after increasing the diameter of the shaft, and then the thread-locking screws were used with additional three-piece thrust ball bearings to keep the free rotation feature. The size of the flanged ball bearings and the three-piece thrust ball bearings were chosen accordingly.

Before the parts were custom manufactured and ordered, a CAD model was created to simulate the design to check the possibility and feasibility as shown in Figure 4.2. Primarily, the size of new components were applied and confirmed by the CAD model. In this process, the aluminum base was also modified to ensure the gap between the improved joints. Once the thickness of the total layers and the gap between the improved joints were verified as shown in Figure 4.2 (a), the original plastic platform was also modified to accommodate the changes in the design of the improved joints and the aluminum base. Though the improved joints were not as compact as the original design, as there was a thick plastic platform under the aluminum base that sits on the dorsum of the hand to match its curvature, the thickness of the improved joints caused no problem.

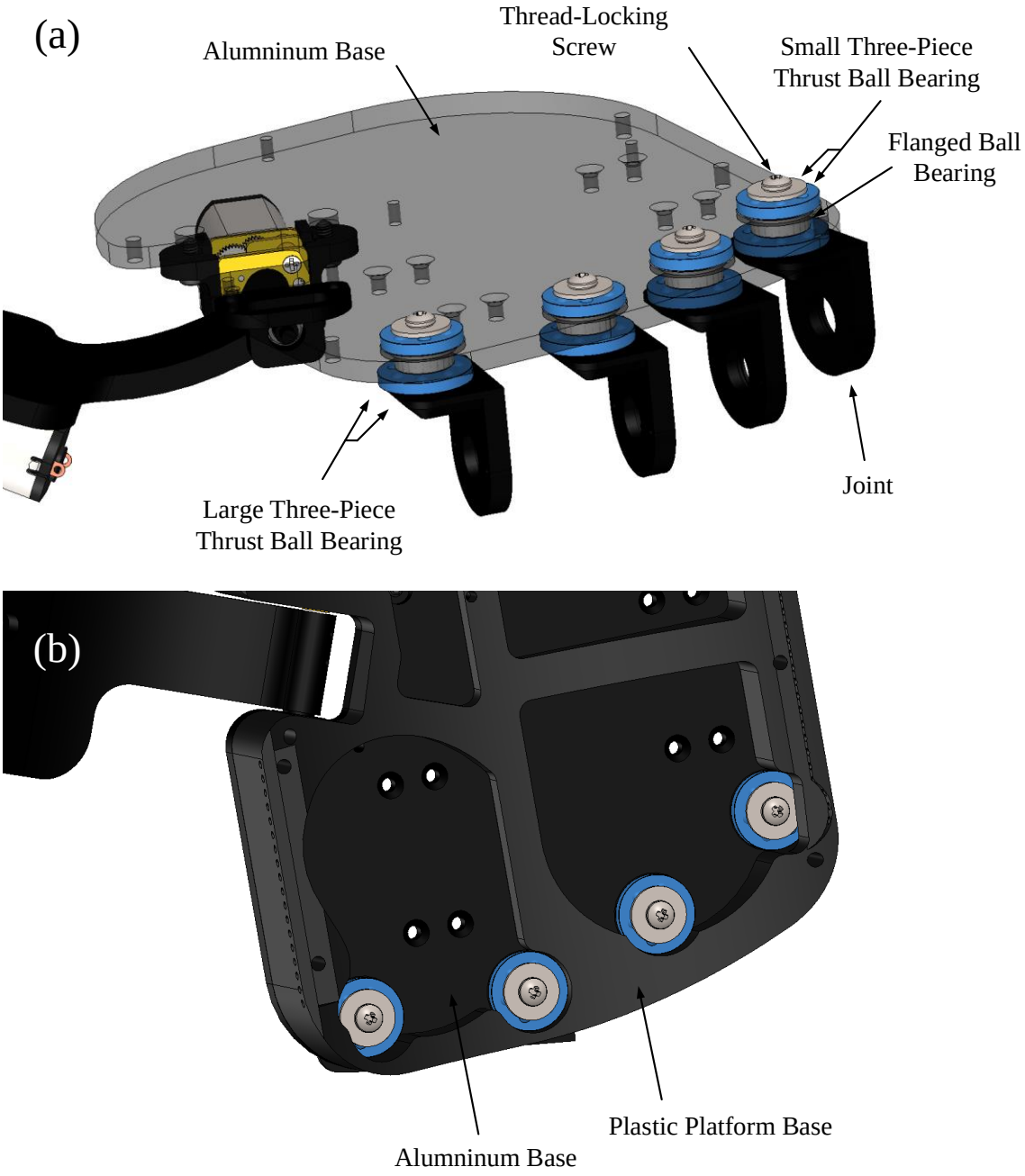

Figure 4.2: (a) CAD assembly model showing the layers of the improved design of the joints (b) CAD assembly model illustrating newly modified platform accommodating the design of improved joints

As shown in Figure 4.2 (b), the improved joints were all contained within the plastic Splatform, and all the modified parts maintained their original functionality.

Following the CAD design validation, the prototype was newly assembled and modified with the improved parts. The aluminum parts of the joints were custom-manufactured, and the ball bearings, thread-locking screws, and three-piece thrust ball bearings were chosen from the off-the-shelf products. For comparison, the joint of SAFER glove, Figure 4.3 (a), and the new robust joint of iSAFER glove, Figure 4.3 (b), are presented below.

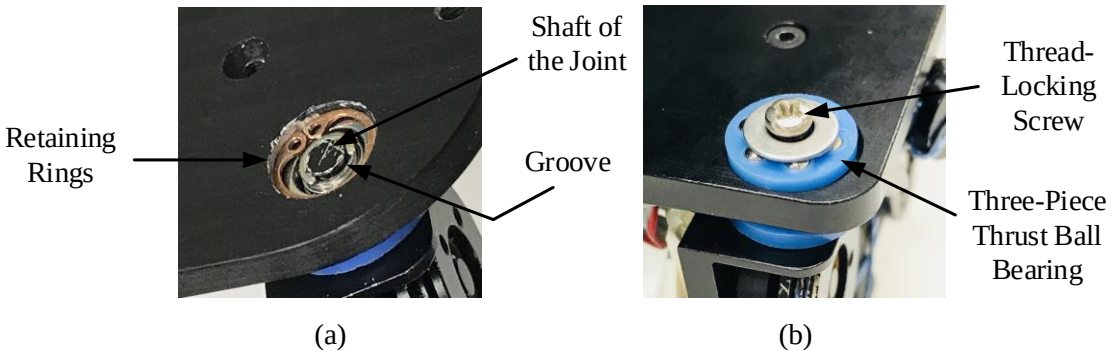

Figure 4.3: (a) Joint of SAFER glove (b) New robust joint of iSAFER glove

4.2 New Force-Sensitive Conductive Elastomer Sensors

Preliminary testing on the previously used FSR sensor showed that it was not suitable for all the desired functional modes. Knowing that a small active sensing area between the finger and an object to detect the force and the stiff plastic cover on the sensor limiting the applicability to a fingertip, a custom-made sensor that could accommodate the shape and the size of a fingertip and was durable across multiple bending motions was required.

4.2.1 Motivation

The motivation behind the sensor came from the variation in friction coefficient when an object slips, transition from static friction to dynamic friction, as demonstrated earlier in the Figure 2.8. For the given application of grasping an object using the exoskeleton glove, the relationship between the external force applied by the glove and the tangential force experienced at the tip of the finger is given by

$$F_t = \mu F_N \tag{1}$$

where, F_t is the tangential force, F_N is the external force, and is the friction coefficient. Now, when the object is at rest, the friction coefficient is static friction coefficient, μ_s. Once the object starts to slip, the coefficient of friction changes to dynamic, μ_d, which is significantly lower than μ_s. This change in friction coefficient for a constant external force results in a change in tangential force experienced at the fingertip. Therefore, by using a sensor that can detect the change in force, the presence of slip can be detected.

Similarly, as the contact is lost periodically due to the transition from static friction to dynamic friction, but not completely, by using a sensor that can detect the loss of contact, a drop in the magnitude of measured voltage, detecting the presence of slip is possible.

4.2.2 Mechanical and Electrical Design

To meet these goals, a sheet made out of a polymeric foil impregnated with carbon black, called Velostat (adafruit, product ID:1361, thickness: .1 mm), was utilized. In order to create the force-sensitive conductive elastomer (FSCE) sensor, Velostat was

layered with two-pieces of fine metallic mesh (adafruit, Product ID:1168, thickness: .08 mm) on both sides, and these layers were concealed by the insulating tape to reduce interference in voltage changes. The layer details of the FSCE sensor design is illustrated in Figure 4.4.

Velostat is a piezoresistive material that possesses a linearly varying conductivity relative to pressure while the fine metallic mesh forms the electrical contact with Velostat acting as the variable resistor in between, which makes it ideal for a new custom-made FSR sensor, FSCE sensor. After soldering individual electrical contact points on the metallic mesh, the resistance between the contacts for a given force applied on the FSCE sensor could be measured. The FSCE sensors were then inset on both the pad and the fingernail of the fingertip thimble of the iSAFER glove.

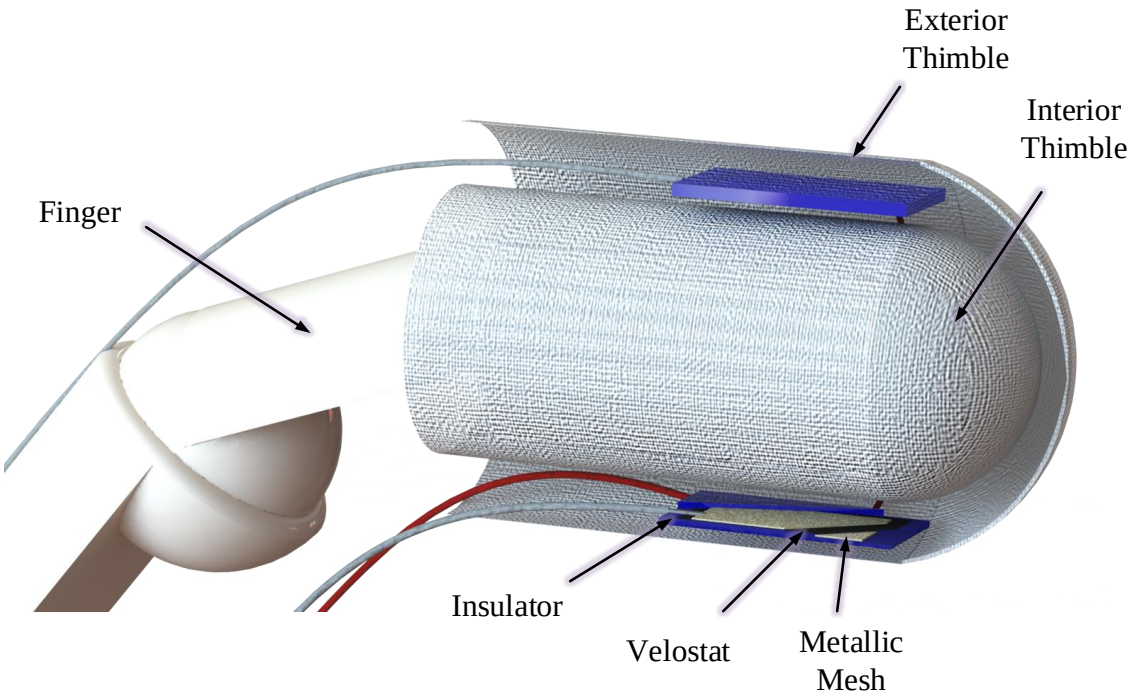

Figure 4.4: Detailed design of the FSCE sensors in between the thimbles

Previously, the SAFER glove used single layer thimble design as depicted in figure 4.5 (a). The FSR sensors were applied in and out of a thimble, and this method increased the damage rate of the FSR sensors. In order to directly measure the multi-directional forces experienced at the fingertips while protecting the FSCE sensors from mechanical damage such as an impact of the fingernail, two layers of the thimbles were utilized, and the FSCE sensors were secured between the layers. The entire sensor setup shown in Figure 4.4 was stitched on to the plastic thimble plate of the iSAFER glove as shown in Figure 4.5 (b). For comparison, the CAD models illustrating the design and sensors in an inside of the thimbles are presented in Figure 4.5 (a) and (b).

In the Figure 4.5 (a), the pink circles indicate the major points of the breakage, where the electrical contact points and the metal tips of the FSR sensors were. This electrical contact points were aligned with the DIP joint, and it was directly affected by the bending motion of the joint. In addition to not having metal tips on the FSCE sensors, locating the

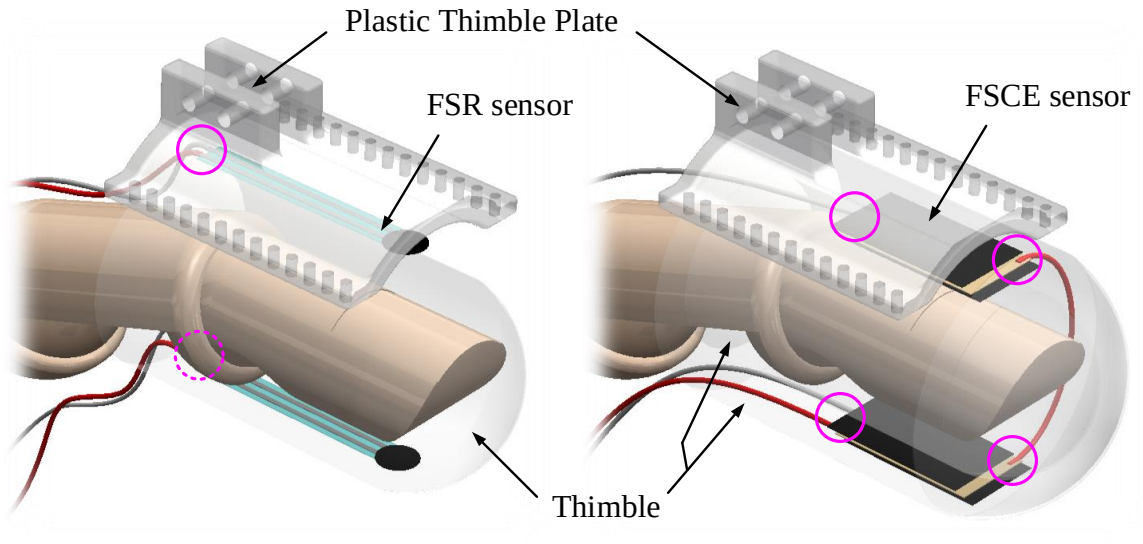

Figure 4.5: (a) FSR sensors in and outside of the single layer thimble for SAFER (b) FSCE sensors in between two layers of thimbles for iSAFER glove

electrical contact points on the distal phalange and distributing the electrical contact points over the sensors as noted in Figure 4.5 (b) ensured the higher durability.

Utilizing the characteristics of Velostat, which is a piezoresistive material, the change in the electrical resistance was measured by the microcontroller. Similar to the off-the-shelf FSR sensor, the FSCE sensor is a two-wire sensor with a resistance that detects the force. Previous studies on resistance of piezoresistive materials between electrical contacts found that resistance-force relationship could be described by [79]

$$R = \frac{\rho \cdot K}{F} \tag{2}$$

where ρ is the resistivity of the contacting surfaces, F is the force applied normal to the contact surfaces, and K is a function of the roughness and elastic properties of the surfaces. This relationship shows the inversely proportional resistance-force relationship. Furthermore, resistance of the sensors can be converted into a voltage signal by utilizing a voltage divider circuit with a resistor shown below in Figure 4.6. Similar type of schematic was also introduced in the off-the-shelf FSR Data Sheet.

The voltage measured can be calculated by applying Ohm's law as follows

$$V_o = V_{in} \cdot \left(\frac{R}{R_R + R} \right) \tag{3}$$

where V_o is the output voltage, V_{in} is the input voltage, which is 3.3 V for the iSAFER system, R_R is the resistance of a resistor that completes the voltage divider, and R is the resistance of the sensor. This method was applied to the iSAFER system, and the microcontroller read the changes in voltage due to the changes in the resistance of the

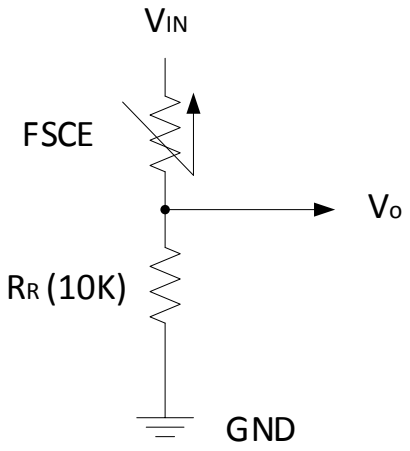

Figure 4.6: Voltage divider circuit with a resistor to convert the resistance to voltage

FSCE sensors. As the resistance of the FSCE sensors is high when there is no force applied to the sensor, while the resistance decreases as applied force increases, the initial V_o without the load will be small and gradually increase.

4.2.3 Calibration of the FSCE Sensor

Before the FSCE sensor was secured between the thimbles, the calibration was performed. To measure the data, the FSCE sensor was attached on a thin polyethylene material to create a deformable feature of human skin, and these layers were placed and fixed on a flat table. A small rectangular block, weighing only 1 g, which can be placed within the FSCE sensor, was placed on the FSCE sensor, and then each mass that weighed 46g, 46g, 46g, and 36g was piled on the rectangular block in such an order. The last 250g data was collected by applying 250g mass on top of the rectangular block. Set of data measured showing a change in the voltage value according to the change in the

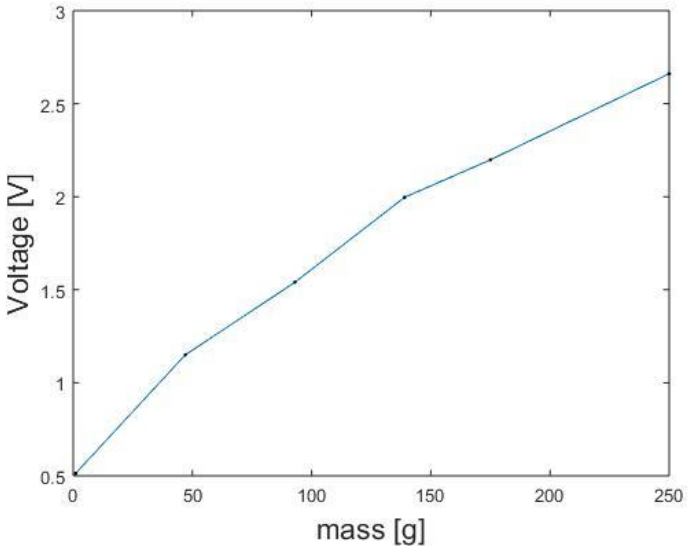

Figure 4.7: Changing voltage magnitude in accordance with the mass change in the normal direction

load is shown below Figure 4.7. As expected, the result showed positive linear relationship between the mass and voltage. The magnitude of the voltage increased as the total mass applied on the sensor increased.

The sensitivity of the sensor can be described as the minimum input of a mass that will result change in the output [80]. During the test, a rectangular block was used to distribute the force evenly. However, whether the block was used or not, the FSCE sensor was sensitive enough to detect a mass of 1g, which is about .00981 N, and the contact between the insulator and the metallic mesh also created initial voltage value. Due to this reason, the minimum force value was measured and saved in the system through the calibration state to adapt to each user's finger geometry. This will be explained further in section 5.2.

In addition to the normal force, as piezoresistive materials demonstrate a sensitivity to multiple force directions, the tangential force was measured and validated to verify the

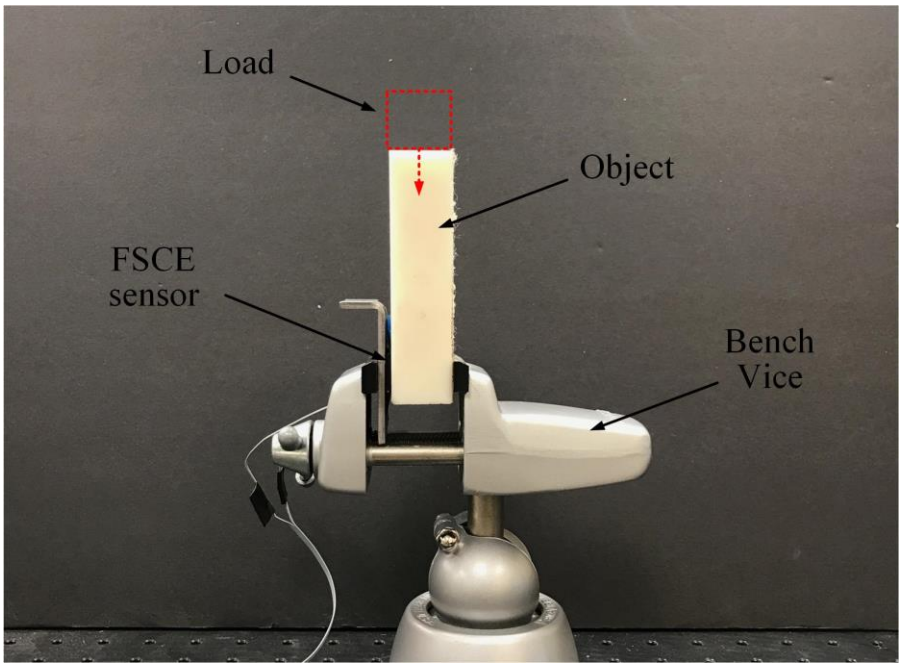

Figure 4.8: Setup of the tangential force calibration

multi-directional forces. The setup of this tangential calibration is shown in Figure 4.8. A small bench vice was used to clamp the sensor between two flat surfaces in parallel. The sensor was clamped lightly, but until the object was visually stable. Once the data was verified to be stable, loads were placed on top of the object. The load was increased in steps until the object started to slide down vertically and visually. The object itself weighed 163g. Therefore, the result shown in Figure 4.9 starts from 163g and ended with 833g. Throughout the test, the sensor did not moves or rotate.

The result showed that the sensor was able to measure the change in tangential load. As the object was softly grasped, the friction force increase due to the increase in load was clearly recorded, and then a visible slip happened around 900g, reaching the maximum static friction force. Stronger grasps would have resulted higher voltage while supporting heavier load. However, that firmer grasp would have showed less change in

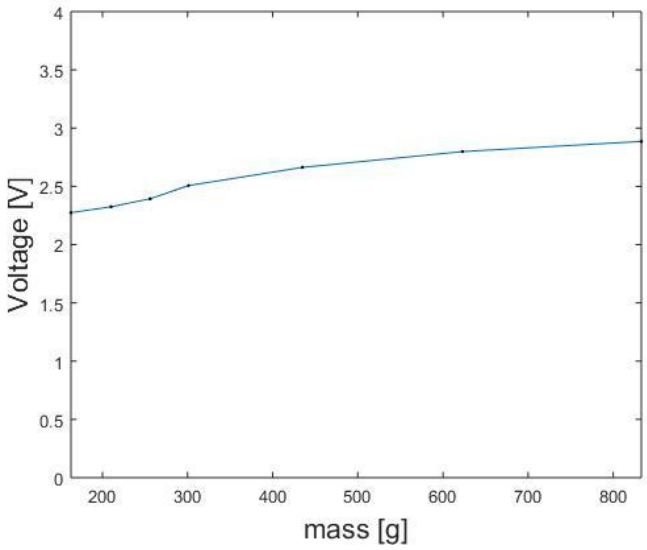

Figure 4.9: Changing voltage magnitude in accordance with the mass change in the tangential direction

the magnitude of the voltage. Therefore, performing the softest grasp to hold an object was desired and practiced.

4.2.4 Conclusion

The benefits of the FSCE sensor are the larger sensing surface, cheaper cost to produce, more resilient, and higher sensitivity than the previous FSR. After calibrating the sensor by applying the masses to a FSCE sensor affixed to a scale, the resultant scale factor was found to be 1.74 N/V.

This FSCE sensors were significantly important in this thesis as it was used to detect the user's intention as well as slips while measuring continuous force-feedback data. Though other options of sensors were considered including an optical sensor mentioned in section 2.5.3, it was not a suitable option for an exoskeleton. Knowing the involvement

of the palm during the grasp, the sensors located on the palm can be further embedded in the prosthetic hand to prevent the interference due to the thickness of the optical sensor, but this cannot be a solution for the hand exoskeleton because the sensors cannot be embedded in the human hand. Therefore, thin FSCE sensors were chosen to be used, and utilizing the calibration information, its capabilities are validated through the experiment.

4.3 Upgraded Electronic Interfaces

The original rapidly prototyped printed circuit board (PCB) on Figure 3.2 was replaced with custom manufactured PCB. In order to improve the interface between the user and the glove, a new second layer PCB was designed to accommodate the addition of an OLED screen, three buttons, and an inertial measurement unit (IMU). The design of the new second layer PCB created by the EAGLE software is shown in Figure 4.10 (a), and the custom manufactured PCB for the new second layer PCB is shown in Figure 4.10 (b) and (c). To fit the system on top of the dorsum of the hand and keep the original form factor, the additional PCB was designed to be located on top of the base PCB. These two boards share the power source, and communicate through one Teensy on the base PCB.

Two of the buttons are used to initiate the changes between the state machines, while the third is implemented as an emergency stop that returns the glove to the idle state when pressed. The IMU is added to detect the hand rotation and position in relation to the wrist and arm position in future work.

The XBee wireless unit was securely relocated to the bottom of the original PCB to reduce the physical damage to the electronic system. When grasping a short object on a table, the little finger side of the hand often touches the table. The location of the Xbee in

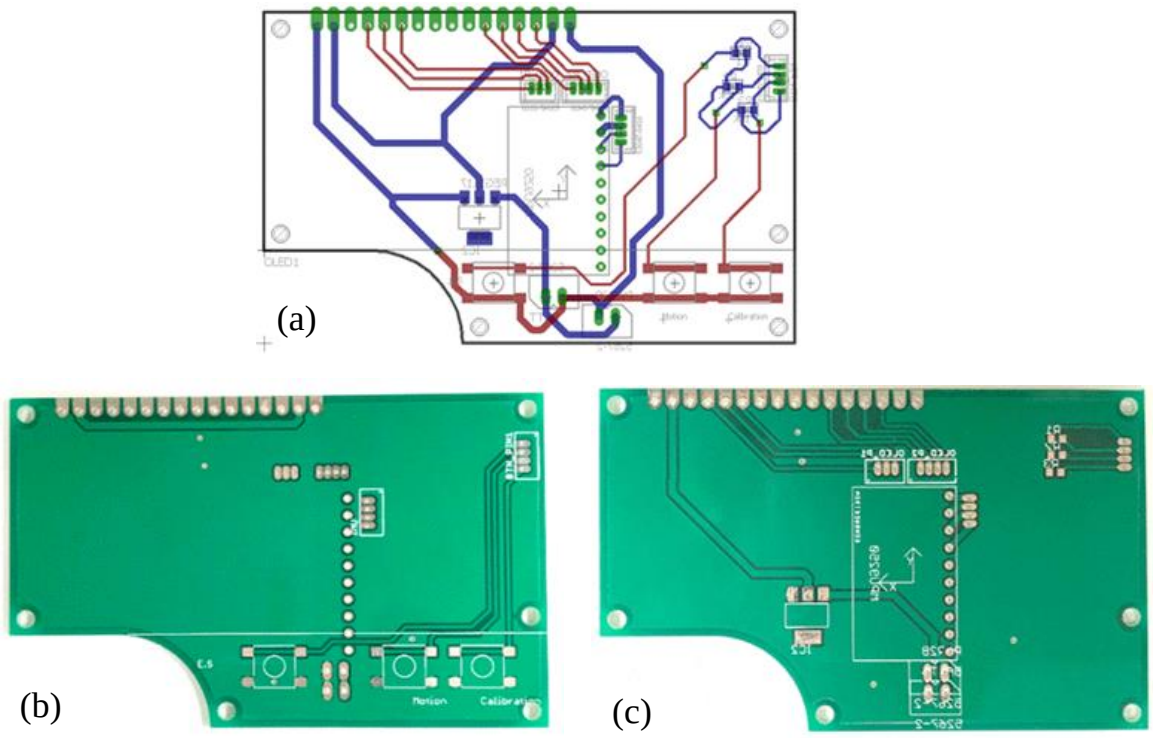

Figure 4.10: (a) Second layer PCB design created by EAGLE software (b) Top view of the manufactured second layer PCB (c) Bottom view of the manufactured second layer PCB

the previous design, as seen in Figure 3.2, caused external impact on the XBee while it acted as an obstruction.

The second layer printed circuit board assembly (PCBA) with OLED screen and three buttons is shown in Figure 4.11. As the second layer PCB was designed to conceal the components on the base PCB, the components mentioned earlier, such as the microcontroller, XBee, and IMU are not shown in this figure, as they are located on or under the base PCB.

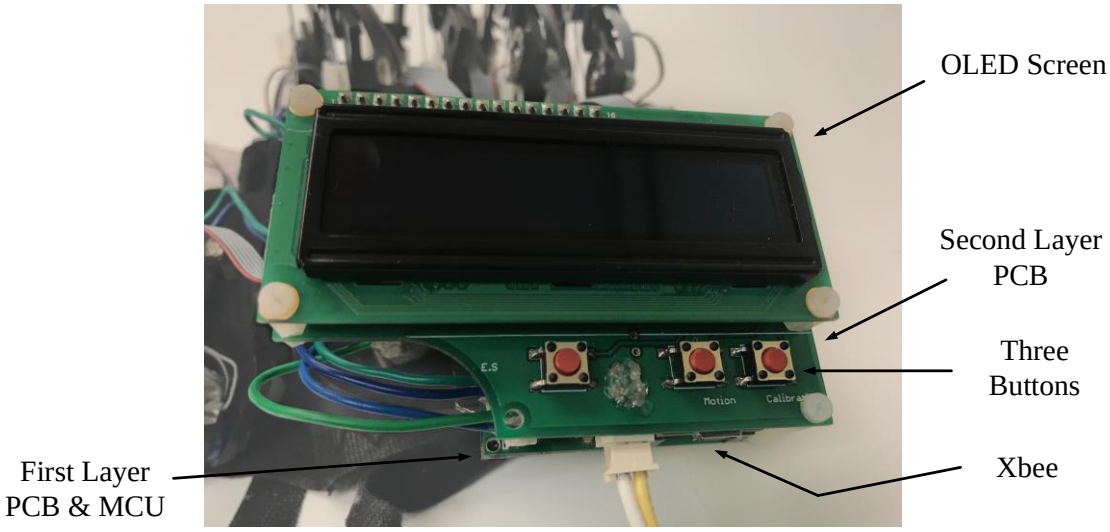

Figure 4.11: Second layer printed circuit board assembly (PCBA) with OLED screen and three buttons

4.4 Conclusion

After creating the new components presented above such as robust joints, aluminum base, plastic platform, FSCE sensors, and second layer PCBA with OLED screen and three buttons, the old components were replaced by the new components. Additionally, the original motors were replaced with 6V 1:1000 high power miniature gearmotors with long-life carbon brushes (HPCB), and the microcontroller was updated with the Teensy 3.2. The assembly of the iSAFER glove with the updated components is shown in Figure 4.12.

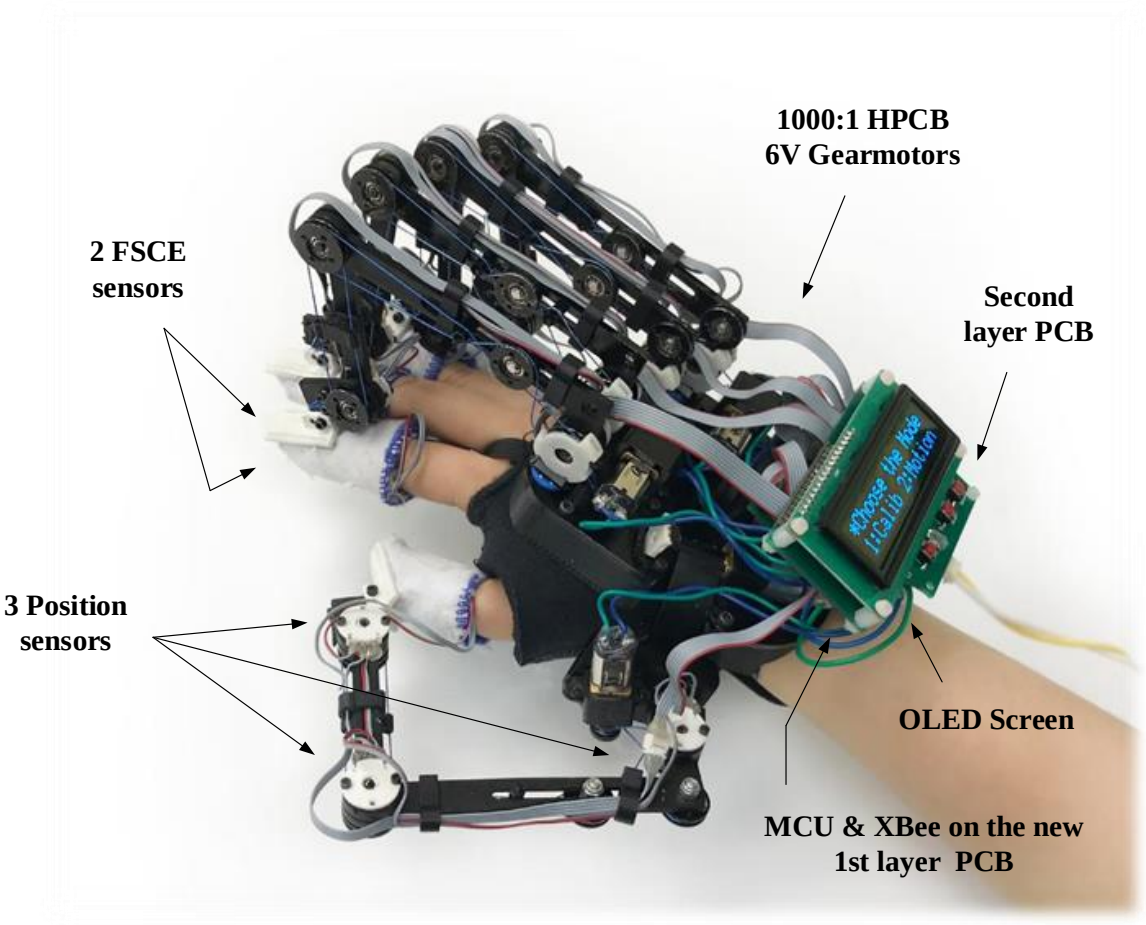

Figure 4.12: Updated components of the iSAFER glove

CHAPTER 5

REHABILITATION AND ASSISTIVE SYSTEM OF THE GLOVE

Recovery from debilitating hand injury is generally evaluated through MAS, which is rated on a 0-5 scale [26], [54]. Previous work with this platform proposed techniques for passive rehabilitation, through repeated passive motion guidance from a learned library of hand motions corresponding to grasps learned from a collection of healthy hand motions, coupled with active resistive rehabilitation through leveraging the glove's haptic feedback capabilities [34]. The current work expands previous functionalities, through the inclusion of grasping assistance as well as user-initiated passive grasping motions. This type of robot-assisted rehabilitation has been shown to result in favorable outcomes such as noticeable reduction in spasticity, decreasing the MAS score of joints, and small increases in the Rivermead Motor Assessment for subacute stroke survivors [26]. In a similar way, the study with MIT-Manus interacted with stroke patients actively and/or passively and showed statistically significant improvement including favorable trends in strength change, Fugl-Meyer Scale, and motor status scale [30]. Thus, robotic rehabilitative aids can greatly benefit a patient recovering from loss of dexterity or strength in their hand.

The iSAFER system is designed to have different modes that can perform either passive or active rehabilitation. In general, passive exercise can benefit patients in all MAS levels to alleviate atrophy, while also a necessary rehabilitation exercise for the patients at MAS level 0. Once the patients advance to level 1 and have the capability to

initiate minor muscle activation, such as a twitch, active rehabilitation with adjustable resistance can be applied depending on the level of the recovery from the injuries.

5.1 Intelligent Object Grasping Rehabilitation System Overview

Simple force control of an exoskeleton requires an informed input force for the system. However, in real life, people not only interact with rigid objects, i.e. a glass cup, but also with deformable objects, i.e. a paper cup. In this analogy, an overly firm grasp of a paper cup can easily result in crushing and spillage of the cup. With this in consideration, the iSAFER glove has been developed to provide a wide range of acceptable grip forces by applying a soft initial force and then adapting to the environment and the object through the detection of slip conditions.

A discrete, minute force step increase is applied when slip is detected, and continuously applied until the system detects that it is no longer in a slip condition. In order to maintain programing simplicity and provide an expandable operational paradigm, the system is designed to be finite state machine. The system overview is shown in Figure 5.1, and the block diagram of pseudo code for the system is included in the Appendix A. The system consists of the three state machines: Calibration, Active Rehabilitation and Assistance, and Main Idle. The method of activation for the system was given considerable thought during the design of the controller. For patients possessing some degree of bilateral paralysis or weakness, using a switch or EMG, for example, could require extensive rehabilitation just to regain this function. The current system instead uses motion amplification as its primary activation mode, referred to here as a “twitch” signal. The glove’s FSCE sensors are capable of detecting even minor force

fluctuations and treat inward or outward forces, relative to the finger pad, as a signal to close or open the fist, respectively. The control can then be adjusted to filter oscillatory signals, as well as to increase or decrease the activation force threshold, to accommodate patients who may have tremors or imprecise motion early in their rehabilitation.

While a small initial grasp force is of value when interacting with deformable objects,

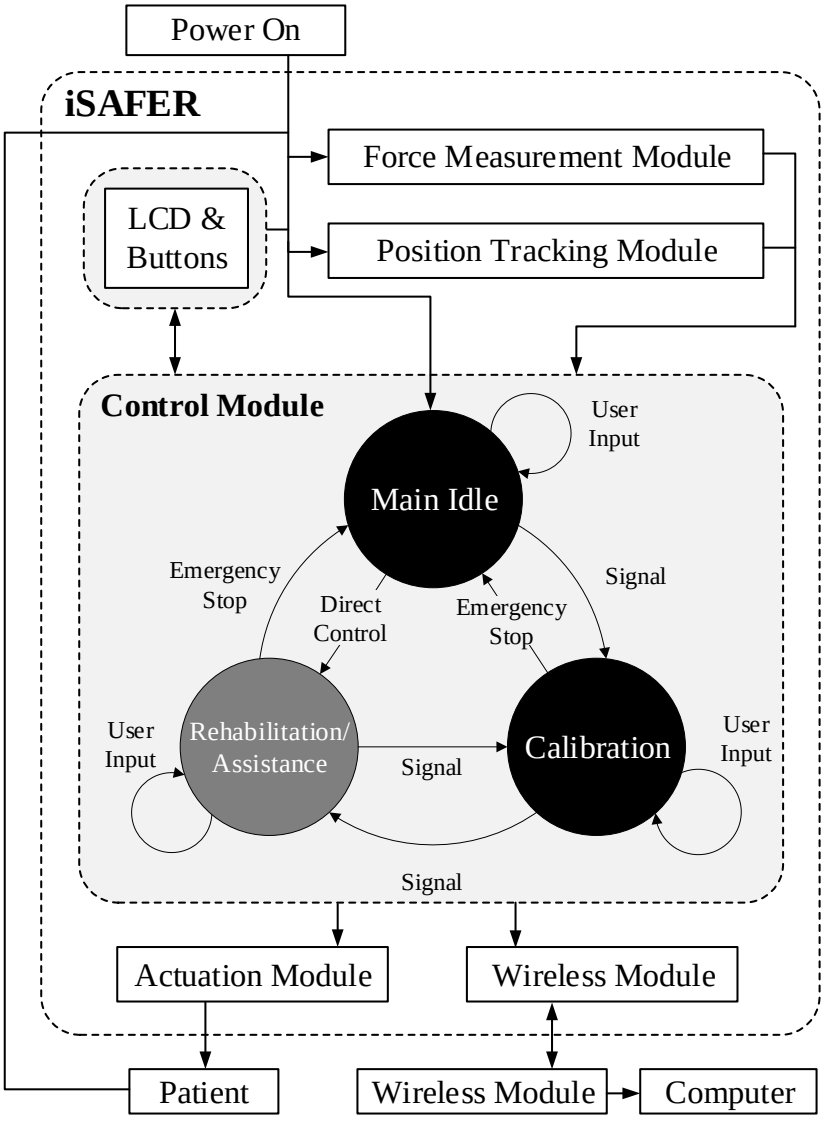

Figure 5.1: Operational flowchart for the iSAFER glove

humans generally respond to tactile vibrational signals to gauge required force and adjust dynamically as required to interact with an object [19], [22], [60], [62], [64]. To continue the previous analogy, an empty paper cup can be grabbed without a slippage with a very small force, but should it be filled with water, this small force will no longer be sufficient. Therefore, detecting the shape, surface roughness or orientation alone may result in failed grasps unless the exoskeleton applies its maximum feasible force on the object in all cases in order to preclude any slippage. Therefore, the functional design of the iSAFER glove is more similar to the biological evaluation of grip stability.

A basic outline of the operational structure of the iSAFER glove is as follows: The system initially applies a calculated minimum force. Should the object shift within the grip of the glove, it will detect the slippage. Once the slippage detection is triggered, the grip force will be adjusted until the object no longer slips.

5.2 State Machine Architecture

The initial and main operative state for the glove following powering on is the Main Idle. While in Main Idle, the fingers will remain at rest in the current position, and the system will wait for a command. When the emergency stop button is pressed in any other states or cases, the system will come back to this Main Idle state while resetting all the saved sensor, state, or case data.

The second state is the Calibration state. A hurdle faced in previous iterations of the glove is adapting the system to variously sized hands. The glove has the ability to be fit to a variety of hand widths and thicknesses through its design; however, the control will vary with the hand geometry. Therefore, in order to take into account the initial pressure

applied to the FSCE sensors due to variations in wearer, the glove must initially move to a calibration state machine.

In Calibration, the iSAFER glove performs warm up rehabilitation motions while simultaneously learning the minimum force values of each fingers. These motions progress through multiple concerted and individual flexions and extensions, in order to both provide a full stretch for the patient's fingers and hand, as well as obtain measurements in a variety of finger positions and locations. The minimum baseline forces are stored and used as a compensatory feedforward term in the glove controller. After the calibration, the glove will automatically change the state to Main Idle while keeping the fingers at the neutral position. The Calibration progression of passive hand and finger exercises can be repeated as necessary at the user's pace in order to enact a full passive rehabilitation session.

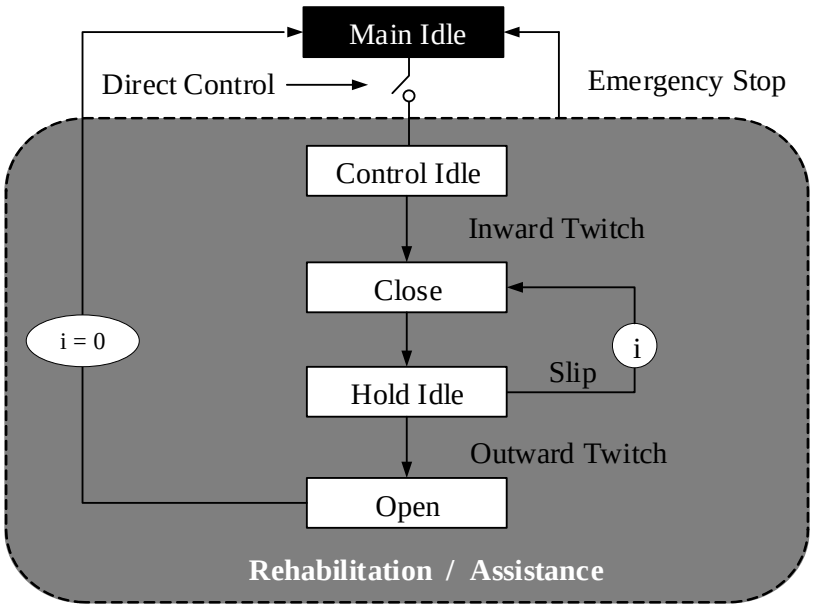

Figure 5.2: Rehabilitation/Assistance state machine detail

Once in the Active Rehabilitation/Assistance state machine, the program proceeds through a sequence of substates, as seen as Figure 5.2. The initial substate is the Control Idle substate. In this substate, the fingers will remain at rest at the current position, and the glove will wait for a twitch signal. Once an inward twitch signal is detected, a substate change is triggered and the glove proceeds to the Close substate.

The Close substate contains closed-loop hysteresis force controllers utilized to flex each finger independently until the force reference is reached for all. A hysteresis controller was utilized due to its optimality for applications that require the fastest possible response [81]. The use of multiple controllers enables geometrically adaptive grips to interact with objects of varying shape. Upon the first such iteration through the Close substate, the initial force input is utilized to control the first grip, and this 'initial soft grip force' is experimentally determined through interaction with compliant objects. The controller then outputs a PWM signal to the motor for each finger until the initial soft grip force input is reached.

Once the force input has been realized, the program proceeds to the Hold Idle substate, wherein the position is held and slip detection routine is activated. If slip is detected, the glove then returns to the Close substate, increasing the force input and velocity reference in a stepwise manner in order to grip more firmly and quickly in the event of successive slip events. The program again then returns to the Hold Idle substate. This sequence continues until slip is no longer detected, with the force reference increasing with each iteration. A diagram depicting a single finger's controller is shown in Figure 5.3. The controller and force reference equations are as follows:

$$F_{IN} = F_{FF} + F \cdot i \tag{4}$$

$$v_{ref} = \begin{cases} v_{FF} + v \cdot i, & if \quad e > 0 \\ 0, & if \quad e \le 0 \end{cases} \tag{5}$$

where F_{IN} is the stepwise input force, F_{FF} is the 'initial soft grip force', F is the force increase gain, v_{ref} is the velocity reference, v_{FF} is the initial velocity, v is the velocity increase gain, e is the error as measured by F_{IN} - $F_{feedback}$ and i is the iteration feedback that drives the increase in the stepwise force and velocity functions.

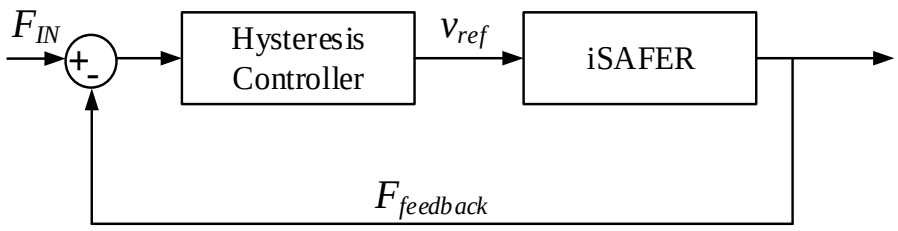

Figure 5.3: Force Control Diagram in Close Substate

If an outward twitch is detected, the system then proceeds to the Open substate. Here, the fingers extend to an open hand position using a closed-loop hysteresis position controller, utilizing feedback from potentiometers located on the finger joints. The force references and substate iteration counters are reinitialized to zero. Once the open position is achieved, program returns to Main Idle.

CHAPTER 6

SENSORY DATA ANALYSIS

The sensory stream provided by the array of sensors embedded within the glove's design provides a rich feedback environment. This data is utilized for multiple purposes, including setting fail-safe protections for the wearer, sensing motion commands, and detecting and analyzing contact forces when the glove is used to grasp an object.

6.1 Mean Filter for Serial Data

When both force measurement and position tracking modules generate data, a set of raw data was collected initially. Raw data was often noisy enough, having meaningless outliers, to mislead the system. To solve this problem, a mean filter was applied to the algorithm, producing processed data, and the result was clean and stable. Adding the benefit of mean filter to the system, the processed data was utilized to track the finger position and measure the force feedback data.

The base PCB consists of ADG725, monolithic 32-channel analog multiplexers, and a synchronous serial data protocol called Serial Peripheral Interface (SPI) was used by microcontroller to communicate with ADG725. Out of 32 channels, 25 channels, 3 potentiometers and 2 FSCEs per one finger, were used to transfer the data. These serial communication data was automatically logged in the buffer size of 640, which contains 20 buffers for each of 32 channels. Using 20 buffers, mean values were computed and logged in the buffer size of 32 for 32 channels.

A sample of mean filter processed data is illustrated in Figure 6.1 along with a raw data visually showing the effect of a mean filter application.

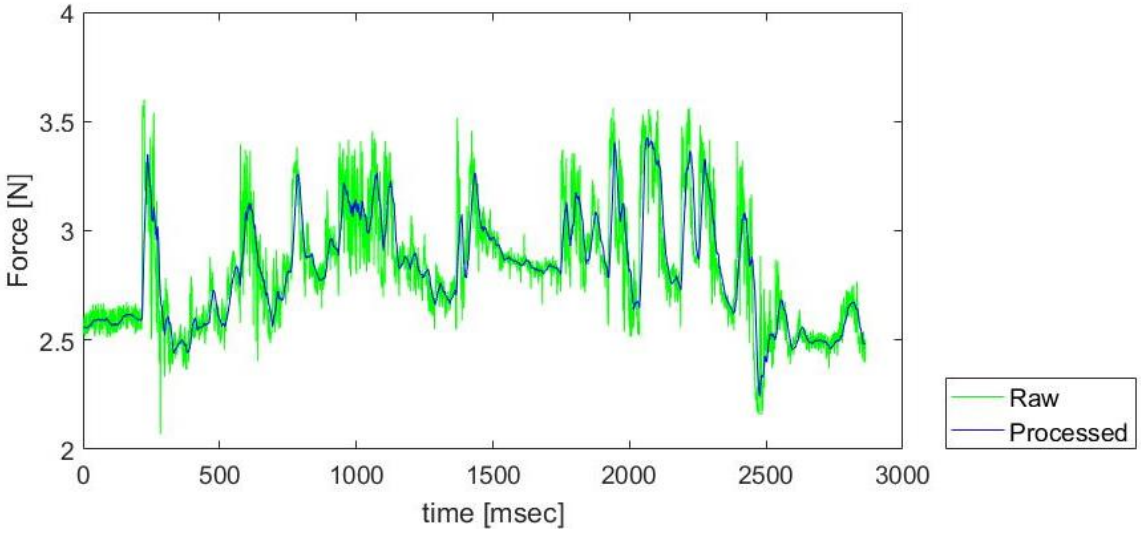

Figure 6.1: Comparison between a raw data and mean filter processed data

6.2 Finger Position Tracking

Where each finger linkage joins the dorsal plate, a rotary potentiometer tracks the angular position. Using this data allows for the tracking of the finger through the kinematic relations of the cabling system. The main application of tracking the finger position is to ensure the safety of the wearer and protect their fingers from being extended beyond the set limits. During the Calibration state, the fingers are gently guided from full flexion to full extension, at which time the limits on the motion of the joints can be adjusted as necessary to ensure an ideal fit as well as to maintain wearer comfort.

6.3 Finger Forces Measurement

In order to verify the operation of the new FSCE sensors, data was recorded while grasping a paper cup, and analyzed in order to confirm that the performance matched or exceeded that of the previously reported system [34].

In Figure 6.2 below, 30 grasps were performed with the glove recording force data passively. The data presented are the results from just one finger, depicted in a raw form in the top image in Figure 6.2. Utilizing dynamic time warping (DTW) in order to temporally align the various grasp sequences, as in [34], the feedback shows strong resemblance to the previously reported data, with greater force resolution and detail.

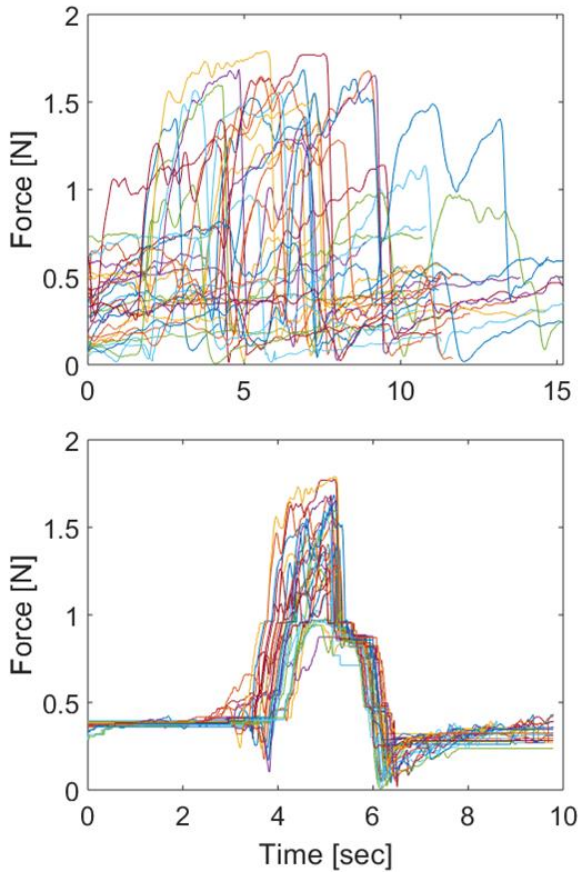

Figure 6.2: Index force data from new sensor. (top): raw data; (bottom): DTW result

While the performance between sensors is comparable, the new FSCE is superior in terms of flexibility and thus conformance to the finger for a more accurate force profile for the fingertip, resilience against breakage, and cost. Thus, the new FSCE sensors demonstrate a robust improvement on the previous system.

The grip demonstration data shown above was collected while a healthy user was gently grasping and lifting an empty paper cup. As such, an average of peak grasp force from the trials is implemented as the initial soft grip force in the system, providing a low initial contact force for the glove in order to enable interaction with compliant objects.

6.4 Finger Motion Amplification

The main activation method of motion amplification requires the detection of finger motion by the wearer. In order to test the sensitivity of the method as well as to demonstrate the applicability for patients with minimal hand functionality, the activation limit is designed to trigger at a minor twitch in the most sensitive configuration. The force feedback resulting from a user flexional twitch followed by a return to starting hand position while wearing the glove is depicted in Figure 6.3, with the data from each finger normalized about a common mean initial value for readability. While the signal is oscillatory, the major feature is the positive force impulse, indicating an increase in force in the direction of finger flexion. The following negative impulse is driven by the elastic properties of the FSCE materials.

In order to detect the positive impulse associated with a flexional twitch, positive derivative detection logic is utilized to trigger a state change. While the glove is in the Control Idle substate, the data from the FSCE sensors for each finger are central

differentiated in real time. Utilizing the user twitch data such as that depicted in Figure 6.3, a positive derivate limit of .012 N over 10 ms was determined. If the differentiated value is found to exceed the twitch slope limit, the progression to the Close substate is triggered.

In Figure 6.4, the force characteristics utilized for the outward twitch motion detection are shown. Unlike inward twitch or slip detection, the outward force change is

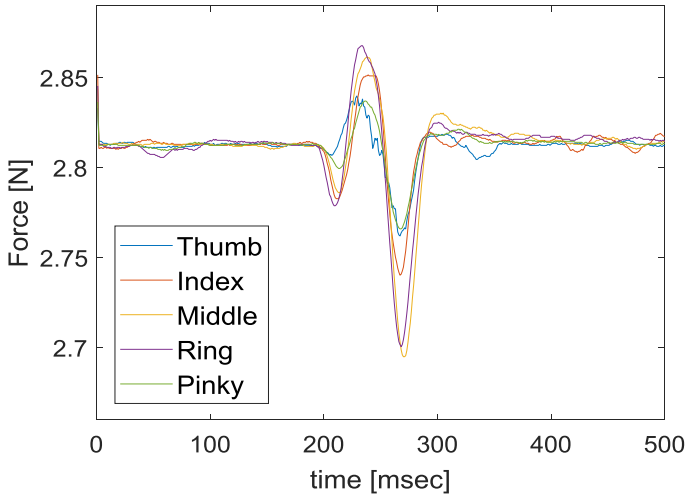

Figure 6.3: Inward twitch force characteristics of fingers

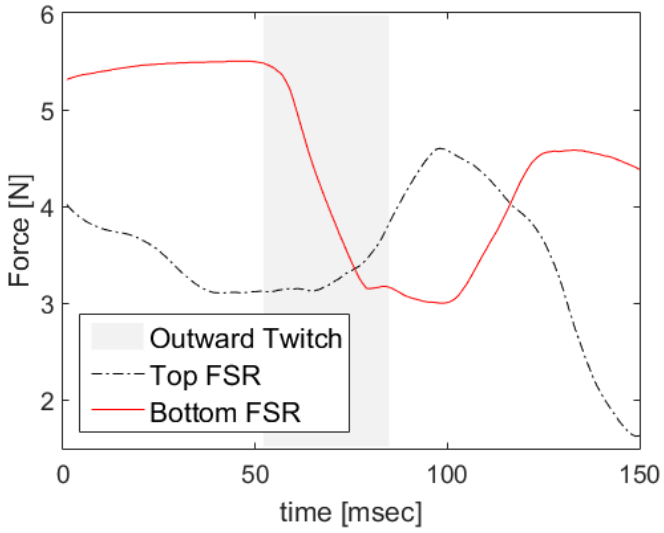

Figure 6.4: Outward twitch force characteristics of fingers

measured through monitoring both the top and bottom FSCE sensors for each finger. In this case, the bottom force reading decreases as it loses contact with the finger, while the top sensor detects a slight increase. Similar to the inward twitch, derivative limits are set. The outward twitch is detected while the program is in the Hold Idle substate, and the top FSCE sensor crosses the positive derivate threshold while the bottom simultaneously crosses the negative. In the Figure 6.4, the outward twitch can be seen to occur within the grey shaded area. Here, a positive derivate limit of .007 N over 10 ms and a negative derivative limit of .040 N over 10 ms were used.

6.5 Object Slip Detection

Insufficiently stable grip configurations must be detected to dynamically adjust the grip assistance supplied by the glove. Research on the tangential forces during slip situations for human grips has shown that the advent of a slip event is indicated by a sudden drop in normal force [68]. Experimental data collected from the fingertip FSCE sensors of the iSAFER glove in generated slip events corroborate these findings, as shown in Figure 6.5.

This event signature can thus be incorporated into the state machine in order to trigger a substate change when a poor grip configuration is detected. While in the Hold Idle substate, the central difference of the data from the FSCE sensors is compared to a negative deriviative force limit, computed from aggregated experimentally-generated slip events. If the approximated force derivative from a finger is found to drop below the derivative limit, a state change is thus triggered and the glove proceeds to the Close substate. Once complete, the glove returns to the Hold Idle state, where it again can

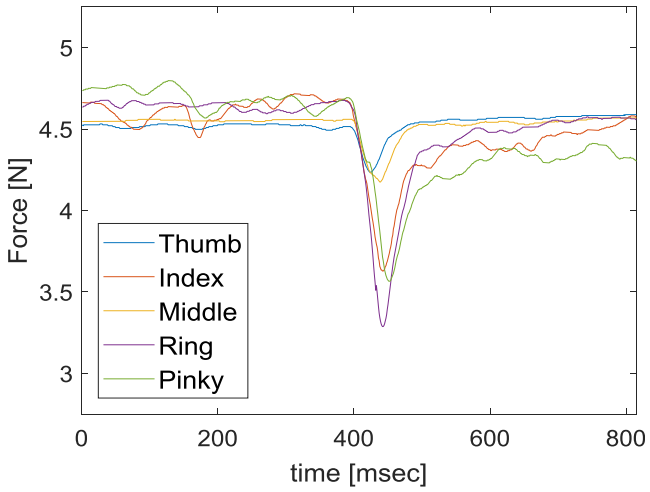

Figure 6.5: Slip event force feedback of fingers

detect any slip events. This state cycle will repeat until a secure grasp is realized, with the reference force incrementing upward monotonically.

CHAPTER 7

EXPERIMENTS

After defining the characteristics of the twitch, slip, and initial soft grip force values, the system was first validated through feedback from a single finger, and a cylindrically shaped object with a smooth surface. Once validated, more experiments involving five fingers were conducted, and then the experiment was expanded to four more objects of different shapes and textures, shown in Figure 7.1. The weight of each of the four objects was as follows: (a) 322 g, (b) 350 g, (C) 513 g, and (d) 238 g.

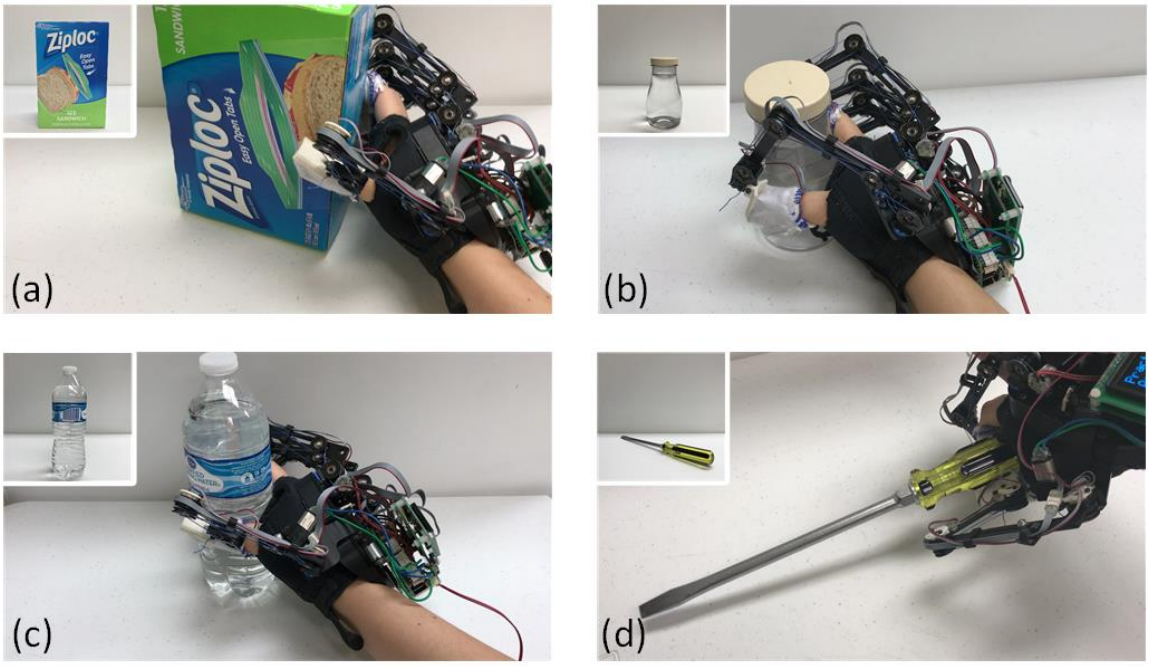

Figure 7.1: Four objects of different shapes and textures for the experiments: (a) cardboard box, (b) variable diameter cylinder, (c) water bottle, (d) screw driver

The data was collected from all five FSCE sensors on the pads of fingertips and the analysis is presented below. Previous work with this platform often used a wooden hand to represent the impaired hand for experimentation. However, in order to perform the twitch activation and accurately illustrate the degrees of freedom possessed by a human hand, the wooden mannequin hand was insufficient. Thus, in the following, a human participant with healthy hands was told to initiate the closing motion by producing short twitch motion, but not to apply any force while grabbing the object.

Utilizing the grasp taxonomy system developed by Feix in [48], for Objects (a)-(d), the iSAFER glove performed a parallel extension grasp, a large diameter grasp that transitions to a small diameter grasp as the object slips to its tapered top, a medium wrap grasp, and a ring grasp, respectively. The glove acts by actuating all five fingers to securely lift the objects off the table. The individually force controlled fingers allow the system to overcome variations in object geometry and adaptively conform to the object as necessary.

7.1 Intelligent Object Grasping

The single finger validation experiment proved the glove was able to perform both the soft grip and detect slippage. Once the slip detection triggers the Close substate, incrementally increasing force was applied to the object to compensate the weight of the object in order to grip it securely. The result of the experiment is illustrated in Figure 7.2.

This figure depicts the entire sequence of a grasp, from twitch input to secure grasp. Event 1 marks where the twitch input is received and the force applied by the glove can be seen to increase. Event 2 then shows the first slip occurrence following the

achievement of the soft grasp force. This slip had a much larger drop in normal force than the second slip, indicated by Event 3. As more force was applied to stabilize the grasp, the drop force reduced as well as the noise in the force.

The cylindrical shape of the grasped object lends itself to the shown force profile, as the uniform diameter results in a roughly stepwise force increase as the grasp is secured. This is a clear illustration of the stepwise reference force function and the hysteresis controller's quick response to the slip events, as designed.

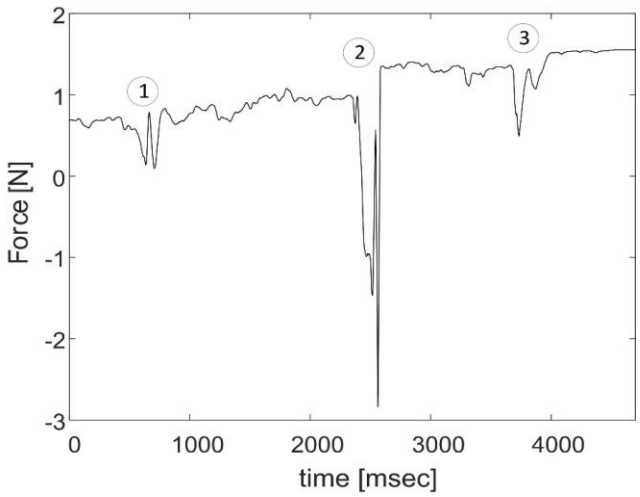

Figure 7.2: Force feedback profile for a single finger grasping a cylindrical object

7.2 Five Finger Object Interaction

While wearing the glove, the user first performed the calibration exercises in order to correctly calculate the initial force offsets due to finger geometry. Once calibrated, the program proceeded to the active rehabilitation and assistance state machine, wherein the human participant attempted to grasp the desired object. When the twitch motion was

produced by the wearer, the glove detected the twitch and initiated flexion. Following the initial flexion, the glove stopped closing when the soft grip force was detected. Soon after, when the human participant tried to lift the object, the occurrence of slip triggered closing until it met new limit. In Figure 7.3 below, the grasp interaction between the wearer and the cylindrical validation object is depicted for all five fingers.

The five-finger twitch can be seen at 1100 msec, at which time the finger flexion is triggered. At 1600 msec, a slip event can be seen to occur, at which time the controller recognizes this and proceeds to close the fingers and increase the grip force. A small spike in normal force can be observed prior to the slip-induced force drop. This is due to the object's overcoming of static friction prior to slippage.

It can be seen that the four fingers have very similar force profiles. As the grasped object is cylindrical and thus necessitated a medium wrap grasp, the majority of the oppositional force is palmar. The thumb does provide the largest force, due to its oppositional nature in a cylindrical grasp. However, as the proximal phalange of the

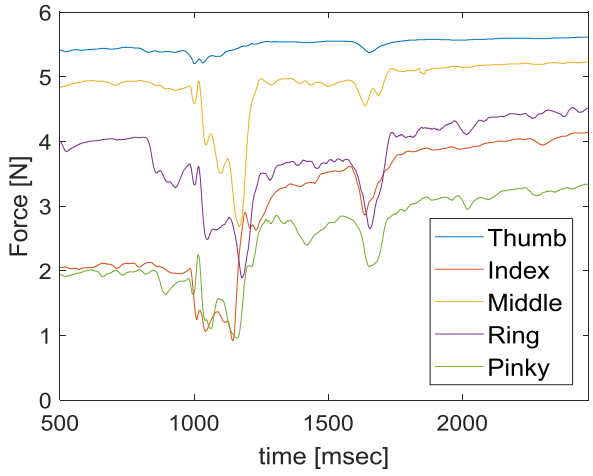

Figure 7.3: Force feedback profile for five fingers grasping a cylindrical object

thumb as well as the webbing of the hand are also in contact with the object, the tip force measurements of the thumb do not show a oppositional force equal to the sum of the other fingers. A future improvement for the sake of grip force analysis is the addition of a palmar force-sensing array to provide a more comprehensive force characterization.

7.3 Multi-Object Grasp Experiment

In Figure 7.4 below, data is presented comparing the force profiles of the grasps of the four experimental objects shown in Figure 7.1. Force data from a single finger in each case is presented for readability. The twitch commands are indicated by the grey shaded area at the initial motion. Following the twitch command, a momentary drop in force can be observed. This is caused by the beginning of the iSAFER glove's finger flexion motion, in concert with the elastic effects of the FSCE. As the linkages push the backside of the fingers toward a closed grip, the contact exerted by the finger upon the pad FSCE decreases below the calibrated offset, until the fingers make contact with the object and the force again increases.

The increasing reference force can be clearly seen following each slip event. The quick response of the slip recovery can also be seen in the short time difference between the start of a slip and the corresponding force increase. In addition, the wearer finished each trial by lifting the object from the table, and the force feedback at the final state is thus directly proportional to the mass of the objects. This is clearly shown by the final recorded values for each object.

The effect of the geometrical shape of the grasped objects on the grasp force is also illustrated by the data. For instance, Object (b), the variable diameter cylinder, shows two

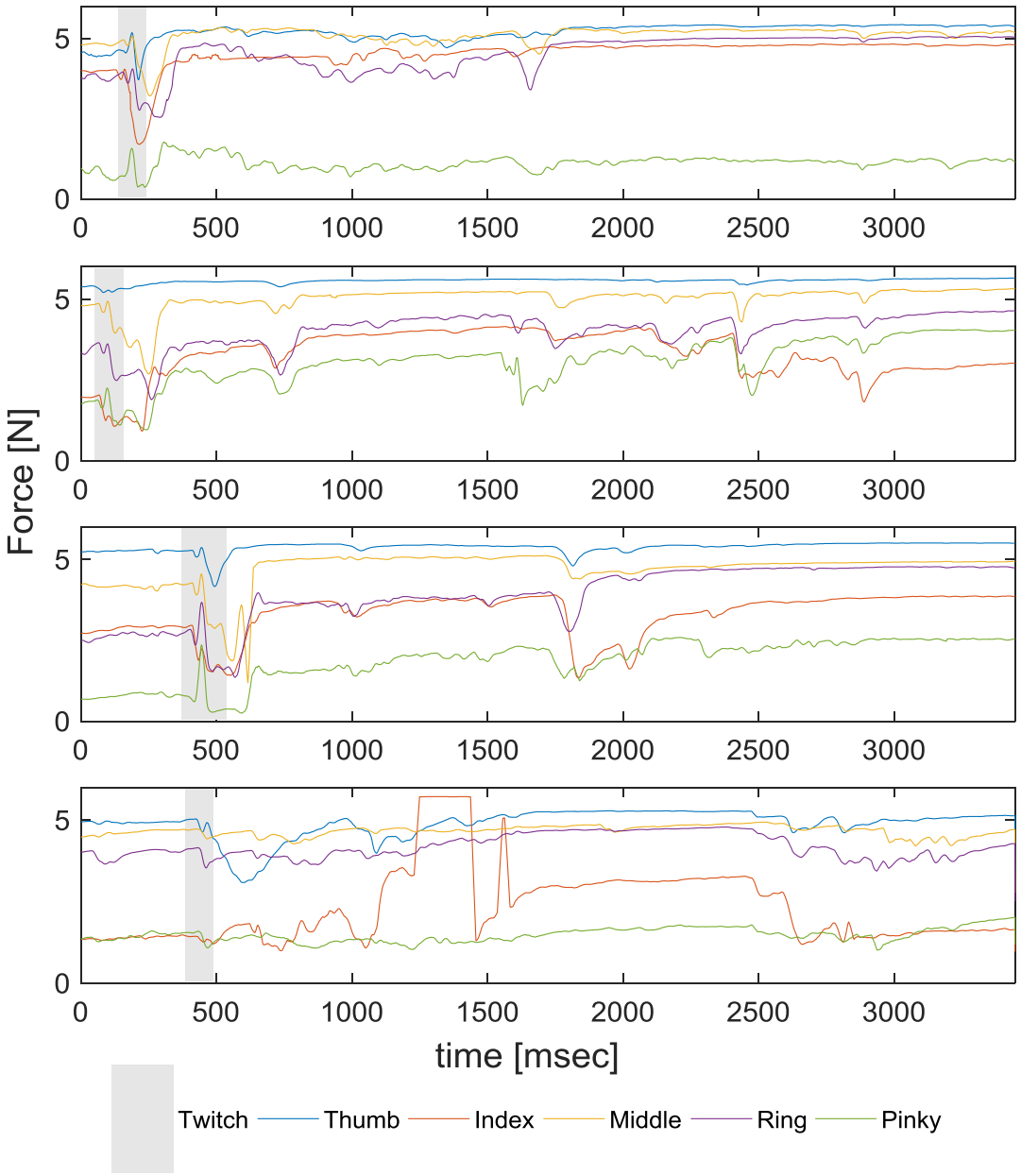

Figure 7.4: Force feedback for four objects: (a) cardboard box, (b) variable diameter cylinder, (c) water bottle, (d) screwdriver

significant slip events at 1600ms and 2500ms as well as two anomalous smaller s lip events at 2200ms and 3000ms. The smaller events occur when the objects shifts within the glove to a smaller diameter section, resulting in a slower decrease in normal force,

followed by a sudden initiation of slip that triggers the closing controller of the glove. The variable diameter also causes the much higher degree of noise in the normal force feedback. Similarly, Object (a), the cardboard box, shows a high level of normal force noise early on in the grip, prior to the firmer grip following the slip event. This is driven by the slight deformation of the box as it is gripped until a firm grip is achieved.

In addition, it can be seen that for the constant width or diameter Objects (a) and (c), the box and the water bottle, the iSAFER glove only required one major slip event and subsequent finger closure to achieve a stable grip upon the object. However, for the non-uniform diameter of Object (b), the variable diameter cylinder, multiple slip events are required in order to stabilize the grip. These slip events can be seen to have varying magnitude, as with each event the diameter of the object being gripped changes, resulting in decreased contact between the iSAFER glove and the object, which the system then compensates for. Furthermore, the data presented shows that with the uniform Objects (a) and (c), the iSAFER glove reaches a steady-state secure grip more quickly than while interacting with a non-uniform object. This holds with the expected results, as greater object complexity would at times require more grip closures in order to achieve a stable grasp.

In performing a ring grasp to pick up Object (d), the screwdriver, the iSAFER glove demonstrated that its slip adaptive grasping can also be applied to grips beyond full hand grasps. The major slip event at 1100ms is followed by a recovery and the noisy force feedback period where the screwdriver shifts within the grip of the glove. The force measurements of middle, ring and pinky fingers can be seen to remain mostly stable as the only forces sensed are due to the motion of the fingers with the finger thimbles. The

index finger sensor can be seen to saturate and then fall off as the screwdriver rotated within the grip until it only made tangential contact on the sensor and was supported by the lower section of the finger that is not covered by the sensor. This can be remedied through the inclusion of larger FSCEs to cover more of the finger.

7.4 Deformable Object Grasp Experiment

In addition to the four objects used in previous experiments, an empty water bottle was used to test the intelligent object grasping with a deformable object. Figure 7.5 shows the difference in result between the SAFER system and the iSAFER system introduced in this paper. Previously, SAFER system was programmed to have simple force control with a static reference force. Therefore, its grasp crushed the deformable object as shown in Figure 7.5 (a) while flexing all fingers to reach the reference force as

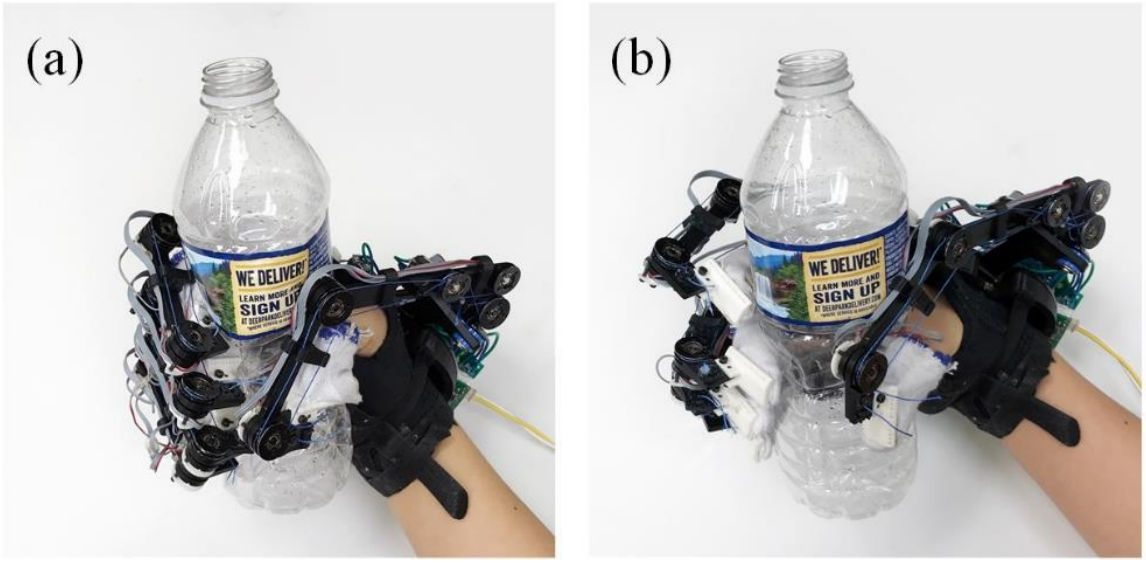

Figure 7.5: (a) SAFER system, (b) iSAFER system with intelligent object grasping algorithm

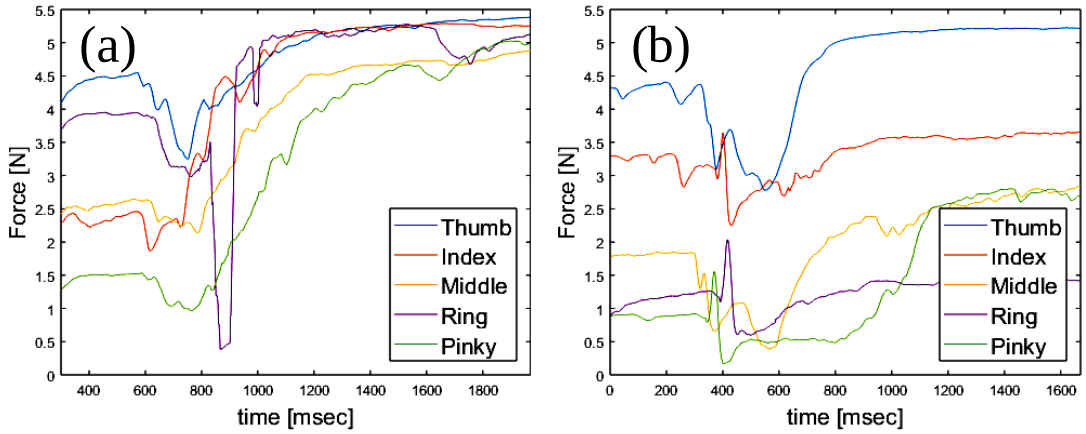

Figure 7.6: Force feedback for five fingers of (a) SAFER and (b) iSAFER system

required by the original SAFER controller, as shown in Figure 7.6 (a) [34]. When the iSAFER system with intelligent object grasping was used to pick up the empty water bottle, the iSAFER system stopped closing once the FSCE sensors touched the surface and reached the soft contact force as shown in Figure 7.5 (b) and 7.6 (b). As the bottle itself only weighed 10g, the slip event did not occur, and the initial soft grip force was firm enough to hold the bottle.

7.5 Time Constant of the First Order System

The parameter indicating the response to a step input of a first order system is called the time constant. Generally, the Greek letter τ, tau, is used to represent the time constant in engineering. The time constant for an increasing system can be described as the time that reaches the value presented in equation (3) of its settling time, as shown in Figure 7.7 [82].

$$1 - \frac{1}{e} \approx 63.21\% \quad (6)$$

As the grip adjustment of iSAFER system is a first order increasing system due to its increasing force value after the slip, using above information and 36 grip adjustment samples, the time constant was determined to be approximately 74.2 ms.

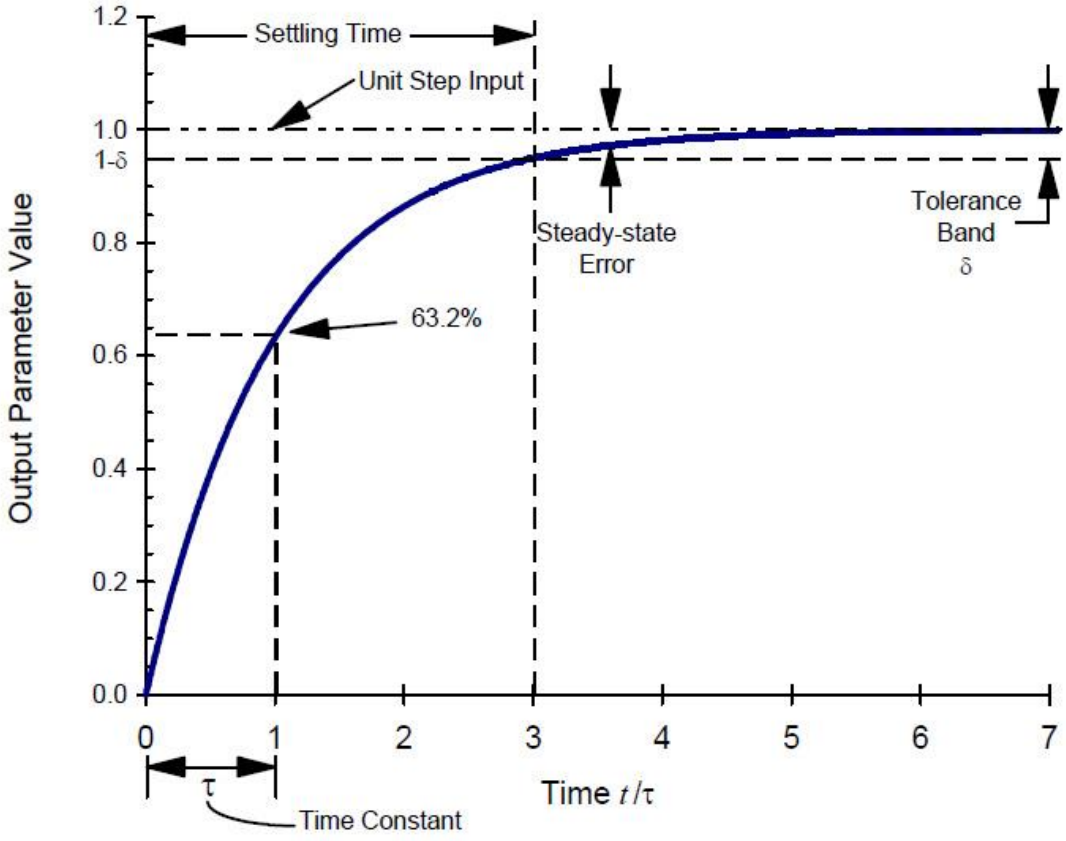

Figure 7.7: First order response behavior [80]

CHAPTER 8

CONCLUSION & FUTURE WORK

This chapter concludes the thesis with a summary of the current research while presenting potential topic of future study.

8.1 Summary

This thesis started with a comprehensive literature review on hand anatomy and function, taxonomy of human grasp types, impairment of hand function, input control method, and slip detection method as well as the prototype review of the SAFER glove. Both mechanical and electrical design and system of the SAFER glove was described as well as the proposed rehabilitation and learning system to provide details of the previous work as this thesis is the extended work of the SAFER glove. Aiming to develop an intelligent grasping controller, the areas that could be improved or enhance the performance of the SAFER glove were identified.

Along with the introduction of improvements, such as robust joints, new FSCE sensors, and upgraded electronic interfaces, the prototype improvement section covered the design of new components and prototype integration. Once the prototype was reconstructed, the intelligent grasping controller, which utilized the FSCE sensors to support slip-aware grasping in order to provide an adaptive force profile for robotic glove exoskeletons, was developed. By sensing variations in the normal force and tangential force between the fingers and the object grasped, the prototype was able to detect slip and

adaptively recover in situations in which the object began to fall from the hand. Therefore, the updated prototype with the intelligent grasping controller consummated the iSAFER glove.

The glove can provide both passive rehabilitation exercise as well as active grasping rehabilitation and assistance. This widens the applicability of the system as a rehabilitative and assistive device. The use of a soft grip force enables the system to interact with delicate objects, while also adapting the grasp force as needed for heavier objects. Though the speed of general grasp was not considered as an important parameter in this thesis, the time constant for a grip adjustment was computed because the grip adjustment should instantly occur to prevent the drop of an object. With time constant of 74.2 ms, the iSAFER system was able to recover its grasp and prevent the drop in the experiment.

Additionally, the potential topics of future work are addressed and introduced in details. Once the pressure distribution map of the hand grasp is fully understood in the future, the addition of a sensory array on the palm of the wearer's hand in accordance with needs will provide improved force profiles and drive further grasp adaptability. Moreover, integration of artificial neural networks will benefit more patients as it could possibly broaden a range of the patients who can use the exoskeletons in an active way. Another imaginable future project, a modular exoskeleton system, was presented with preliminary design.

8.2 Future Work

This section presents potential topics of future work. In addition to the suggested improvement on the current iSAFER system, a modular system consisting of iSAFER glove and a wearable 3 DOF forearm exoskeleton for rehabilitation and assistive purposes (FE.RAP) is proposed.

8.2.1 Future Work on Intelligent Object Grasping

In future work, improved sensing and automation capabilities will be explored. In this thesis, RSCEs were applied on the finger pads and fingernails. During the experiments, some results highlighted the effect of contacts between the palm and the objects. These inevitable contacts seemed to be the reason of the reduced force of the thumb pad. After reviewing the literatures on the pressure distribution map of hand [59], [83], [84], the result explained how much the palm was involved in the grip. Figure 8.1 illustrates the palm involvement in the grasp. Not only the contact of palm, but also the skin deformation that happens at the contact seemed to affect the pressure distribution. The addition of a sensory array on the palm of the wearer's hand will provide improved force profiles and drive further grasp adaptability.

In addition, integration of artificial neural networks can utilize wearer data to provide decreased response time in order to achieve a stable grip upon identification of the geometric profile of the object via the linkage positional feedback provided by the potentiometer, while also learning and adapting to the capabilities of the wearer as their abilities improve throughout rehabilitation. Likewise, other benefits will include matured detection of user's intention. If the iSAFER system could learn the patterns of slight

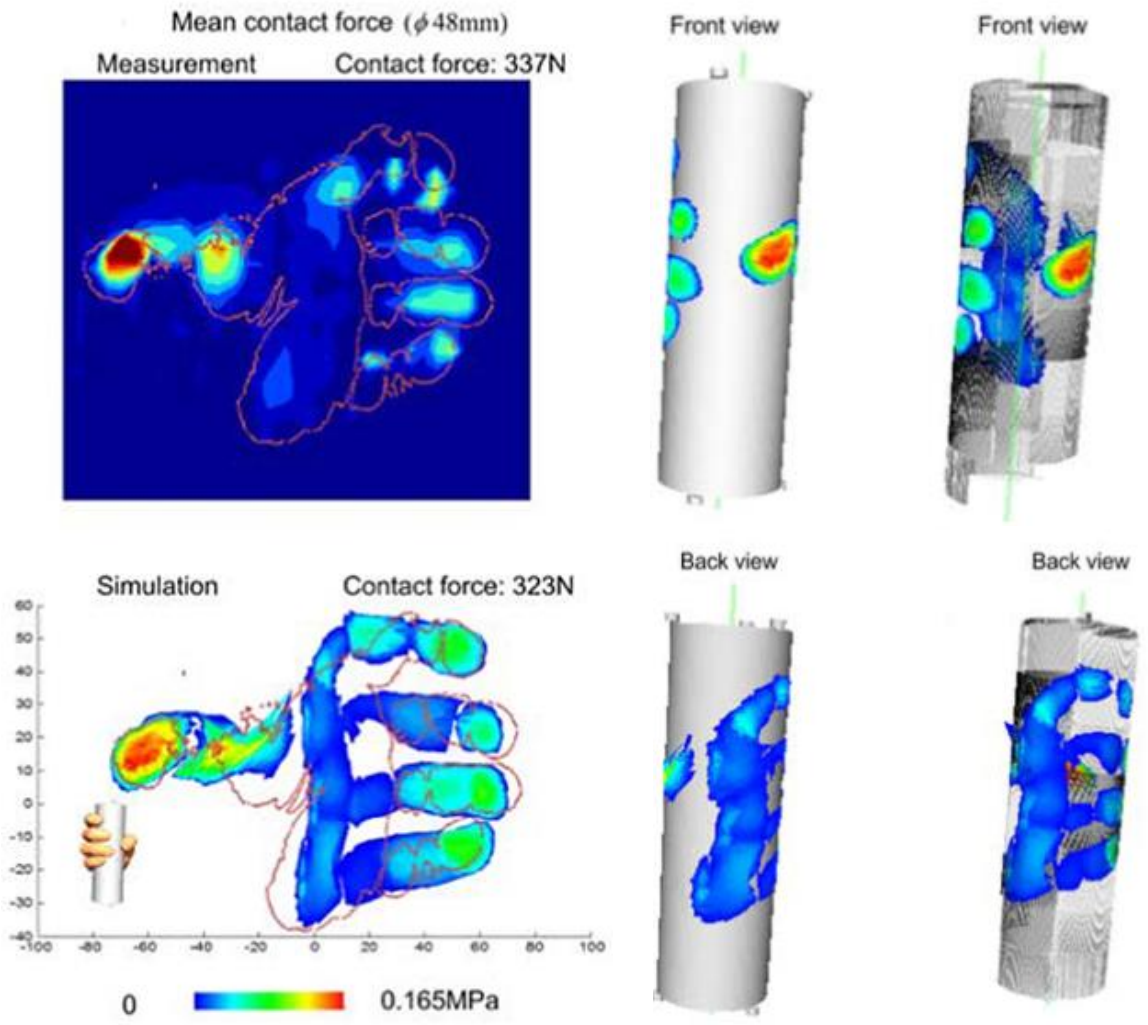

Figure 8.1: Pressure distribution validation using 48mm diameter cylinder grasp [81]

finger movements for frequently used grips, then even the users, who may have very little movement to almost no movement, would be able to perform numerous types of grasps actively without having numerous buttons or switches for each grasp.

Clinical trials with a variety of participants can be conducted in order to provide a more detailed analysis of the system's rehabilitation capabilities in the future.

8.2 Modular Exoskeleton System

The patients who lost motor function on hand often suffer forearm motor function loss as well. A study focused on delays in grip initiation and termination in persons with stroke concluded that supporting the weight of arms could reduce the delay in grip initiation and termination [85]. However, projects often focus on one part of the human body parts, such as hand, and develop an exoskeleton glove [34], [35], [86]–[89]. On the other hand, there are also projects, which focus on limbs as a whole system, such as arms, resulting in upper extremity exoskeletons [46], [89]–[96]. For rehabilitation and assistive purposes, these upper extremity exoskeletons will guide the users to move the upper limbs involving multiple human body parts from shoulder to wrist. In fact, as upper extremity or upper limb generally represents the region from shoulder to hand, current upper extremity exoskeletons that covered the human body parts from shoulder to wrist are not quite complete, yet, some of the other upper extremity exoskeletons covered less parts by omitting the wrist or shoulder support [46], [89]–[94]. In addition, as the human body parts covered by each upper limb exoskeleton were different, the amount of degrees of freedom (DOF) supported for each joint also varied per each upper limb exoskeleton [6]. For instance, though the forearm has three DOF, certain forearm exoskeletons and upper limb exoskeletons covered less than three DOF for the forearm [46], [94]–[98].

Besides the facts, standardizing how many DOF per joint or deciding what parts must be covered by one exoskeleton is not possible in reality. Furthermore, groups of patients require different rehabilitation processes, and individuals in those groups have different recovery speed. To provide personalized rehabilitation training with exoskeletons, an exoskeleton that has multiple modular sub-exoskeletons can be advantageous to the

patients. Considering a case where a patient lost motor function of both the wrist and the hand, this patient may no longer need to use the exoskeleton for the wrist rehabilitation once that patient starts to recover the motor function of the wrist while the hand is still impaired. If the exoskeleton was modular exoskeleton that had two sub-exoskeletons, the patient may detach the wrist exoskeleton, and continue using the hand exoskeleton for the hand rehabilitation.

Utilizing that idea, the forearm exoskeleton called the FE.RAP was designed and analyzed [9]. Following Figure 8.2 illustrates the optimized design of the FE.RAP after

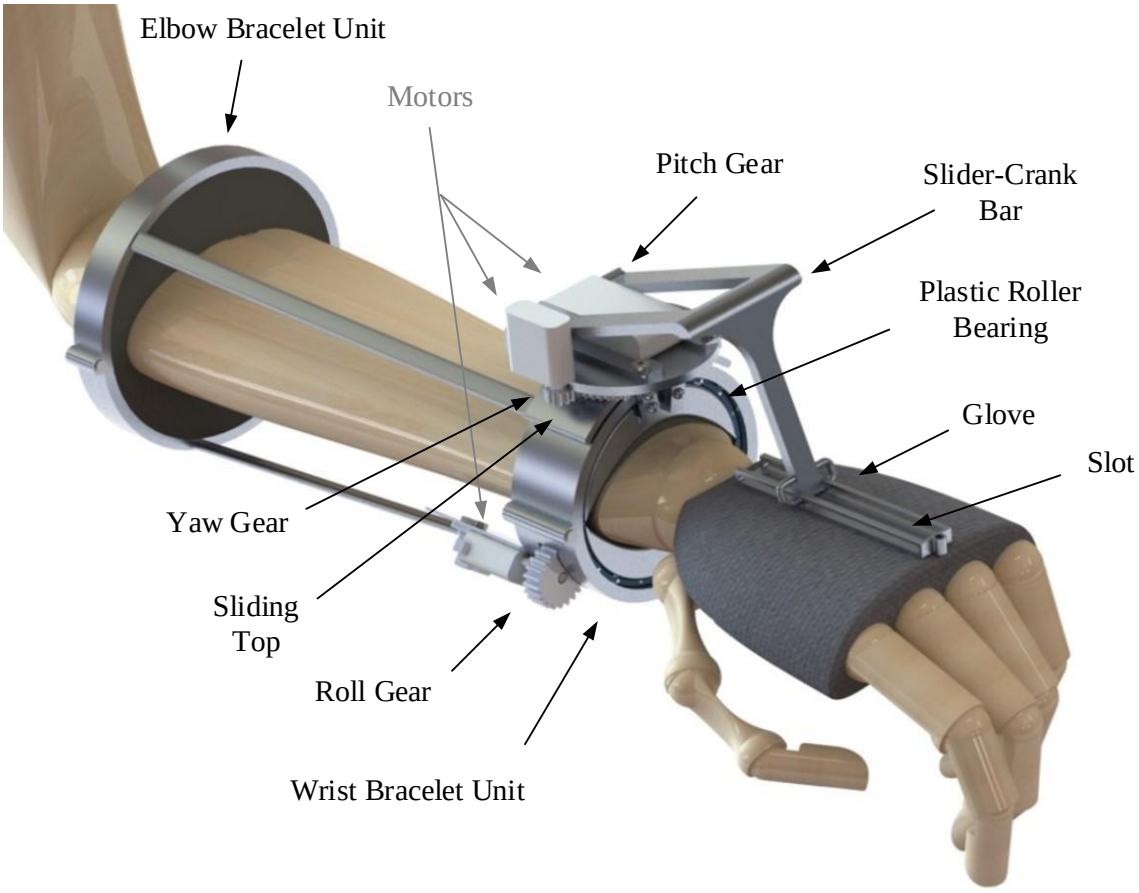

Figure 8.2: Optimized design of the FE.RAP

the workspace analysis and optimization. During the optimization, movable range of human hand expressed in angle, shown in the Table 2, was used. Knowing that there are factors that can affect the data of the ROM, such as gender or method used to measure the ROM, the ROM data shown in Table 2 was decided after an intense literature review. After the optimization, the workspace of the FE.RAP was verified to satisfy most of the ROM data in Table 2. The ROM of the ulnar deviation, radial deviation, forearm pronation, forearm supination, and wrist flexion were fully satisfied, but the optimized point of rotation chosen to keep the compactness of the FE.RAP, it limited the ROM of the wrist extension. As the FE.RAP can extend the human hand up to 49°, which is about 82% of the full ROM, an improved design to further increase the wrist extension to 60° are desired to be considered in the future.

If this FE.RAP and the iSAFER glove can work together as a system while each works as an individual exoskeleton, this will increase the modularity and have multiple application. At the beginning stage of the rehabilitation, the patients can start

Table 2: Movable Range of Human Hand

Joint Motion		Range of Motion
Pitch	Wrist Extension	60
	Wrist Flexion	70
Yaw	Ulnar Deviation	30
	Radial Deviation	20
Roll	Forearm Pronation	90
	Forearm Supination	90

rehabilitation with full system, but adjusting to the recovery condition of the patient, one of the modules, either iSAFER glove or FE.RAP, can be detached from a system reducing unnecessary weight of a full system. In the future, when individuals start to own exoskeletons for rehabilitation purpose, this modularity will be beneficial in many ways for those users as one system can transfer from rehabilitation exoskeleton to assistance exoskeleton. An option of attaching and detaching modules as necessary will continue to provide rehabilitation while assisting ADL for the patients, who were not able to recover full range of motion in a short period.

A preliminary design of the modular upper extremity exoskeleton consisting of the FE.RAP and iSAFER glove is depicted in Figure 8.3. To fit the component of the

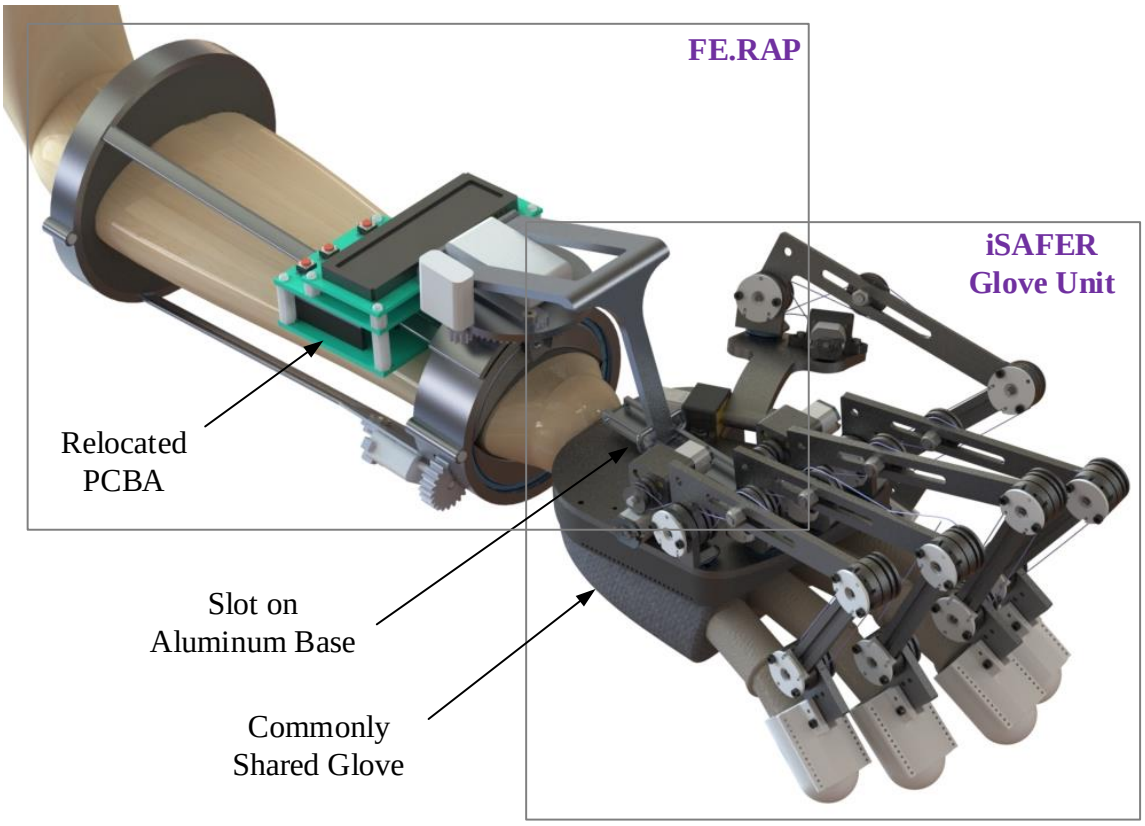

Figure 8.3: A preliminary design of the modular upper extremity exoskeleton consisting of the FE.RAP and iSAFER glove

FE.RAP on the iSAFER glove body, a number of components iSAFER glove were relocated to show an abstract concept.

REFERENCES

[1] G. B. Prange, M. J. A. Jannink, C. G. M. Groothuis-Oudshoorn, H. J. Hermens, and M. J. IJzerman, "Systematic review of the effect of robot-aided therapy on recovery of the hemiparetic arm after stroke," *J. Rehabil. Res. Dev.*, vol. 43, no. 2, p. 171, 2006.

[2] B. H. Dobkin, "Rehabilitation after Stroke," *N. Engl. J. Med.*, vol. 352, no. 16, pp. 1677–1684, Apr. 2005.

[3] I. D. Cameron and S. E. Kurrle, "1: Rehabilitation and older people," *Med. J. Aust.*, vol. 177, pp. 387–391, 2002.

[4] T. Future and H. L. Expectancy, "The Future of Human Life Expectancy :," *Source*, vol. 14, no. 8, pp. 1–4, 2006.

[5] J. et al Dipiro, *Pharmacotherapy A Pathophysiologic Approach*, vol. 53, no. 9. 2008.

[6] P. Maciejasz, J. Eschweiler, K. Gerlach-Hahn, A. Jansen-Troy, and S. Leonhardt, "A survey on robotic devices for upper limb rehabilitation.," *J. Neuroeng. Rehabil.*, vol. 11, no. 1, p. 3, 2014.

[7] "Post-Stroke Rehabilitation," National Institutes of Health, 2014.

[8] R. Riener, M. Wellner, T. Nef, J. von Zitzewitz, A. Duschau-Wicke, G. Colombo, and L. Lunenburger, "A View on VR-Enhanced Rehabilitation Robotics," in *2006 International Workshop on Virtual Rehabilitation*, 2006, pp. 149–154.

[9] J. Lee and P. Ben-Tzvi, "Design of a Wearable 3-DOF Forearm Exoskeleton for Rehabilitation and Assistive Purposes," in *Proceedings of the 2017 ASME*

International Mechanical Engineering Congress and Exposition (IMECE 2017) Volume 3: Biomedical and Biotechnology Engineering, 2017, pp. 1–10.

[10] E. Refour, B. Sebastian, and P. Ben-Tzvi, "Design and Integration of a Two-Digit Exoskeleton Glove," in *Proceedings of the ASME 2017 International Design Engineering Technical Conferences and Information in Computers and Engineering Conference IDETC/CIE 2017*, 2017, pp. 1–9.

[11] B. R. Brewer, S. K. McDowell, and L. C. Worthen-Chaudhari, "Poststroke Upper Extremity Rehabilitation: A Review of Robotic Systems and Clinical Results," *Top. Stroke Rehabil.*, vol. 14, no. 6, pp. 22–44, 2007.

[12] M. Gobbo, P. Gaffurini, L. Vacchi, S. Lazzarini, J. Villafane, C. Orizio, S. Negrini, and L. Bissolotti, "Hand Passive Mobilization Performed with Robotic Assistance: Acute Effects on Upper Limb Perfusion and Spasticity in Stroke Survivors," *Biomed Res. Int.*, vol. 2017, pp. 1–6, 2017.

[13] M. A. Diftler, L. B. Bridgwater, and J. M. Rogers, "RoboGlove – A Grasp Assist Device for Earth and Space," *45th Int. Conf. Environ. Syst.*, no. July, pp. 1–8, 2015.

[14] P. Polygerinos, Z. Wang, K. C. Galloway, R. J. Wood, and C. J. Walsh, "Soft robotic glove for combined assistance and at-home rehabilitation," *Rob. Auton. Syst.*, vol. 73, pp. 135–143, 2015.

[15] P. Ben-Tzvi and Z. Ma, "Sensing and Force-Feedback Exoskeleton (SAFE) Robotic Glove," *IEEE Trans. Neural Syst. Rehabil. Eng.*, vol. 23, no. 6, pp. 992–1002, Nov. 2015.

[16] E. D. Engeberg and S. G. Meek, "Adaptive Sliding Mode Control for Prosthetic

Hands to Simultaneously Prevent Slip and Minimize Deformation of Grasped Objects," *IEEE/ASME Trans. Mechatronics*, vol. 18, no. 1, pp. 376–385, Feb. 2013.

[17] I. Jo and J. Bae, "Design and control of a wearable and force-controllable hand exoskeleton system," *Mechatronics*, vol. 41, no. c, pp. 90–101, 2017.

[18] Z. Su, K. Hausman, Y. Chebotar, A. Molchanov, G. Loeb, G. S. Sukhatme, and S. Schaal, "Force Estimation and Slip Detection for Grip Control using a Biomimetic Tactile Sensor," *IEEE-RAS Int. Conf. Humanoid Robot.*, pp. 297–303, 2015.

[19] R. M. Crowder, V. N. Dubey, P. H. Chappell, and D. R. Whatley, "A multi-fingered end effector for unstructured environments," in *Proceedings 1999 IEEE International Conference on Robotics and Automation (Cat. No.99CH36288C)*, 1999, vol. 4, no. May, pp. 3038–3043.

[20] A. A. S. Al-Shanoon, S. A. Ahmad, and M. K. b. Hassan, "Slip detection with accelerometer and tactile sensors in a robotic hand model," *IOP Conf. Ser. Mater. Sci. Eng.*, vol. 99, no. 1, p. 12001, Nov. 2015.

[21] L. Roberts, G. Singhal, and R. Kaliki, "Slip detection and grip adjustment using optical tracking in prosthetic hands," in *Proceedings of the Annual International Conference of the IEEE Engineering in Medicine and Biology Society, EMBS*, 2011, pp. 2929–2932.

[22] R. Fernandez, I. Payo, A. S. Vazquez, and J. Becedas, "Slip Detection in Robotic Hands with Flexible Parts," in *ROBOT2013: First Iberian Robotics Conference, Advances in Intelligent Systems and Computing 253*, 2014, pp. 153–167.

[23] D. J. Clarke and A. Forster, "Improving post-stroke recovery: The role of the

multidisciplinary health care team," *J. Multidiscip. Healthc.*, vol. 8, pp. 433–442, 2015.

[24] H. Lee, W. Kim, J. Han, and C. Han, "The Technical Trend of the Exoskeleton Robot System for Human Power a=Assistance," *Int. J. Precis. Eng. Manuf.*, vol. 13, no. 8, pp. 1491–1497, Aug. 2012.

[25] S. M. Hatem, G. Saussez, M. Della Faille, V. Prist, X. Zhang, D. Dispa, and Y. Bleyenheuft, "Rehabilitation of Motor Function after Stroke: A Multiple Systematic Review Focused on Techniques to Stimulate Upper Extremity Recovery.," *Front. Hum. Neurosci.*, vol. 10, no. September, p. 442, 2016.

[26] S. Hesse, G. Schulte-Tigges, M. Konrad, A. Bardeleben, and C. Werner, "Robot-assisted arm trainer for the passive and active practice of bilateral forearm and wrist movements in hemiparetic subjects.," *Arch. Phys. Med. Rehabil.*, vol. 84, no. 6, pp. 915–20, Jun. 2003.

[27] G. Kwakkel, B. J. Kollen, and H. I. Krebs, "Effects of Robot-Assisted Therapy on Upper Limb Recovery After Stroke: A Systematic Review," *Neurorehabil. Neural Repair*, vol. 22, no. 2, pp. 111–121, Sep. 2007.

[28] V. Rajasekaran, J. Aranda, A. Casals, and J. L. Pons, "An adaptive control strategy for postural stability using a wearable robot," *Rob. Auton. Syst.*, vol. 73, pp. 16–23, Nov. 2015.

[29] S. K. Charles, H. I. Krebs, B. T. Volpe, D. Lynch, and N. Hogan, "Wrist Rehabilitation Following Stroke: Initial Clinical Results," *Rehabil. Robot. 2005. ICORR 2005. 9th Int. Conf.*, pp. 13–16, 2007.

[30] M. L. Aisen, H. I. Krebs, N. Hogan, F. McDowell, and B. T. Volpe, "The Effect of

Robot-Assisted Therapy and Rehabilitative Training on Motor Recovery Following Stroke," *Arch. Neurol.*, vol. 54, no. 4, pp. 443–446, Apr. 1997.

[31] J. H. Crosbie, S. Lennon, J. R. Basford, and S. M. McDonough, "Virtual reality in stroke rehabilitation: Still more virtual than real," *Disabil. Rehabil.*, vol. 29, no. 14, pp. 1139–1146, 2007.

[32] N. Takeuchi and S.-I. Izumi, "Rehabilitation with poststroke motor recovery: a review with a focus on neural plasticity.," *Stroke Res. Treat.*, vol. 2013, p. 128641, 2013.

[33] J. A. Martinez, P. Ng, Son Lu, M. S. Campagna, and O. Celik, "Design of Wrist Gimbal: A forearm and wrist exoskeleton for stroke rehabilitation," in *2013 IEEE 13th International Conference on Rehabilitation Robotics (ICORR)*, 2013, pp. 1–6.

[34] Z. Ma, P. Ben-Tzvi, and J. Danoff, "Hand Rehabilitation Learning System With an Exoskeleton Robotic Glove," *IEEE Trans. Neural Syst. Rehabil. Eng.*, vol. 24, no. 12, pp. 1323–1332, Dec. 2016.

[35] M. Ngai, "Design of a Forearm Exoskeleton for Supination / Pronation Assistance in Daily Activities," 2010.

[36] P. Polygerinos, K. C. Galloway, E. Savage, M. Herman, K. O'Donnell, and C. J. Walsh, "Soft robotic glove for hand rehabilitation and task specific training," *Proc. - IEEE Int. Conf. Robot. Autom.*, vol. 2015–June, no. June, pp. 2913–2919, 2015.

[37] A. M. Zaid, T. C. Chean, J. A. Sukor, and D. Hanafi, "Development of hand exoskeleton for rehabilitation of post-stroke patient," in *AIP Conference Proceedings*, 2017, vol. 1891, no. 2017, p. 20103.

[38] B. E. Mustard and R. G. Lee, "Relationship between EMG patterns and kinematic

properties for flexion movements at the human wrist," *Exp*, vol. 66, pp. 247–256, 1987.

[39] P. Polygerinos, K. C. Galloway, S. Sanan, M. Herman, and C. J. Walsh, "EMG controlled soft robotic glove for assistance during activities of daily living," *IEEE Int. Conf. Rehabil. Robot.*, vol. 2015–Septe, pp. 55–60, 2015.

[40] R. Looned, J. Webb, Z. Xiao, and C. Menon, "Assisting drinking with an affordable BCI-controlled wearable robot and electrical stimulation: a preliminary investigation," *J. Neuroeng. Rehabil.*, vol. 11, no. 1, p. 51, 2014.

[41] K. S. Türker, "Electromyography: Some Methodological Problems and Issues," *Phys. Ther.*, vol. 73, no. 10, pp. 698–710, 1993.

[42] P. K. Levangie and C. C. Norkin, "Joint Structure and Function: A Comprehensive Analysis," *F. A. Davis Co.*, pp. 393–436, 2005.

[43] L. Wang, T. Meydan, and P. Williams, "A Two-Axis Goniometric Sensor for Tracking Finger Motion," *Sensors*, vol. 17, no. 4, p. 770, Apr. 2017.

[44] O. Rettig, L. Fradet, P. Kasten, P. Raiss, and S. I. Wolf, "A new kinematic model of the upper extremity based on functional joint parameter determination for shoulder and elbow," *Gait Posture*, vol. 30, no. 4, pp. 469–476, 2009.

[45] A. Tözeren, *Human Body Dynamics: Classical Mechanics and Human Movement*, vol. 87, no. 2. Springer, 2000.

[46] M. R. S. John, N. Thomas, and V. P. R. Sivakumar, "Design and Development of Cable Driven Upper Limb Exoskeleton for Arm Rehabilitation," *Int. J. Sci. Eng. Res.*, vol. 7, no. 3, pp. 1432–1440, 2016.

[47] "Guitar Player Anatomy." [Online]. Available: https://www.mangore.com/player-

anatomy-3-15-56.

[48] T. Feix, J. Romero, H.-B. Schmiedmayer, A. M. Dollar, and D. Kragic, “The GRASP Taxonomy of Human Grasp Types,” *IEEE Trans. Human-Machine Syst.*, vol. 46, no. 1, pp. 66–77, Feb. 2016.

[49] J. Liu, F. Feng, Y. C. Nakamura, and N. S. Pollard, “A taxonomy of everyday grasps in action,” in *2014 IEEE-RAS International Conference on Humanoid Robots*, 2014, pp. 573–580.

[50] T. Feix, R. Pawlik, H.-B. Schmiedmayer, J. Romero, and D. Kragi, “A comprehensive grasp taxonomy,” *Robot. Sci. Syst. Conf. Work. Underst. Hum. Hand Adv. Robot. Manip.*, pp. 2–3, 2009.

[51] T. Feix, I. M. Bullock, and A. M. Dollar, “Analysis of Human Grasping Behavior: Object Characteristics and Grasp Type,” *IEEE Trans. Haptics*, vol. 7, no. 3, pp. 311–323, Jul. 2014.

[52] N. Kamakura, M. Matsuo, H. Ishii, F. Mitsuboshi, and Y. Miura, “Patterns of Static Prehension in Normal Hands,” *Am. J. Occup. Ther.*, vol. 34, no. 7, pp. 437–445, 1980.

[53] N. N. Ansari, S. Naghdi, T. K. Arab, and S. Jalaie, “The interrater and intrarater reliability of the Modified Ashworth Scale in the assessment of muscle spasticity: limb and muscle group effect.,” *NeuroRehabilitation*, vol. 23, no. 3, pp. 231–237, 2008.

[54] U. Naqvi and A. l. Sherman, *Muscle Strength Grading*, vol. 12, no. 6. 2017.

[55] L. Peternel, T. Noda, T. Petrič, A. Ude, J. Morimoto, and J. Babič, “Adaptive Control of Exoskeleton Robots for Periodic Assistive Behaviours Based on EMG

Feedback Minimisation.," *PLoS One*, vol. 11, no. 2, p. e0148942, 2016.

[56] R. A. R. C. Gopura, K. Kiguchi, and Y. Li, "SUEFUL-7: A 7DOF upper-limb exoskeleton robot with muscle-model-oriented EMG-based control," in *2009 IEEE/RSJ International Conference on Intelligent Robots and Systems*, 2009, pp. 1126–1131.

[57] Z. Tang, K. Zhang, S. Sun, Z. Gao, L. Zhang, and Z. Yang, "An upper-limb power-assist exoskeleton using proportional myoelectric control," *Sensors (Basel).*, vol. 14, no. 4, pp. 6677–6694, 2014.

[58] Z. G. Xiao, A. M. Elnady, J. Webb, and C. Menon, "Towards a brain computer interface driven exoskeleton for upper extremity rehabilitation," *5th IEEE RAS/EMBS Int. Conf. Biomed. Robot. Biomechatronics*, pp. 432–437, 2014.

[59] H. In and K. Cho, "Exo-Glove : Soft wearable robot for the hand using soft tendon routing system," *IEEE Robot. Autom.*, vol. 22, no. March 2015, pp. 97–105, 2015.

[60] R. S. Johansson and J. R. Flanagan, "Coding and use of tactile signals from the fingertips in object manipulation tasks," *Nat. Rev. Neurosci.*, vol. 10, no. 5, pp. 345–359, May 2009.

[61] C. Melchiorri, "Slip Detection and Control Using Tactile and Force Sensors," *Mechatronics*, vol. 5, no. 3, pp. 235–243, 2000.

[62] R. Fernandez, I. Payo, A. S. Vazquez, and J. Becedas, "Micro-Vibration-Based Slip Detection in Tactile Force Sensors," no. i, pp. 709–730, 2014.

[63] E. G. M. Holweg, H. Hoeve, W. Jongkind, L. Marconi, C. Melchiorri, and C. Bonivento, "Slip detection by tactile sensors: algorithms and experimental results," *Proc. IEEE Int. Conf. Robot. Autom.*, vol. 9, no. 7, pp. 3234–3239, 2007.

[64] S. Kosaka, M. Nakajima, T. Fukuda, and H. Matsuura, “Slipping Detection with Integrated Piezoelectric Vibration Tactile Sensors,” in *2008 IEEE/SICE International Symposium on System Integration*, 2008, pp. 111–116.

[65] R. Romeo, C. Oddo, M. Carrozza, E. Guglielmelli, and L. Zollo, “Slippage Detection with Piezoresistive Tactile Sensors,” *Sensors*, vol. 17, no. 8, p. 1844, Aug. 2017.

[66] M. R. Tremblay and M. R. Cutkosky, “Estimating friction using incipient slip sensing during a manipulation task,” in *[1993] Proceedings IEEE International Conference on Robotics and Automation*, 1993, pp. 429–434.

[67] B. Kim, H. Cho, D. Kim, U. Kim, H. R. Choi, H. P. Moon, J. C. Koo, Y. Lee, and J. D. Nam, “Design of slip detection sensor for artificial skin,” in *2012 9th International Conference on Ubiquitous Robots and Ambient Intelligence (URAI)*, 2012, pp. 510–511.

[68] H. Kinoshita, L. Bäckström, J. R. Flanagan, and R. S. Johansson, “Tangential Torque Effects on the Control of Grip Forces When Holding Objects With a Precision Grip,” *J. Neurophysiol.*, vol. 78, no. 3, pp. 1619–1630, Sep. 1997.

[69] Z. Ma and P. Ben-Tzvi, “Tendon transmission efficiency of a two-finger haptic glove,” in *2013 IEEE International Symposium on Robotic and Sensors Environments (ROSE)*, 2013, no. October, pp. 13–18.

[70] Z. Ma and P. Ben-Tzvi, “RML Glove; An Exoskeleton Glove Mechanism With Haptics Feedback,” *IEEE/ASME Trans. Mechatronics*, vol. 20, no. 2, pp. 641–652, Apr. 2015.

[71] Z. Ma and P. Ben-Tzvi, “Design and Optimization of a Five-Finger Haptic Glove

Mechanism," *J. Mech. Robot.*, vol. 7, no. 4, p. 41008, 2015.

[72] Z. Ma, P. Ben-Tzvi, and J. Danoff, "Modeling Human Hand and Sensing Hand Motions With the Five-Fingered Haptic Glove Mechanism," *Proc. ASME 2014 Int. Des. Eng. Tech. Conf. Comput. Inf. Eng. Conf. IDETC/CIE 2014*, p. V05AT08A008, 2014.

[73] P. Ben-Tzvi, J. Danoff, and Z. Ma, "The Design Evolution of a Sensing and Force-Feedback Exoskeleton Robotic Glove for Hand Rehabilitation Application," *J. Mech. Robot.*, vol. 8, no. 5, p. 51019, 2016.

[74] Z. Ma and P. Ben-Tzvi, "An Admittance Glove Mechanism for Controlling a Mobile Robot," *Proc. ASME 2012 Int. Des. Eng. Tech. Conf. Comput. Inf. Eng. Conf. IDETC/CIE 2012*, p. 1109, 2012.

[75] Z. Ma, P. Ben-Tzvi, and J. Danoff, "Sensing and Force-Feedback Exoskeleton Robotic (SAFER) Glove Mechanism for Hand Rehabilitation," in *Proceedings of the ASME 2015 International Design Engineering Technical Conferences & Computers and Information in Engineering Conference, IDETC/CIE 2015*, 2015, vol. 8, no. 5, p. V05AT08A036.

[76] Z. Ma and P. Ben-Tzvi, "An Admittance Type Haptic Device: RML Glove," in *Proceedings of the ASME 2011 International Mechanical Engineering Congress & Exposition, IMECE 2011*, 2011, pp. 1219–1225.

[77] Z. Ma and P. Ben-Tzvi, "RML glove-an exoskeleton glove mechanism with haptics feedback," *IEEE/ASME Trans. Mechatronics*, vol. 20, no. 2, pp. 641–652, 2015.

[78] Y. Hiramatsu, D. Kimura, K. Kadota, T. Ito, and H. Kinoshita, "Control of

precision grip force in lifting and holding of low-mass objects," *PLoS One*, vol. 10, no. 9, 2015.

[79] D. A. Valle-Lopera, A. F. Castraño-Franco, J. Gallego-Londoño, and A. M. Hernández-Valdivieso, "Test and fabrication of piezoresistive sensors for contact pressure measurement," *Rev. Fac. Ing. Univ. Antioquia*, no. 82, pp. 47–52, Mar. 2017.

[80] J. J. Carr and J. M. Brown, *Introduction to Biomedical Equipment Technology, Third Edition*. Prentice Hall, 1998.

[81] Z. Shen and S. B. Andersson, "Minimum time control of a second-order system," *49th IEEE Conf. Decis. Control*, vol. 2, no. 1, pp. 4819–4824, 2010.

[82] Worcester Polytechnic Institute, "Vibrations Measurements." [Online]. Available: https://users.wpi.edu/~sullivan/ME3901/Lectures/Vibration/Vibrations Measurements.htm.

[83] Y. Xie, S. Kanai, and H. Date, "An Efficient Simulation of Skin Contact Deformation for Virtual Ergonomic Assessments of Handheld Products," *Int. J. CAD/CAM*, vol. 13, no. 1, pp. 81–95, 2013.

[84] J. W. Nicholas, R. J. Corvese, C. Woolley, and T. J. Armstrong, "Quantification of hand grasp force using a pressure mapping system," *Work*, vol. 41, no. SUPPL.1, pp. 605–612, 2012.

[85] N. J. Seo, W. Z. Rymer, and D. G. Kamper, "Delays in grip initiation and termination in persons with stroke: effects of arm support and active muscle stretch exercise.," *J. Neurophysiol.*, vol. 101, no. 6, pp. 3108–3115, 2009.

[86] J. H. Beekhuis, A. J. Westerveld, H. van der Kooij, and A. H. A. Stienen, "Design

of a self-aligning 3-DOF actuated exoskeleton for diagnosis and training of wrist and forearm after stroke," in *2013 IEEE 13th International Conference on Rehabilitation Robotics (ICORR)*, 2013, pp. 1–5.

[87] T. Noda, N. Sugimoto, J. Furukawa, M. A. Sato, S. H. Hyon, and J. Morimoto, "Brain-controlled exoskeleton robot for BMI rehabilitation," in *IEEE-RAS International Conference on Humanoid Robots*, 2012, pp. 21–27.

[88] J. Blake and H. B. Gurocak, "Haptic Glove With MR Brakes for Virtual Reality," vol. 14, no. 5, pp. 606–615, 2009.

[89] B. Kim, "Controls for the Shoulder Mechanism of an Upper-Body Exoskeleton for Promoting Scapulohumeral Rhythm," pp. 538–542, 2015.

[90] P. Letier, M. Avraam, S. Veillerette, M. Horodinca, M. De Bartolomei, A. Schiele, and A. Preumont, "SAM : A 7-DOF portable arm exoskeleton with local joint control," in *2008 IEEE/RSJ International Conference on Intelligent Robots and Systems*, 2008, pp. 3501–3506.

[91] E. Mohammadi, H. Zohoor, and S. M. Khadem, "Control system design of an active assistive exoskeletal robot for rehabilitation of elbow and wrist," *2014 2nd RSI/ISM Int. Conf. Robot. Mechatronics, ICRoM 2014*, vol. 23, pp. 834–839, 2014.

[92] T. Noda, T. Teramae, B. Ugurlu, and J. Morimoto, "Development of an upper limb exoskeleton powered via pneumatic electric hybrid actuators with bowden cable," in *IEEE International Conference on Intelligent Robots and Systems*, 2014, pp. 3573–3578.

[93] K. Kiguchi, M. H. Rahman, M. Sasaki, and K. Teramoto, "Development of a 3DOF mobile exoskeleton robot for human upper-limb motion assist," *Rob. Auton.*

Syst., vol. 56, no. 8, pp. 678–691, Aug. 2008.

[94] Y. Mao and S. K. Agrawal, "Design of a cable-driven arm exoskeleton (CAREX) for neural rehabilitation," *IEEE Trans. Robot.*, vol. 28, no. 4, pp. 922–931, 2012.

[95] U. Keller, H. J. A. van Hedel, V. Klamroth-Marganska, and R. Riener, "ChARMin: The First Actuated Exoskeleton Robot for Pediatric Arm Rehabilitation," *IEEE/ASME Trans. Mechatronics*, vol. 21, no. 5, pp. 2201–2213, Oct. 2016.

[96] M. H. Rahman, M. J. Rahman, O. L. Cristobal, M. Saad, J. P. Kenné, and P. S. Archambault, "Development of a whole arm wearable robotic exoskeleton for rehabilitation and to assist upper limb movements," *Robotica*, vol. 33, no. 1, pp. 19–39, Jan. 2015.

[97] C. V Gilman, P. Ben-Tzvi, G. Yessin, and J. Danoff, "A Robotic Exoskeleton Device for Augmenting Wrist Movement and Grip Function in Debilitated Patients," in *ASME 2011 International Mechanical Engineering Congress and Exposition*, 2011, pp. 1041–1050.

[98] J. Allington, S. J. Spencer, J. Klein, M. Buell, D. J. Reinkensmeyer, and J. Bobrow, "Supinator extender (SUE): A pneumatically actuated robot for forearm/wrist rehabilitation after stroke," in *Proceedings of the Annual International Conference of the IEEE Engineering in Medicine and Biology Society, EMBS*, 2011, pp. 1579–1582.

APPENDIX A

Block Diagram of the iSAFER System